A Study of Primary Neural Stem Cell Differentiation *In Vitro*, Focusing on the Three Amino acid Loop Extension (TALE) Homeobox Transcription Factors

by

Benjamin A. Barber

Thesis submitted to the Faculty of Graduate Studies of

The University of Manitoba

In partial fulfilment of the requirements of the degree of

MASTER OF SCIENCE

Department of Biochemistry and Medical Genetics

University of Manitoba

Winnipeg

Abstract

Neural stem cells are capable of self-renewal and multilineage differentiation into the main cell types of the central nervous system, which are the neurons, astrocytes, and oligodendrocytes. These properties make neural stem cells an attractive cell source for potential cell-based therapies; however, thoroughly describing their gene expression programs is required to predict their safety and efficacy. In this study, we reveal that mouse embryonic day (E14) forebrain-derived primary neural stem cells have an astrocytic gene expression profile. We show that the NOTCH and BMP signalling pathways exhibit transcription profiles that are specific to the proliferation and differentiation of this neural stem cell source. Finally, we report the expression patterns of the *Hox* and TALE family homeobox genes in the E14 forebrain, E14 forebrain-derived primary neural stem cells, and their differentiating progeny. Protein expression analysis suggests that PREP2 is involved in neural stem cell proliferation and neuronogenesis, and that MEIS1 is involved in astrocyte differentiation. This is the first report on the expression patterns of TALE genes in forebrain-derived NSC differentiated *in vitro*, which provides a starting point to investigate the role of TALE genes in forebrain neurogenesis.

Acknowledgements

First and foremost I would like to thank my supervisor Dr. Mojgan Rastegar for the opportunity to work on this project and for her unyielding support throughout. Mojgan's dedication to her students cannot be appreciated enough. Her work ethic and the support she gives her lab members are truly something to aspire to, and I wish her all the success in the world with her research program.

I would like to thank my advisory committee members Dr. Jeff Wigle, Dr. David Eisenstat and Dr. Tom Klonisch for their invaluable insight and suggestions throughout my project. The wealth of knowledge that these individuals demonstrate during the course of an advisory committee meeting is humbling to say the least.

Thank you to my lab members, especially our technician Carl, who is the pillar we all know we can rely on most. And to my fellow students Robby and Vichy, thank you for all the help, advice, discussions, and fun!

Last but certainly not least I would like to thank Lara Gushulak. Lara's capability, compassion and devotion to family are exemplary of what keeps the world turning 'round. On behalf of everyone, thanks for being who you are, and for being there.

I would like to acknowledge the following agencies for their financial support: NSERC (Discovery Grant 372405-2009), Canada Foundation for Innovation, Manitoba Health Reasearch Council, University of Manitoba Reasearch Grant Program, Manitoba Institute of Child Health, Scottish Rite Charitable Foundation of Canada (Grant 10110), Health Sciences Centre Foundation and The Dr. Paul HT Thorlakson Foundation Fund.

Table of Contents

List of Abbreviations

ALP	alkaline phosphatase
CNS	central nervous system
CNTF	ciliary neurotrophic factor
DG	dentate gyrus
EGF	epidermal growth factor
ESC	embryonic stem cell
FGF	fibroblast growth factor
ICD	notch intracellular domain
ICM	inner cell mass
IF	immunofluorescence
IPC	intermediate precursor cell
iPS cell	induced pluripotent stem cell
LGE	lateral ganglionic eminence
MGE	medial ganglionic eminence
NSC	neural stem cell
PDGF	platelet-derived growth factor
RA	retinoic acid
RG	radial glia
SVZ	subventricular zone
T3	thyroid hormone triiodothyronine
VEGF	vascular endothelial growth factor
VZ	ventricular zone

List of Tables

List of Figures

1.1 Introduction

The aim of this work is to contribute to our knowledge of stem cell biology and the potential of these cells for regenerative therapy and disease research. Since the successful isolation and culture of mammalian pluripotent stem cells in 1981 [1], the stem cell field has rapidly expanded. During this time, significant advances have been achieved including the identification of different types of stem cells, stem cell culture systems and stem cell based therapies in animal models that have shown varying degrees of improvement [2-6]. Current methods in genetics and biochemistry enable us to describe the character of these cells at a depth previously unattainable. These new technologies better equip us to predict both the beneficial and the dangerous outcomes of stem cell implantation. Our work contributes to describing the genetics of neural stem cell (NSC) self-renewal and differentiation *in vitro* using RNA and protein expression analysis, with a focus on homeodomain transcription factors. Neural stem cells provide a source of self-renewing primitive cells with the ability to give rise to all three major cell lineages of the central nervous system (CNS): neurons, astrocytes and oligodendrocytes [2,7-8]. *In vitro* culture of these cells provides a means to generate vast quantities of cells required for cell screening, transplant techniques, and for studying the effects of pharmacological agents on specific CNS cell types. A detailed understanding of cell environmental response and the cell fate decision process is first required before therapeutic NSC delivery should be attempted.

1.2 The Stem Cell Hierarchy

The stem cell hierarchy identifies different types of stem cells and places them in order based on the degree of their differentiation and lineage restriction (Fig. 1). Atop the hierarchy are totipotent stem cells which have the capacity to give rise to all of the cell types necessary to generate the entire organism. In the case of mammals, this includes the embryo proper as well as the supportive extraembryonic tissue. Proceeding down the stem cell hierarchy, cell potential becomes more lineage restricted. Below totipotent stem cells are pluripotent stem cells, which have the capacity to generate all of the cell types that make up the mature organism. Next are multipotent stem cells that are restricted to specific germ layers or cell lineages, and can produce the cells necessary to generate specific organs or tissues [9]. Examples of multipotent stem cells include neural stem cells, mesenchymal stem cells and haematopoietic stem cells [10-12]. More restricted cell types include oligopotent (few cell types), bipotent (two cell types) and unipotent (one type of progeny) cells.

1.3 Embryonic Stem Cells

Embryonic stem cells (ESC) are pluripotent, and arguably have the greatest potential for experimentation, development, and regeneration. After fertilization of the oocyte, the zygote undergoes several rounds of symmetric cell divisions. The cell mass created by these cell divisions is known as the morula, and at the 32 cell stage compaction occurs leading to the definition of a compact inner cell mass (ICM), and a surrounding cell layer comprising the trophectoderm. The ICM gives rise to the embryo proper and the trophectoderm generates the supportive extraembryonic tissues [13]. This structure is

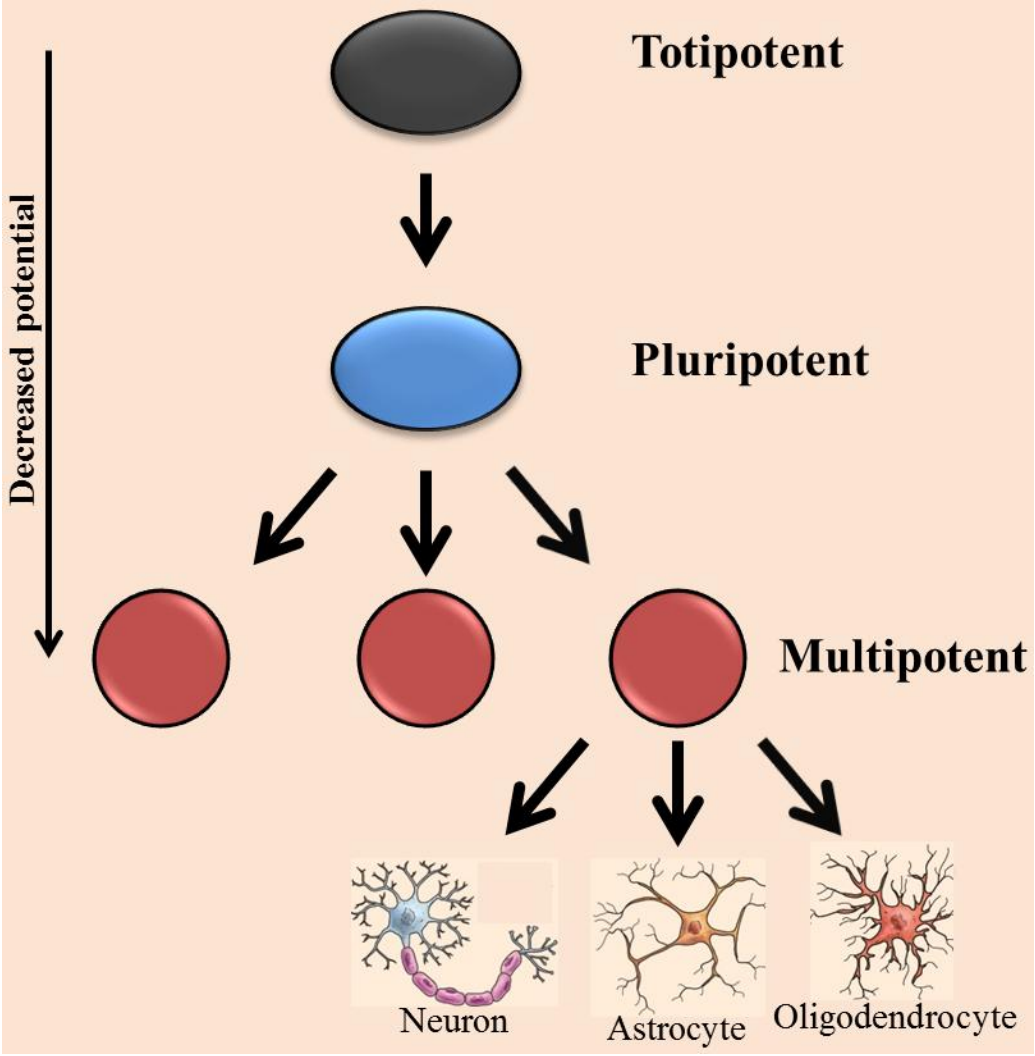

Figure 1. The stem cell hierarchy. This is a hierarchical arrangement of the types of stem cells based on differentiation potential. The most primitive cells, totipotent stem cells, are capable of generating the most cell types and are at the top of the hierarchy. Differentiation potential is more restricted in the cells positioned lower in the hierarchy, until fully differentiated cells are generated from either multipotent stem cells directly or *via* more restricted stem/progenitor cells. In this case, the differentiated neural cell types (neurons, astrocytes, and oligodendrocytes) are generated from multipotent neural stem cells. (*Including adaptations from Olynik and Rastegar, in preparation.*)

known as the blastocyst and it is the ICM cells within the blastocyst that are the source of pluripotent embryonic stem cells [14-15]. There are a variety of assays used to verify the pluripotent character of isolated embryonic stem cells. In cell culture, surrogate assays include detecting the expression of so-called "pluripotency genes" such as *Oct4* and *Nanog*, which display their strongest expression in pluripotent stem cells and play key roles in maintaining the ESC state [16-17]. In culture, addition of the alkaline phosphatase (ALP) substrate ρ-nitrophenyl phosphate will produce a robust yellow colour when dephosphorylated by ALP, which is strongly expressed in pluripotent cells [18-19]. Functional assays include transplantation of these cells into immunodeficient mice to determine whether these cells can generate teratomas that include cell lineages of all three germ layers [1,20]. The best demonstration of pluripotency comes from the formation of chimeric mice and contribution to all three germ layers within the chimera. This is done by introducing the cells into a blastocyst and allowing the chimeric embryo to develop in a pseudopregnant host, then subsequently detecting ESC progeny within all three germ layers *via* a transgene reporter [21].

In the absence of extrinsic signals or serum *in vitro*, ESC undergo neural differentiation, which is described as the default mechanism [22-23]. Studies have shown that this differentiation produces cells of mainly telencephalic (forebrain) identity [24-25]. When cultured at low density and in the presence of leukemia inhibitory factor (LIF), a small percentage of embryonic stem cells produce NSC colonies, and passaging of these leads to fibroblast growth factor 2 (FGF2) dependence and many characteristics shared with adult brain derived neural precursor cells. This includes the *in vitro* neural differentiation patterns of the cells and their *in vivo* differentiation patterns upon

transplantation [22-23,26]. It has been found that combining serum and all trans-retinoic acid (RA) can accelerate neuronal maturation and suppress cell proliferation of embryonic stem cells. This practice is common in ESC experimentation [27-29]. Electrophysiological experiments show that the differentiated neurons include functional excitatory and inhibitory neurons, and protocols have been modified to produce specific neuron types such as dopaminergic, motor, and cerebellar neurons [30-33]. The use of RA has also been shown to decrease the telencephalic identity of the differentiating cells and induce a caudalization of cell identity based on gene expression profiles [25,28]. The genes found to be induced under the influence of RA included several *Hox* genes, and *in vivo* studies report the caudalization of neural structures under the influence of retinoic acid during development, indicating that ESC neural differentiation may provide a reliable cell source for region specific nervous system repair in the future [34-36].

While embryonic stem cells may provide a cell source capable of indefinite self-renewal *in vitro*, with differentiation characteristics similar to those observed *in vivo*, there are significant ethical concerns regarding collection and use of human embryonic stem cells [37-38]. Some of the strongest resistance comes due to the fact that deriving human embryonic stem cells from the ICM involves destroying the embryo. Recent developments in somatic cell reprogramming towards an ESC-like state offer one approach to overstep this ethical hurdle [39].

1.4 Induced Pluripotent Stem Cells

Early experiments involving the transfer of somatic cell nuclei into enucleated oocytes demonstrated the generation of genetic clones [40]. It was observed that

unidentified factors within the enucleated oocyte were able to influence the state of the somatic nucleus toward that of a more primitive pluripotent state. In 2006, Takahashi and Yamanaka reported their findings that a set of four genes (*Oct4*, *Sox2*, *Klf4*, *c-Myc*) were capable of reprogramming mouse embryonic or adult fibroblasts into a pluripotent state, when introduced by retrovirus vectors [3]. The technique was subsequently performed in human cells [41], but recognizing the risks of viral integration, alternative reprogramming approaches have since been developed including plasmid transfection, episomal vectors and direct transduction of chimeric proteins [42-44]. There are now numerous ways to de-differentiate somatic cells into what are known as induced pluripotent stem cells (iPS cells).

It has also been shown that less differentiated cell types, although difficult to isolate, are more readily reprogrammed to an ESC-like state than differentiated cells. Experimental results have shown a higher number of successful reprogramming events and the need for introducing fewer reprogramming factors when generating iPS cells using less differentiated cells [45-47]. These findings suggest that there are intrinsic programs determining the extent of differentiation regardless of tissue type, and that less differentiated cells can be more easily reprogrammed to the pluripotent stem cell state.

The concept of iPS cells was a significant advancement for the field of regenerative medicine as it provided a source of pluripotent cells that did not require the destruction of a blastocyst. This removes a considerable ethical hurdle in the pursuit of pluripotent stem cell based therapies. Other advantages include their ability to generate patient specific stem cells that can be differentiated into specific cell types to recapitulate diseased cell phenotypes or provide a cell source for autologous transplants. The advantage of

autologous cell transplants is that there is a reduced chance of immunoresistance to the therapy as compared to exogenous cell transplants. Challenges thus far include the efficiency of reprogramming and the quality of the reprogrammed cells [41,48-49]. The success rate in producing iPS colonies is very low and there is mounting evidence that the gene expression profile is actually very different from embryonic stem cells [50-52]. This means that data generated in the ESC field will not necessarily apply to iPS cells and all experiments must be repeated to best describe each pluripotent stem cell source. Data from neural stem cell research such as ours will provide an excellent comparison for pluripotent cells being used for neural differentiation. The primary neural stem cells used in our lab progress through embryonic development, acquiring their neural lineage restriction and genetic programming *in vivo*.

1.5 Transdifferentiation and Cell Plasticity

Transdifferentiation or lineage conversion refers to the capacity of cells from one lineage to directly convert to functional cells of another lineage, without reprogramming through a pluripotent state. Studies in this field are gradually revealing the true extent of cellular plasticity. Examples of this include the following: forced expression of neural-lineage-specific transcription factors *Ascl1*, *Brn2* and *Myt1l* converted fibroblasts into neurons [53], the same combination of factors convert differentiated hepatocytes to neurons [54]. The conversion of fibroblasts into brown fat cells and contracting cardiomyocytes has been achieved using specific combinations of transcription factors [55-57]. Transcription factors in particular have a significant influence on cell phenotype with respect to fate specification and lineage potential. This is likely due to the ability of these proteins to directly influence gene expression, which makes their activity more efficient than for

example, a protein that works upstream of a signalling cascade. This is why our investigation into the genetic programming of neural stem cell fate decisions centers around transcription factors. Furthermore, the homeobox transcription factors are well recognized for their essential roles in early development and cellular identity. This includes specification of cells within the central nervous system [58].

1.6 Central Nervous System Patterning

At approximately one week post fertilization of the mouse oocyte, gastrulation occurs in the developing mouse embryo. This is a process of cellular rearrangements and tissue folding in the blastula and defines the endoderm, mesoderm and ectoderm. All subsequent tissues of the adult mouse are traceable back to these three germ layers or lineages. Cell lineages derived from the endoderm include those of endocrine glands as well as epithelial linings of the digestive and respiratory tracts. The mesoderm gives rise to connective tissue, muscle, and bone, and the ectoderm gives rise to the epidermis and nervous system [13]. Positional identity along the anterior-posterior axis, in the mesoderm and ectoderm is specified by homeobox genes. These are highly conserved developmental genes, with axial patterning roles retained throughout evolution from fruit fly to humans [58]. During the gastrulation process, the neural plate structure is specified from the ectoderm on the dorsal surface of the embryo. It is from the neural plate that all cells of the nervous system are derived. Near the end of gastrulation the neural plate folds into the neural tube and during this time neural crest cells migrate away from the neural tube. Neural crest cells give rise to the peripheral nervous system and the neural tube gives rise to the central nervous system: the brain and spinal cord [13]. Neural tube induction in vertebrates has been linked to FGF signalling and inhibition of bone

morphogenic protein (BMP) signalling [13,59-61]. It is within the neural tube that a succession of spatial and temporal specification events regionalizes the primordial central nervous system along dorso-ventral and anterior-posterior axes [62-63].

The floor plate of the neural tube, situated above the notochord, actively expresses sonic hedgehog (SHH) and receives retinoic acid (RA) input from the adjacent mesoderm. The concentration of factors secreted from the floor plate decreases towards the dorsal neural tube or roof plate. These inputs promote the specification of motoneurons from the ventral neural tube [64-65]. The number of neurons generated is further influenced by WNT protein signalling, which appears to occur in a gradient descending from the dorsal to ventral neural tube [66]. The dorsal plate secretes BMP4 and BMP7 which are required for specification of dorsal interneurons [67]. The concentrations of BMP decrease when approaching the ventral neural tube from the dorsal plate source (Fig. 2(A)). These opposing molecular gradients are critical for dorso-ventral patterning of the spinal cord and the neuronal networks derived from here. The anterior-posterior patterning of the spinal cord is initiated by FGF signalling in the neural tube, which is strongest in the caudal regions and weaker progressing rostrally [68]. FGF signalling stimulates *Hox* gene expression which is also influenced by RA signalling in the anterior spinal cord [69-70]. These signals establish the expression profiles of transcription factors such as HOX and homeodomain proteins of the LIM (named after Lin11, Isl-1 and Mec-3 proteins) family, which then specify neuronal identity along the anterior-posterior axis [71-72].

1.7 Forebrain Development

Neural tube regionalization gives rise to the forebrain, midbrain, hindbrain and spinal cord regions. Within these regions primitive cells of the neurectoderm lineage exist, which exhibit mixed degrees of differentiation potential and propensity for self-renewal [73]. The stem and progenitor cells within this region are responsible for constructing the vertebrate nervous system. The region of the neural tube adjacent to the ventricle (lumen) is known as the ventricular zone (VZ). The VZ is a region of cell proliferation and contains the neural progenitor cells that generate neurons and glia, the two main cell types of the nervous system. In the telencephalon (anterior forebrain) region of the neural tube, the VZ lines the lateral ventricles, where the multipotent neural progenitor cells are situated. Cells isolated from the VZ have the capacity to self-renew and differentiate into the three main cell lineages of the nervous system [74-75]. These are the properties that define neural stem cells.

The dorsal region of the telencephalon is the pallium and the ventral region is called the subpallium. Distinct progenitor cell populations in these regions give rise to the cerebral cortex, and the striatum which includes the lateral (LGE) and medial (MGE) ganglionic eminences under the guidance of transcription factors [76]. As early as E8.5 in mouse embryos, *Pax6* expression is detectable in progenitor cells of the pallium. Transcription factors such as NGN2, DBX, TBR1 and TBR2 accompany PAX6 in defining pallial progenitors, versus subpallial progenitors that are actively expressing the transcription factors GSX2, NKX2.1, DLX1, DLX2, VAX1, MASH1 and SIX3 among others (Figure 2.(B)) [77-83]. These transcription factors actively maintain regional identity

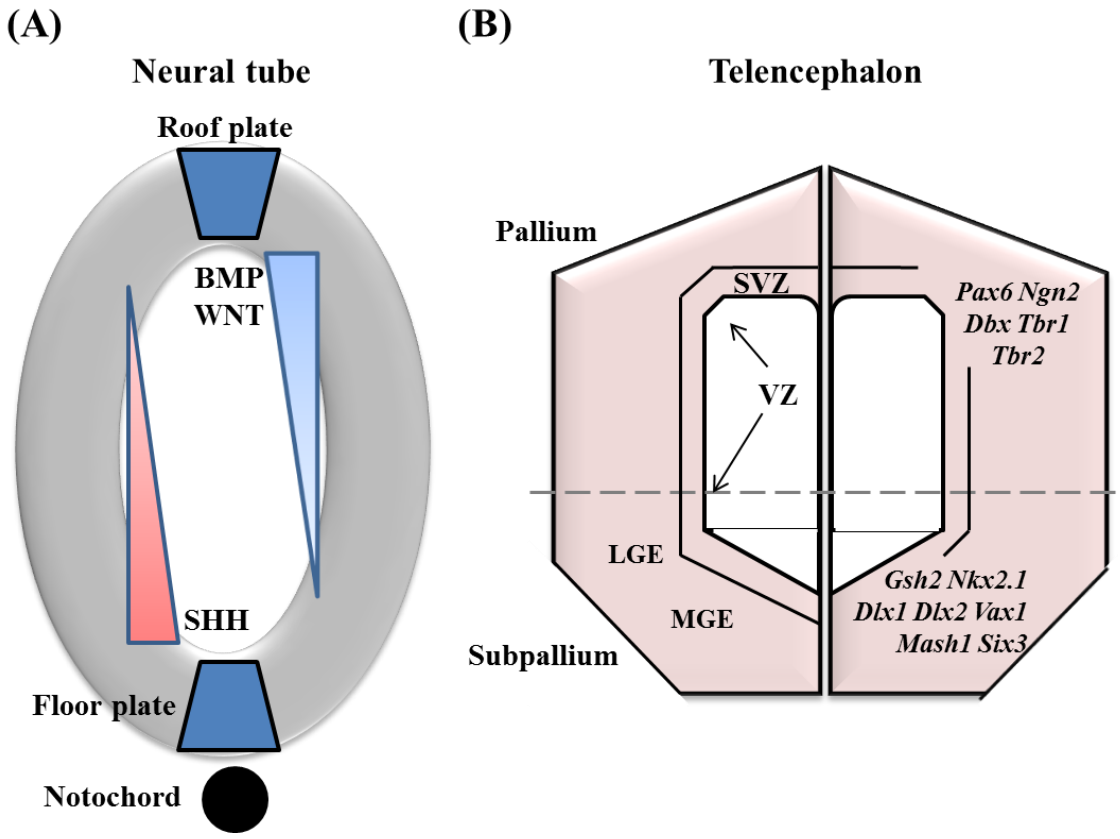

Figure 2. Early development of the vertebrate central nervous system. Morphogen gradients establish the identity of cells in the dorsal-ventral axis of the developing neural tube (A). These include BMP and WNT from the roof plate and SHH from the floor plate. Restricted expression patterns of transcription factors in the dorsal-ventral axis of the developing telencephalon establish the identity of progenitors that develop in the forebrain (B).

of progenitor spatial domains. *Pax6* and *Gsh2* appear to be particularly important in maintaining the pallial-subpallial interface. PAX6 is concentrated in the pallium but expression also overlaps with GSH2 in the dorsal most region of the subpallium. In *Pax6*$^{-/-}$ embryos, the subpallial transcription factor expression boundaries are lost and there is a loss of physical distinction between pallium and subpallium, with lateral ganglionic eminences developing at the cost of ventral pallium [81]. In *Gsh2*$^{-/-}$ embryos, there is a ventral expansion of pallial gene expressing cells at the cost of subpallial gene expressing cells from the striatum [78]. It has been proposed that the mechanism by which transcription factors maintain regional boundaries is by regulating expression of extracellular proteins such as cadherins, which regulate cell-cell adhesion [84].

Some of the progenitor cells lining the ventricles include the so-called radial glial (RG) cells because of characteristics that are shared with glial cells, and a radial morphology that includes processes reaching from the ventricles to the cortical plate [85]. In the mouse embryo, corticogenesis begins at approximately E9 and at this time the neurepithelial cells of the VZ undergo morphological changes. The cell body remains in the ventricular zone but processes maintain contact with ventricular and pial surfaces, and in doing so elongate as neurogenesis ensues. These processes provide the scaffold for neuronal migration from the ventricular zone into the cortical plate [86-87]. During the neurepithelial to radial glia phenotypic change, the cells also begin to express astroglial markers GLAST, BLBP, RC1, RC2 and TN-C, and neurepithelial tight junctions are replaced by adherens junctions [88-90].

The RG cells of the ventricular zone undergo either symmetric or asymmetric rounds of division. Symmetric divisions increase the pool of progenitors, and asymmetric

divisions maintain the progenitor pool, while also generating neurons at first and then glial cells as development proceeds. Forebrain development proceeds by generating consecutive layers of neurons on top of the ventricular layer. Neuronal progeny of asymmetric divisions are post-mitotic and migrate outward from the luminal lining to establish what is called the pre-plate [86]. The pre-plate is a sheath of neurons and each subsequent layer of neurons derived from the VZ migrates outwards to situate itself between two cell layers of the pre-plate. The multiple layers that are generated between the pre-plate layers are known as the cortical plate. The mammalian cortex is ultimately composed of six identifiable layers that are generated through repeated rounds of cell divisions and migrations from the ventricular zone. Dividing radial glia cells can give rise to neurons directly or *via* intermediate progenitor cells (IPC) that divide symmetrically, but are lineage restricted, giving rise to either two IPCs or two neurons. Neuronal IPCs occupy the embryonic subventricular zone (SVZ) and contribute to the process of neurogenesis [91]. Evidence suggests that NOTCH signalling activated by the surrounding cells antagonizes differentiation and maintains the proliferative state of the progenitor cells as well as radial glia [92-93].

1.8 Neural Stem Cells

Neural stem cells are the founding cells of the functional nervous system. These cells exhibit the properties of multipotent stem cells capable of self-renewal and differentiation into multiple cells types including neurons, astrocytes and oligodentrocytes that comprise the nervous system (Fig. 3) [94-95]. Recent studies have revealed that NSC have more

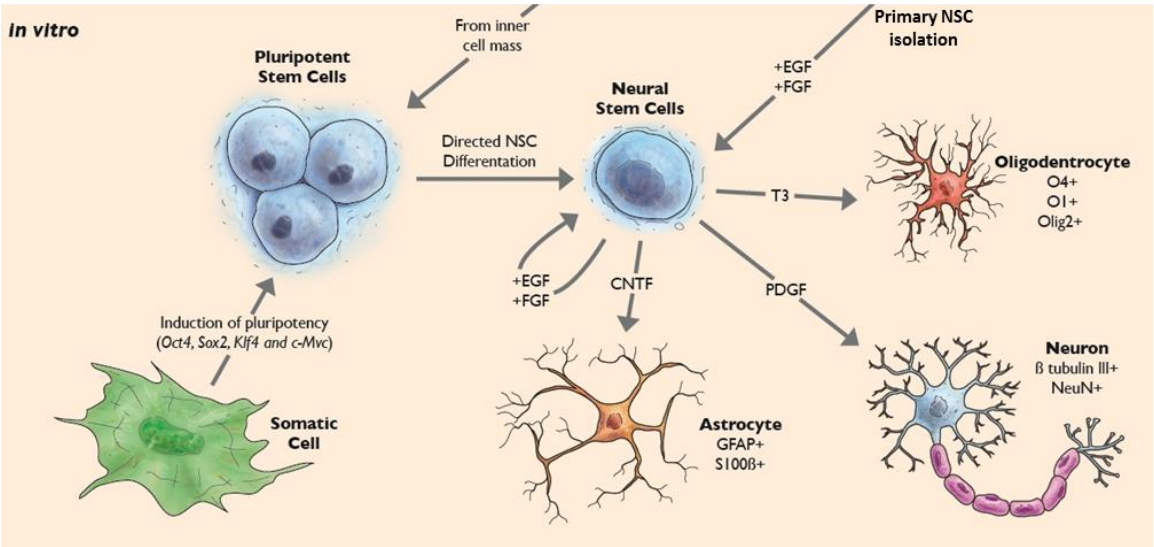

Figure 3. Neural stem cell differentiation in vitro. Neural stem cells can be derived from the embryonic or adult organism as well as pluripotent stem cells. Neuronal and glial differentiation can be promoted by the addition of different factors and subsequently identified by their expression of specific cell type markers. (*Olynik and Rastegar, in revision, 2012.*)

plasticity than originally presumed, and that given the correct combination of inductive cues, may be driven towards other lineages as well [96-98]. However, *in vivo* the developmental role of NSC is restricted to the nervous system. In the adult, there remains multipotent NSC within the nervous system, capable of continuous neurogenesis. These cells are localized to specific niche regions that provide the appropriate environment for survival and preventing differentiation [99]. Within the adult forebrain region, there are two main regions where neural stem cells reside; these are the SVZ and the dentate gyrus (DG) of the hippocampus [100-101]. The hippocampus is responsible for learning and memory, and neurogenesis here is presumed to be involved in memory formation [102]. Studies have shown that the rate of new neurons being born has associations with the time of day as well as participation in learning tasks [103-105]. In the adult brain, the SVZ is the main site of neurogenesis. New neurons born here migrate to the olfactory bulbs to replace interneurons which frequently turn over [86].

The ventricular walls of the lateral hemispheres, particularly during development, provide a rich source of NSC to be studied. Both the ventricular zone and the subventricular zone are very complicated regions with respect to the extracellular environment, which includes vasculature, cerebral spinal fluid and a mix of different cell types performing distinct functions [106]. This is in addition to the inherent complexity of neural stem cells that respond differently to stimuli depending on the stage of development. An example of this is BMP signalling in early development, which promotes the formation of neurons, while later stage BMP signalling encourages glial differentiation from progenitors [107-108]. *In vitro* cell culture conditions do not recapitulate this environment. However, providing the minimum means necessary to support the

neural stem cells generates an excellent model system to study gene expression patterns involved in the environmental response and phenotypic changes of the cells. For example, NSC can be cultured and subsequently differentiated along specific lineages, given the correct inductive cues, and the gene expression profiles can be assayed during acquisition of various cell fates. Previous studies have been effective in identifying signalling pathways and transcription factors important for NSC self-renewal and differentiation [109-111].

Neural stem cells can be cultured in monolayer or as floating aggregates called neurospheres. The dissociated cells of dissected embryonic VZ/SVZ are cultured in serum free media with the supplemented mitogens fibroblast growth factor 2 (FGF2) and epidermal growth factor (EGF). Monolayer culture requires an adhesive coating such as fibronectin, while neurospheres are generated in uncoated cell culture plates. The proliferation rate is higher in neurospheres which is advantageous for conducting experiments that require cell bulk [112]. However, a disadvantage is that the composition of neurospheres is difficult to analyse due to their large cluster formation. The neurospheres are heterogeneous, composed of NSC, progenitors and more differentiated cell types [113]. Still, as a functional assay the neurosphere culture has significantly impacted our current knowledge about NSC regulation. Serial passaging and limiting dilution assays are quite effective for measuring proliferation and self-renewal capacity of neural stem cells [114-115]. Serial passaging involves passing the cells indefinitely while measuring the frequency and size of neurosphere formation in culture. The limiting dilution assay involves determining the minimum number of cells required to produce a specific number or frequency of neurospheres. The impact of exogenous factors or expression levels of

particular genes can be correlated with outcomes in these assays, to see how these variables impact NSC self-renewal. The multipotency of NSC can also be assayed by placing neurosphere cells into differentiation conditions with or without first dissociating the spheres. When mitogen is withdrawn and serum is added to the culture, differentiation ensues, producing neurons, astrocytes, and oligodendrocytes [116].

There are variations of differentiation protocols that have been found to influence lineage acquisition. Neuronal differentiation can be promoted by including platelet derived growth factor (PDGF) in the cell culture media. Including thyroid hormone T3 has been shown to promote oligodendrocyte differentiation, and ciliary neurotrophic factor (CNTF) supports astrocyte differentiation [117-118]. The developmental stage of NSC isolation can influence lineage output. Neural stem cells harvested earlier, during periods that correspond with neurogenesis (E10) in the developing mouse give more neurons upon differentiation, whereas NSC isolated from the gliogenic period (E14) give rise to more astrocytes proportionally [119]. Neurospheres differentiated as aggregates also generate more neurons whereas dissociated cells in monolayer generate more astrocytes proportionally. The manipulation of intrinsic factors has also been achieved using viral vector transduction to induce lineage specific gene expression programs and promote differentiation of specific neuron subtypes [120-121].

The intrinsic identity of neural stem cells also appears to have a significant impact on the character of differentiated cell types, including their gene expression patterns and capacity to integrate upon transplantation. Lineage tracing experiments using reporter mice have revealed distinct NSC populations that give rise to specific progeny and replacement cells for specific regions of the central nervous system [122-123]. It has been

shown that primary NSC retain a spatial identity based on the region of the nervous system from which they are isolated, even after *in vitro* expansion. Upon transplantation, however, neural stem cells have been reported to either retain their regional identity, giving rise to the same cells regardless of where they are transplanted [124], or respond to local inductive cues to generate neurons specific to the site of transplantation [125-126]. Other studies have shown that the degree to which neural stem cells retain their regional identity in culture depends on the culture conditions [125,127-128].

The character of a neurosphere is quite variable depending on many factors. Developmental stage of the host, tissue of origin, cell confluency, sphere passage number, media composition and the frequency of media replacement may all influence the neurospheres either genetically or functionally [126,129-133]. It is therefore very important to maintain consistency within an experimental set for comparison between experimentals and controls.

Neural stem cells may be propagated in culture to generate vast quantities of cells with the ability to differentiate into the different cell types of the nervous system. These properties make NSC arguably the best source of material for potential cell-based therapies targeting the nervous system. The endogenous plasticity of the CNS provides some optimism that primary or ESC-derived neural stem cells expanded *in vitro* will be able to contribute to tissue regeneration under the influence of the local environment. Endogenous progenitors have been shown to proliferate and generate new hippocampal neurons in response to ischemia [134], oligodendrocyte precursors proliferate and differentiate more rapidly in regions of neurodegeneration in amyotrophic lateral sclerosis mice [135], and quiescent astocytes begin to proliferate and differentiate into glia

upon injury [136]. Transplantation experiments in rodents have shown promising results for the ability of local tissue to accept and integrate transplanted neural stem cells. Examples include neural progenitors transplanted into rat hippocampus, where the cells integrated as region-specific neurons and were functional. Neural stem cells also differentiated at lesion sites in rodent models of multiple sclerosis, brain ischemia and haemorrhage. Such transplant experiments have even reported cases of functional recovery in the animal model, including motor recovery in spinal cord injury [137-140].

Translation to the clinic has been hampered by the complexity of these cells and challenges in controlling other types of stem cell based therapies [141-143]. A more complete description of the genetic programs behind NSC self-renewal and lineage specification will better enable us to develop protocols for cell selection, integration, and transplant assessment. Neural stem cells have great potential with respect to regeneration and repair. Stem cell-based therapy in the haematopoietic system has yielded positive results for years [144]. A thorough assessment of the genetic programming in proliferating and differentiating NSC is essential before attempting NSC-based therapy, so as to prevent any potential negative consequences for the patients.

1.9 Neural Stem Cell Signalling Pathways

Specific cell signalling pathways have been documented to influence neural stem cell fate. For instance the EGF and FGF pathways promote NSC survival and propagation [145]. The NOTCH signalling pathway acts to antagonize NSC differentiation, though further studies are required to delineate the specific roles of each ligand and receptor variant belonging to this pathway [146]. Activation of the PDGF and vascular endothelial growth

factor (VEGF) pathways is known to promote oligodendrocyte generation and NSC migration respectively, while BMP activity is associated with astrocyte versus neuronal lineage commitment [108,147-148]. Temporal and regional context influence how cells respond to these signalling pathways. This makes it important to investigate the role of these pathways at different stages of development, in NSC located in different regions, and during differentiation of the neural stem cells.

NOTCH signalling. Vertebrate Notch signalling involves direct cell-cell interactions through four receptors NOTCH1-4, which interact with ligands of the delta-like ligand (*Dll*) and jagged (*Jag*) family Dll1, Dll3, Dll4, JAG1 and JAG2. Upon interacting with the ligand, the notch receptor is cleaved extracellularly by a metalloprotease TACE, and intracellularly by gamma-secretase. The cleavage by gamma-secretase at the internal cell membrane releases NOTCH intracellular domain (ICD) from the transmembrane portion of the receptor, which then translocates to the nucleus to activate NOTCH target genes. In the nucleus, ICD recruits transcription activators to convert the CSL (suppressor of hairless) mediated transcription repressor complex into a transcription activator [149]. *Notch* is associated with neural progenitor maintenance and it is believed this occurs by preventing differentiation. It is proposed that maintenance of the progenitor pool occurs through a process known as lateral inhibition. When a mother cell divides asymmetrically during neurogenesis, a differentiating daughter cell expressing NOTCH ligands is produced and interacts with NOTCH receptors on the other daughter progenitor cell to antagonize differentiation and maintain a progenitor state. This lateral inhibition ensures that a sufficient pool of progenitors is maintained to generate the quantity of cells necessary for CNS development. This concept was well described in *Drosophila*

melanogaster notch signalling originally [150-151] and since then in NSC neurogenesis [152-154].

Target genes of NOTCH signalling include HES1 and HES5 protein encoding genes, which are active in neural stem cells. HES1 and HES5 are bHLH transcription factors and have been shown to suppress neurogenesis by silencing proneuronal bHLH transcription factors such as *Mash1* and *Neurogenin* [155]. In promoting this cascade of events, NOTCH signalling prevents neuronal differentiation in favour of NSC maintenance, but also permits astrogliogenesis. If NOTCH signalling is impaired through loss of *Notch*, *Hes1* or *Hes5*, the result is premature neuronal differentiation and impaired proliferation. The effects of NOTCH signalling in neural stem cells are dependent on *Hes1* and *Hes5*. Mice lacking these genes do not have progenitor maintenance restored with constitutively active NOTCH signalling [156].

Bone Morphogenic Protein (BMP). BMPs are secreted proteins belonging to the TGFβ superfamily of secreted polypeptide growth factors. They are ligands of serine-threonine kinase receptors types I and II. Upon interaction with receptor heteromers, there is a transactivation between receptors and a cascade ensues whereby SMAD proteins are activated and translocate to the nucleus to regulate gene transcription. Myriad cellular processes are influenced by these pathways [157]. In mouse embryonic stem cells, the BMP4-SMAD cascade works to antagonize differentiation *via* Id (inhibitors of differentiation) proteins [158]. In the early embryo, opposing gradients of SHH and BMP work to pattern the neural tube. These factors act as morphogens evoking different developmental responses based on their concentrations. The signalling activities regulate transcription factors that work to specify neuronal cell types in the developing nervous

system. BMP signalling has been shown to have an effect on NSC differentiation towards neurons versus oliogodendrocytes. See *et al.* observed reduced astrocyte differentiation of NSC in BMP-receptor double knockout mice [159]. Increasing BMP7 levels has been shown to drive astrocyte differentiation from radial glia in embryonic mice. The same group revealed that *in vivo* BDNF instructs neurons to express BMP7 which then contributes to the gliogenic phase of radial glia in embryos midgestation [160]. *In vitro,* BMP4 induces neurosphere adhesion, astrocytic differentiation, and migration [161].

1.10 Homeobox Genes

The homeobox is a well conserved 180 base pair deoxyribonucleic acid (DNA) sequence that encodes for the 60 amino acid homeodomain common to all of the homeobox gene superfamily of transcription factors. The homeodomain structure includes three alpha helices involved in DNA binding, with one helix sitting in the DNA major groove and the other two helices lying over top, providing stability and indirectly participating in the DNA binding function [162-163]. The homeobox superfamily is comprised of clustered *Hox* genes and other non clustered homeobox genes. *Hox* genes are distinct from other homeobox genes based on their linear arrangement in paralog groups that are found within clusters on separate chromosomes. The 39 mammalian *Hox* genes are arranged in 13 paralog groups in four clusters. *Hox* genes exhibit spatial and temporal collinear expression. Genes located more 3' in a cluster are expressed earlier and more anteriorly along the anterior-posterior axis. Genes situated more 5' in each cluster are expressed later and more posteriorly [58].

Homeobox genes are master regulators of development and *Hox* genes are essential in axial segmentation of the developing embryo, providing instructions for cell identity, survival, apoptosis and differentiation [164-169]. These genes were originally discovered when their misexpression was found to be the cause of homeotic transformation in *Drosophila*. A homeotic transformation is an event whereby aberrant gene expression causes a segment of an embryo to take on the identity of another [170-171]. *Hox* genes are also involved in proximal distal patterning of developing limbs in vertebrates [172-174].

Functional redundancies are common among *Hox* genes, making it difficult to study the role of these genes through overexpression or knock down experiments. Overlapping expression patterns of HOX proteins has revealed a posterior dominance or phenotypic suppression effect. This concept describes the situation where HOX proteins derived from more 5' paralogs can overrule the instructions of more 3' situated HOX when generating spatial phenotype [175-176]. Recent work has revealed that DNA elements that are mutually targeted by several HOX proteins will be occupied by the HOX protein that has a stronger association with the DNA-binding cofactor(s) when situated on the DNA. In the fly it was shown that the HOX ortholog *AbdA* has a motif that is absent in the ortholog *Src*, which enables it to form more stable complexes with the DNA binding cofactor Exd at the DNA recognition sequence [177].

The recognition sequence for HOX proteins is a simple ATTA/TAAT motif, which is found frequently throughout the genome, making the identification of specific HOX-DNA targeting rather challenging. The interaction with cofactors such as PBX (*Exd*) and MEIS (*Hth*) has been shown to influence the specificity of HOX DNA binding and has aided in identifying some of the target genes that are regulated by HOX transcription

factors. It has been shown that multimer complexes of these proteins impact DNA binding affinity for specific sites and transcriptional activity [178-182].

The most anterior region of *Hox* activity in the developing mouse is the hindbrain region. Correct expression of *Hox* genes is essential for proper segmentation of the hindbrain into regions of distinct gene expression profiles that develop into the rhombomeres, which are the site of origin for specific cranial nerves belonging to the peripheral nervous system. Aberrant *Hox* expression in this region leads to craniofacial abnormalities that are traceable back to incorrect segmentation of this region [183-185]. *Hox* gene expression occurs posteriorly from the hindbrain and throughout the spinal cord. Neural stem cells that are derived from different regions of the CNS maintain a regional identity and this is reflected in the *Hox* profile of the cultured cells [126]. Interestingly, RA induced neuronal differentiation of embryonal carcinoma P19 cells activates expression of *Hox* genes, despite having no CNS regional identity [181,186]. This begs the question whether *Hox* expression may be induced in differentiating NSC derived from *Hox*-free regions. Due to their strong association with specifying cell identity, the *Hox* family of transcription factors are a good benchmark to compare cells cultured *in vitro* to their *in vivo* counterparts, for which they are raised to replace in stem cell therapy.

1.11 TALE Proteins

The name three amino acid loop extension (TALE) protein is derived from an extra three amino acids in the loop between helix 1 and 2 of the homeodomain in this family of homeodomain transcription factors. The TALE genes are further categorized into subfamilies based on the conservation of their sequences. Two of these subfamilies are the PBC or PBX and the MEINOX or MEIS/PREP families. TGFβ-induced factor (TGIF) proteins form a third subfamily of the TALE factors; however, they are not known as cofactors of HOX transcription factors [187]. PBC and MEINOX proteins commonly participate in transcription factor dimers and multimers cooperatively with HOX proteins, whereby the TALE proteins provide complimentary DNA binding specificity. PBX1 interacts with HOX paralogs 1-10 while MEIS1 interacts with paralogs 9-13 [188-189]. These proteins have important roles in providing regional information and axial patterning. But they are also important for cell proliferation, differentiation and organogenesis [190-193].

PBX is the conserved mammalian ortholog of *Drosophila Exd* [194]. Originally PBX was identified in pre-B cell leukemia due to a chromosomal translocation that generated the E2A-PBX1 fusion protein [195-196]. The mammalian homologs include PBX1-4 [197-198]. *Pbx1* and *Pbx3* null mice die at E15.5 and soon after birth, respectively. *Pbx1* null mice exhibit a wide array of hypoplastic organ phenotypes due to loss of cell proliferation and aberrations of peripheral nervous system development, while *Pbx3* null mice die specifically of respiratory failure [199-200]. Long-term survival is unaffected in *Pbx2* null mice and they display no detectable abnormalities [201]. *Meis1* has a known role in leukemia stem cell self-renewal [202].

MEIS/PREP proteins are orthologs of *Drosophila Hth* [203]. *Meis1* was originally isolated as a viral integration site for murine leukemia virus in BXH-2 mice [204]. Mammalian homologs include *Meis1-3* and *Prep1-2*. Studies in *Meis1* knock out mouse models have shown that *Meis1* is essential for development and embryos survive to maximum gestation of E14.5. Defects occur in eye development, maintenance of definitive hematopoiesis, and angiogenesis [205-206]. Expression profiling of *Meis2* suggest it may have a role in development of the forebrain striatum [207-208], the midbrain [209] and the retina [210]. *Meis3* is involved in vertebrate hindbrain patterning [211-213]. The *Prep1*$^{-/-}$ knockout mouse is embryonic lethal at around embryonic day E7, when cell expansion fails to proceed due to *p53*-dependent apoptosis [214]. Mice homozygous for a hypomorphic *Prep1*$^{i/i}$ mutation reveal that *Prep1* functions as a tumor suppressor and maintains genomic stability [215-218]. *Prep2* mRNA has been detected in mouse oocytes and shows a restricted expression pattern in adult mouse tissues [219-220]. A function for PREP2 has yet to be verified; however, PREP2 dimerizes with PBX proteins, and is expressed in multiple isoforms that show regulated subcellular localization dependent on cytoskeletal systems [220-221].

It is well documented that *Pbx1*, *Meis1*, *Prep1* and *Prep2* are expressed in the brain [207,220,222]. In contrast, no information exists regarding TALE expression in neural stem/progenitor cells or their differentiating progeny. Of these genes, only *Pbx1* a definite role *in vivo* that relates to neurogenesis[223224224]. PBX1 has been observed in the caudo-rostral migratory tract of rats, where it is expressed in migrating and maturing neurons that are bound for the olfactory bulb [223]. Both PBX1 and MEIS1 are expressed in the VZ and SVZ of the developing mouse brain, which houses neural stem cells [207]. The

exact location and timing of PREP1 and PREP2 protein expression in the central nervous system has yet to be studied.

1.12 TALE Protein Expression and Function

Independent mutations involving PBX1 and MEIS1 proteins are associated with leukemia. The chimeric E2a-PBX1 protein causes pediatric pre-B cell leukemia and can induce myeloid and T-lymphocyte leukemia in mice [224-225]. MEIS1 is commonly over-expressed in acute myeloid leukemia (AML) and acute lymphoblastic leukemia (ALL), which is associated with HOXA9 deregulation [226-229]. In addition MEIS1 over-expression is capable of accelerating leukemogenesis and its levels are associated with hematopoietic stem cell self-renewal [230]. The *Pbx1*$^{-/-}$ mouse displays severe anemia and a reduction in hematopoietic progenitor proliferation. In human adipocyte progenitors, loss of PBX1 reduces proliferation and promotes adipocyte differentiation. Reduced progenitor proliferation has also been observed in chondrocytes and in the spleen anlagen during skeletal and spleen development, respectively, in association with reduced PBX1 activity [231]. These findings suggest a potential role for the TALE factors in regulating stem cell phenotype that is not specific to tissue type.

There is a high degree of cooperation and interdependence among TALE and HOX proteins. The earliest evidence of this came from observations that mutations in *Exd* lead to homeotic transformations in *Drosophila* [232-233]. Early studies on PBX/MEIS interactions have revealed that in certain cell types, dimerization occurs in the cytoplasm, which is required for PBX translocation into the nucleus and subsequent interactions with HOX proteins [234-237]. However, recent studies have shown that PBX1 nuclear localization

can occur independent of interaction with MEIS. Other determining factors of subcellular localization are PBX1 phosphorylation state, which can be regulated by Protein Kinase A, and cell cycle stage [238-239]. There also appears to be cross-regulation of protein levels between the TALE proteins. In F9 cells, PREP1 stabilizes PBX2 by decreasing its proteasomal degradation [240]. In *Prep1*$^{i/i}$ mutant mice, reduced PBX1, PBX2 and MEIS1 protein levels are observed relative to wild type, but there are no differences in the mRNA levels detected [192].

MEINOX and PBX also interact in complex with DNA. Together, MEIS1 and PBX1 interact with the promoter of *Sox3* to regulate its expression in NT2/D1 cells [241]. In pre-B cells a specific DNA element is bound by PBX1/MEIS1 and PBX1/PREP1 dimers, but the E2a-PBX1 fusion significantly decreases the formation of these dimers as well as their association with this DNA element [242]. Dissection of the *Hoxb1* auto-regulatory enhancer has revealed multiple PBX-HOX and PBX-MEINOX binding sites. *In vivo*, the combinations of these sites have been shown to modulate reporter expression in transgenic mice and chick embryos. TALE dimers composed of PBX1-MEIS1 and PBX1-PREP1 can interact at these DNA sites, as well as dimers of PBX1-HOX proteins. Furthermore, ternary complex formation has been detected, involving PREP1-PBX-HOXB1, which has demonstrated sensitivity to retinoic acid [179,243-245]. Oncogenic roles for specific HOX proteins also rely on interactions with TALE proteins. HOXA9-TALE complexes have been isolated from leukemic cell lines, and these protein associations are required for HOXA9 immortalization of myeloid progenitors [246]. An oncogenic role for HOXB7 in human breast cancer is dependent on interaction with the correct TALE cofactors, and oncogenicity of HOXA1 relies on interaction with PBX1 [247-248]. It is also

known that over-expression of MEIS1 accelerates lukemogenesis induced by HOXA9, and this is dependent upon the C-terminal transactivation domain of MEIS1. A chimera composed of the MEINOX protein PREP1 and this domain confer leukemogenic properties upon PREP1 [249].

Retinoic acid regulates the activation and expression of *Hox* and TALE developmental programs that include multimers, cross-regulation and autoregulatory feedback loops. These gene programs are complicated even further by the recent discovery of HOX and TALE regulation of RA synthesis. In mouse embryos, retinaldehyde dehydrogenase-2 (*Raldh2*) codes for an enzyme responsible for RA synthesis [250-251]. In *Pbx1/Pbx2* null mice and *Hoxa1/Pbx1*-deficient embryos there are reduced levels of *Raldh2* and RA activity. It was recently discovered that a HOXA1-PBX1/2-MEIS2 complex binds a *Raldh2* regulatory element *in vivo* and this element is required for the appropriate transcriptional regulation of *Raldh2* [191].

Despite the neural expression patterns *in vivo* and *in vitro*, it has been shown that PBX1 is dispensable for neural differentiation of mouse embryonic stem cells [252]. The undefined involvement of PBX1 in neurogenesis makes *Pbx1* a target of interest to investigate the mRNA and protein expression patterns in neurospheres and differentiating neural stem cells. The patterns of MEINOX expression in this system is of interest due to their CNS expression patterns and developmental roles.

In vitro culture of primary NSC provides an opportunity to investigate the expression patterns and roles of specific genes during neurogenesis. The results of such experiments, however, must be considered as context specific due to the sensitivity and

variation among NSC sources and culturing methods. As previously mentioned, the effects of cell signalling molecules in vivo, for example, are dependent on the stage of embryonic development. Our current knowledge about the roles of TALE genes lead us to believe that our study, investigating the expression patterns of TALE genes during NSC differentiation, will result in novel findings with significance to CNS development and cell based therapeutics. These genes have important roles in development and stem cell regulation. The data we generate will provide the foundation for functional studies regarding the role of TALE genes in NSC fate decisions and forebrain development.

TALE gene	Lethality	Forebrain expression	Cell proliferation or stem cell aberration
Pbx1$^{-/-}$	E15.5	✓	✓
Pbx2$^{-/-}$	Non-lethal	✓	
Pbx3$^{-/-}$	Perinatal	✓	✓
Meis1$^{-/-}$	E14.5	✓	✓
Meis2$^{-/-}$	?	✓	✓
Meis3$^{-/-}$	?	?	✓
Prep1$^{-/-}$	E7	?	✓
Prep2$^{-/-}$	?	?	

Table 1. TALE gene knockout mouse model phenotypes. The lethality of TALE gene knockout models make primary NSC culture a viable alternative to study the roles of these genes in neural development. The majority of these genes are expressed in the developing forebrain and have roles in cell proliferation and stem cell regulation, making them genes of interest for forebrain NSC regulation.

2.1 Rationale

Neural induction of pluripotent ESC and embryonal carcinoma cells using retinoic acid leads to activation of *Hox* and TALE genes. Modulating the expression of these genes influences ESC-derived neural stem cell fate decisions as well as their essential roles in central nervous system development [191,243,253]. Aberrant expression of homeobox genes for instance is associated with developmental abnormalities including homeotic transformations, hypomorphic organs and human cancer including forebrain-derived tumors [170,199,254]. Phenotypes such as these strongly suggest aberrations in stem cell fate determination and proliferation. TALE proteins have been detected in the developing forebrain, including the VZ and SVZ, where neural stem cells and transient amplifying progenitor cells exist [207]. *Hox* gene expression has not been detected in the forebrain. However, *in vitro* primary NSC culture is dependent on the use of mitogens including FGF and EGF, and during CNS development *Hox* genes are activated in response to FGF [13,116]. The expression of *Hox* and TALE genes in forebrain derived primary NSC and their in vitro differentiated progeny has not been investigated in detail. There is a need for more extensive data on NSC gene expression programs and their relative expression levels in the developing forebrain, versus the neurosphere culture and the *in vitro* differentiating progeny. The *in vitro* study of forebrain-derived neural stem cells offers the opportunity to investigate the expression of these genes and identify correlations between their expression levels and cell lineages or NSC self-renewal.

Forebrain NSC culture also offers an accessible system for studying the expression of TALE transcription factors, which may be independent of the HOX proteins. HOX proteins cooperate with TALE factors in binding DNA, and there are

many redundancies observed amongst the functions of 39 HOX proteins [58]. Our system provides a means to identify potential roles of TALE transcription factors in NSC fate decisions, which may be exercised independently, or in complex with non-HOX DNA-binding cofactors that have not yet been identified.

Our findings will directly extend our knowledge of the gene expression programs involved in forebrain NSC neurogenesis, with special emphasis on the profiles of TALE gene expression. This knowledge is essential for predicting the efficacy and safety of the different stem cell sources available for clinical applications in nervous system repair. We investigated the expression profiles of important NSC signalling pathways and CNS developmental transcription factors in E14 forebrain-derived primary NSC, in the context of astrocyte differentiation. Astrocytic differentiation of neural stem cells occurs during this stage of development *in vivo*, and our NSC differentiation system is strongly biased towards astrocyte generation. Our use of primary generation neurospheres for differentiation minimizes the amount of time the cells are in culture, while at the same time generating sufficient numbers of cells for our experiments. This approach was used to ensure that the associations we draw between gene expression and cell fate *in vitro* are consistent with the situation of neural stem cell neurogenesis *in vivo*.

2.2 Hypothesis

The three amino acid loop extension (TALE) homeodomain transcription factors are expressed in embryonic day E14 forebrain-derived neural stem cells, and the expression profiles of these proteins during NSC differentiation is associated with specific cell type lineages.

2.3 Objectives

1. To reveal the gene expression profiles of important neural stem cell signalling pathways in the E14 developing forebrain, E14 forebrain-derived primary NSC, and their differentiating progeny.
2. To determine the transcript expression patterns of genes encoding for HOX transcription factors as well as genes that are important for neuronal development; in the E14 developing forebrain, E14 forebrain-derived primary NSC and their differentiating progeny.
3. To determine the expression profile of TALE gene mRNA transcripts and proteins in the E14 developing forebrain, E14 forebrain-derived primary NSC and their differentiating progeny.

2.4 Materials and Methods

Ethics statement and animal care

Animals were treated according to the standards of the Canadian Council on Animal Care. The described experimental protocols were performed in accordance with animal experimentation guidelines, and the mice were obtained from an approved source (Central Animal Care Services, University of Manitoba).

Neural stem cell isolation, expansion and differentiation

Timed pregnant female C57 BL/6 mice were humanely euthanized by CO_2 gas followed by cervical dislocation and embryos were removed. The day of the positive vaginal plug was considered as E0.5 of pregnancy and embryos were collected at E14.5 and placed in GIBCO® phosphate buffered saline (PBS) (1.06 mM KH_2PO_4, 155.17 mM NaCl, 2.97 mM Na_2HPO_4-$7H_2O$) solution on ice. The embryos were transferred to ice-cold artificial cerebral spinal fluid (ACSF) (0.124M NaCl, 5 mM KCl, 1.3 mM $MgCl_2$, 26.2 mM $NaHCO_3$, 10 mM glucose, 1.99 mM $CaCl_2$, antibiotic/antimycotic) where the brains were removed, and then forebrains were dissected from embryonic whole brains. Forebrains from one litter (approximately 8 embryos) were mechanically dissociated by fire-polished pasteur pipettes in 2 ml Basic NSC media (DMEM:F12, 10mM HEPES, antibiotic/antimycotic, 0.6% glucose). Full NSC media (Basic NSC media, 2 µg/ml heparin, 20 ng/ml rhEGF, 20 ng/ml bFGF and hormone mix (5X stock: DMEM:F12, 0.6% glucose, 1 mg/ml transferrin, 0.25 mg/ml insulin, 0.097 mg/ml putrescine, 0.3µM sodium selenite, 0.2 µM progesterone) was added to a total volume of 10 ml and the media with dissociated cells was run through a 40 µm filter to remove meninges particles and ensure a single cell suspension. Trypan blue exclusion assay was used to verify

viable cells, and viable cell counts were used for plating. Cells were plated on uncoated tissue culture plates at a density of $10^5/cm^2$, in serum free Full NSC media. The cells were expanded in these conditions for 7 days, and were fed every other day with fresh media. At the end of 7 days, neurospheres were gently dissociated by Accutase (Sigma-Aldrich, Oakville ON) treatment and single cell suspension was verified by microscopy. The cells were counted using trypan blue, and added to tissue culture plates coated with Growth Factor Reduced Matrigel™ (BD Biosciences, Mississauga ON) at a density of 10^5 cells per cm^2 in DMEM containing glutamine, antibiotic/glutamine and 15% heat inactivated fetal bovine serum. The cells were cultured in this condition for 8 days of differentiation, and the media was refreshed every other day throughout the differentiation.

Cortical neuron isolation and culture

Postmitotic cortical neurons were isolated from E18.5 mouse embryos. First, cortices were isolated from whole brain into cold Hank's balanced salt solution (HBSS) (1.26 mM $CaCl_2$, 0.493 mM $MgCl_2$-$6H_2O$, 0.407 mM $MgSO_4$-$7H_2O$, 5.33 mM KCl, 0.441 mM KH_2PO_4, 4.17 mM $NaHCO_3$, 137.93 mM NaCl, 0.338 mM Na_2HPO_4, 5.56mM D-Glucose, GIBCO®). The tissue was dissociated using a combination of digestion by Earle's balanced salt solution (EBSS)- based (5.33 mM KCl, 26.19 mM $NaHCO_3$, 117.24 NaCl, 1.01 mM NaH_2PO_4-H_2O, 5.56 mM D-Glucose, GIBCO®) papain solution (0.1 mg/ml cysteine, 0.51 nM EDTA, 10 U/ml papain), and mechanical dissociation by pasteur pipette[255-256256-257256-257256-257255-256]. Papain solution (3 ml) was added to one litter of dissected cortices for 20 min at 37°C and the reaction was stopped with 300 µl of 10/10 solution (10 mg/ml BSA and 10 mg/ml ovomucoide in EBSS). The

cells were precipitated by centrifugation at 1000 rpm for 10 seconds and the supernatant was aspirated. The cells received 3 ml of 1/10 solution (10/10 solution diluted 10x in EBSS) and 0.1% DNase (Calbiochem®) and were mechanically dissociated by pasteur pipette. The 10/10 solution was added at 1:1 volume with the cell suspension, followed by centrifugation for 2 min at 1000 rpm. The supernatant was removed and cells were suspended in neuronal culture media (Neurobasal™ media, (Life Technologies, Burlington ON), 1% v/v penicillin/streptomycin, 2% B27 supplement, 500 μM L-Glutamine), followed by counting of the cells and plating at a density of 5 x $10^4/cm^2$ on coverslips in neuronal culture media. On day 3 after plating, we removed half of the media volume and replaced this with neuronal selection media (neuronal culture media, 7 μM cytosine arabinoside). Two days later, half of the media volume was removed and this was replaced with neuronal culture media. Two days later, on day 7, the cells were fixed in 4% paraformaldehyde (PFA) for immunofluorescent labelling, as detailed below.

Fixation and immunofluorescent labelling

Neurospheres were rinsed with PBS and fixed with freshly polymerized PFA (0.16 M sodium phosphate buffer, pH7.4 and 2% PFA) for 20 min at room temperature to cross-link proteins, then rinsed with cryoprotectant (25 mM sodium phosphate buffer, pH7.4, 10% sucrose, 0.04% NaN_3). Fixed samples were incubated at 4°C in cryoprotectant solution for at least 24 hours (h). Neurospheres were mounted in optimal cutting temperature compound (OCT) and cryosections (8-10 μm) were obtained on gelatinized slides and stored at -20°C.

Cells differentiating on matrigel coated glass coverslips were rinsed with PBS and fixed in 4% PFA for 15 min at room temperature, while adhered to the coverslips. The

cells were subsequently rinsed in PBS and stored in PBS at 4°C until used in immunofluorescent labelling experiments.

Cryopreserved slides were air-dried for 20 min, and soaked in 0.3% Triton X-100 (tr) tris buffered saline (TBS) (50 mM Tris-HCl, pH 7.4, containing 1.5% NaCl) solution for 20 min. Permeabilization and pre-blocking of neurosphere sections were performed with TBS-tr containing 10% normal goat serum (NGS). For immunofluorescent labeling, primary and secondary antibodies were diluted in TBS-tr containing 10% NGS (refer to tables 1 and 2 for antibody dilutions). Primary antibody incubation was done overnight at 4°C (200 μL/slide). Following primary labeling, the slides were washed three times with TBS-tr (20 min), and incubated in a humidity chamberbox for 1h at room temperature with 200 μL/slide of secondary antibody. Slides were washed once with TBS-tr (20 min) and twice with Tris-HCl (50 mM) buffer, pH 7.4 (20 min). For negative controls, primary antibody omission and IgG (mouse and rabbit derived antibodies) or IgY (chicken derived antibody) whole molecule incubations (1 μg/ml) were used in the protocol along with the corresponding secondary antibodies. For immunofluorescence staining of cells, permeabilization was performed with 2% NP-40 in PBS for 10 min at room temperature, and pre-blocking was performed with PBS containing 10% normal goat serum. Primary antibody incubation was performed one hour at room temperature followed by rinses with PBS and secondary antibodies were applied (1:800 dilution) at room temperature for one hour. Primary and secondary antibodies were diluted in PBS containing 10% normal goat serum. Following antibody incubations, coverslips were slide mounted with glycerol anti-fade medium containing DAPI counter stain (0.5 μg/ml) (Calbiochem, EMD Chemicals,

Gibbstown NJ) and incubated at room temperature for 1h in the dark before observation or storage in the dark at -20°C.

Microscopy and cell quantification

Immunofluorescence was detected using an Axio Observer.Z1 inverted microscope from Carl Zeiss. The illumination system was composed of the Zeiss Colibri LED system and a HXP-120 mixed gas lamp. The software used for detection, imaging and image processing was AxioVision 4.8 (Carl Zeiss). For quantification of cells in the neurospheres, a minimum of two labelling experiments were performed. From each of those two experiments a minimum of 2 sphere sections were selected and divided in half at random to provide a total sample of 4 half-spheres for quantification. All of the cells were counted in the 4 half-spheres based on the detection of DAPI stained nuclei. The minimum total number of cells counted was 500 for each protein of interest. The cells were quantified for detection of the protein of interest, to estimate the proportion of cells that expressed the protein of interest, within the total cell population of the neurosphere cultures. For quantification of differentiating cells, randomized frames of 3 separate immunolabeling experiements were collected. A total of 500 cells were counted from these frames based on DAPI signal, and the number of cells expressing the protein of interest was recorded.

Reverse transcription and real-time polymerase chain reaction (PCR)

Total RNA was extracted from the whole E14.5 forebrain (FB), primary neurospheres (D0) and differentiating cells at day1 (D1) and day8 (D8) of differentiation. The RNeasy Mini Kit (Qiagen Sciences, Maryland) was used for RNA extraction and cDNA synthesis was done with the RT^2 First Strand Kit (Qiagen). Real-time PCR was

performed in customized RT^2 Profiler PCR Array 96 well plates from SABiosciences (Qiagen), using SABiosciences SYBR Green-based RT^2 qPCR Master Mix in an Applied Biosystems (ABI) 7500 Real-Time PCR machine. Primer sequences were designed by SABiosciences™ and were not disclosed by the company. These are designed to give uniform cycling conditions to each gene within the plate, while detecting every transcript of the gene, but avoiding complementation with other regions of the transcriptome. The standardized cycling program provided by the company was used each time a plate was run in the real-time PCR machine. Two housekeeping genes were included for normalization, *Gapdh* and *Actin*, and three internal controls were provided in the plate design to address genomic DNA contamination, reverse transcription performance and PCR cycling performance. For each sample of interest (FB, D0, D1 and D8) three (n=3) plates were run and the difference in threshold cycle values (ΔCt) were calculated for the gene of interest minus the housekeeping gene *Gapdh*. The students t-test was used to detect significant differences between the ΔCt values for FB, D1 and D8 versus D0, based on a p-value of 0.05 (*), 0.01 (**) and 0.001 (***). Analysis was performed using Microsoft Excel 2007 and SABiosciences™ web-based RT^2 Profiler PCR Array Data Analysis. The graphs presented in the results section report the average fold change in transcript expression levels for FB, D1 and D8 versus D0, with bars representing standard error, based on the sample size of n=3.

Total cell extracts and western blot (WB)

Total cell protein extracts were prepared using neural stem cell salt shock protein extraction buffer (50 mM tris pH 8.0, 150 mM NaCl, 5 mM EDTA, pH 8.0, 0.2% sodium deoxycholate, 1% NP-40, 50 mM NaF, 1 mM sodium orthovanadate, Roche Complete

Cocktail protease inhibitor). The isolated protein concentration was determined by Bradford assay using BioRad Protein Assay Reagent and the SpectraMax M2^{e} 96-well plate spectrophotometer (Molecular Devices) with SoftMax® Pro v5.3 analysis software.

Protein samples were denatured by boiling for 5 minutes in loading buffer (50 mM Tris-HCL pH 8.0, 2%SDS, 10% glycerol, 1% β-Mercaptoethanol, 12.5 mM EDTA and 0.02% bromophenol blue). Proteins were run in polyacrylamide gel by electrophoresis to separate based on their molecular weight. A 4% acrylamide gel (0.125 M Tris-HCL(pH 6.8), 0.1% SDS, 0.05% $Na_2S_2O_8$, 0.001% TEMED) was used for the stacking gel and 10% acrylamide gel (0.375. Tris-HCL (pH 8.8), 0.1% SDS, 0.1% $Na_2S_2O_8$, 0.0004% TEMED) for the separating gel. Electrophoresis was performed with the gels at 200V, at 4°C, in electrophoresis running buffer (25 mM Tris, 192 mM glycine, 0.1% SDS, pH 8.3). The proteins were transferred to nitrocellulose membrane in transfer buffer (192 mM glycine, 25 mM Tris, 0.05% SDS, 20% methanol) at 100V for 1 h at room temperature with a cooling pack in the chamber.

For immunolabelling, membranes were pre-blocked in 5-10% milk/TBS for 1 hr at room temperature and primary antibodies were applied in 1-5% milk/TBS-Tween20 (0.2%) for either 1h at room temperature or overnight at 4°C. Chemilluminescence detection was performed using horseradish peroxidase (HRP) conjugated secondary antibody (applied 1 h room temperature in 1-5% milk/TBS-Tweeen20) and Immobilon Western Chemiluminescent HRP Substrate solution (Millipore™) containing luminol and peroxide. Exposures were captured on film and by the Fluor-S™ MAX Multimager (BIO-RAD), and quantification was performed using the Quantity One® 1-D v4.6.9 analysis software (BIO-RAD).

Antibodies

Antibody	Application	Description	Source
GFAP	IF (1:200)	Mouse monoclonal	Life Technologies
NEUN	IF (1:1000)	Mouse monoclonal	Millipore, Temecula CA
βtubIII	IF (1:1000)	Chicken polyclonal	Millipore
SOX2	IF (1:250)	Rabbit polyclonal	Millipore
NESTIN	IF (1:230)	Mouse monoclonal	Developmental Studies Hybridoma Bank, Iowa City IA
OLIG2	IF (1:1500)	Rabbit polyclonal	Millipore
PREP1	WB (1:200)	Mouse monoclonal	Santa Cruz Biotechnology Inc., Santa Cruz CA
PREP2	IF (1:100), WB (1:200)	Mouse monoclonal	Santa Cruz Biotechnology Inc
PBX1	IF (1:100), WB (1:200)	Rabbit polyclonal	Santa Cruz Biotechnology Inc
MEIS1	IF (1:500), WB (1:6000)	Rabbit polyclonal	Millipore
Ki67	IF (1:100)	Rabbit polyclonal	Santa Cruz Biotechnology Inc
GAPDH	WB (1:1500)	Rabbit polyclonal	Santa Cruz Biotechnology Inc
β-Actin	WB (1:2000)	Mouse monoclonal	Sigma-Aldrich

Table 2. List of primary antibodies. The primary antibodies used in the studies are presented with the dilutions used for each application, a description of the type of antibody, and the companies from which these were sourced.

Antibody	Application	Description	Source
Sheep anti-mouse IgG	WB	Peroxidase–conjugated	Jackson ImmunoResearch Laboratories, Inc. West Grove PA
Donkey anti-rabbit IgG	WB	Peroxidase–conjugated	Jackson ImmunoResearch Laboratories, Inc.
Goat anti-chicken IgY	IF	Dylight 649-conjugated	Life Technologies
Goat anti-rabbit IgG	IF	Rhodamine Red-X-conjugated	Life Technologies
Goat anti-rabbit IgG	IF	Fluorescein isothiocyanate (FITC)-conjugated	Life Technologies
Goat anti-mouse IgG	IF	FITC-conjugated	Life Technologies
Goat anti-mouse IgG	IF	Rhodamine Red-X-conjugated	Life Technologies
Goat anti-rabbit IgG	IF	AlexaFluor-488-conjugated	Life Technologies
Rabbit IgG whole molecule	IF	Isotype control	JacksonImmunoResearch Laboratories, Inc.
Mouse IgG whole molecule	IF	Isotype control	JacksonImmunoResearch Laboratories, Inc.
Chicken IgY whole molecule	IF	Isotype control	JacksonImmunoResearch Laboratories, Inc.

Table 3. List of secondary antibodies and immunoglobulin whole molecules. The scondary antibodies and immunoglobulin whole molecules used for isotype controls are pesented with the dilutions used for each application, a description of the antibody type, and the companies from which these were sourced.

3 Results

3.1 Mouse embryonic day E14.5 forebrain-derived neural stem cells generated neurospheres that expressed an astrocyte lineage gene expression profile.

Neurosphere formation is a standard assay used to verify the presence of neural stem cells, and to describe the proliferation characteristics of these cells. Neurospheres are known to consist of neural stem cells, progenitors and more differentiated cells. Depending on the NSC culture conditions used, the cell type composition of the spheres will be impacted [112]. In order to establish the character of our neurosphere and NSC differentiation system, we performed immunofluorescent (IF) labelling and real-time PCR experiments to detect the expression levels and frequencies of specific cell-type markers. These data could then be used to associate the expression levels of NSC signalling pathways and transcription factors detected in the differentiating cells, with NSC fate decisions. We used IF labelling of specific cell type markers in sectioned neurospheres, to describe the differentiated and undifferentiated cell type composition of the neurospheres. We counted a minimum of 500 cells (identified by DAPI stained nuclei) for each marker by randomly dividing the sectioned spheres in half and counting a minimum of 4 halves from four different spheres, from a minimum of two separate labelling experiments. We confirmed the presence of NSC, neurons and glia in the sectioned neurospheres. The transcription factor SOX2 is a stem cell marker expressed in ESC and neural stem cells with established roles in attenuating self-renewal [257]. We found that 82% of cells in a given neurosphere express detectable levels of SOX2 and these cells co express the NSC marker NESTIN, which is an intermediate filament protein (Fig. 4). To detect neurons and astrocytes we used NEUN and GFAP

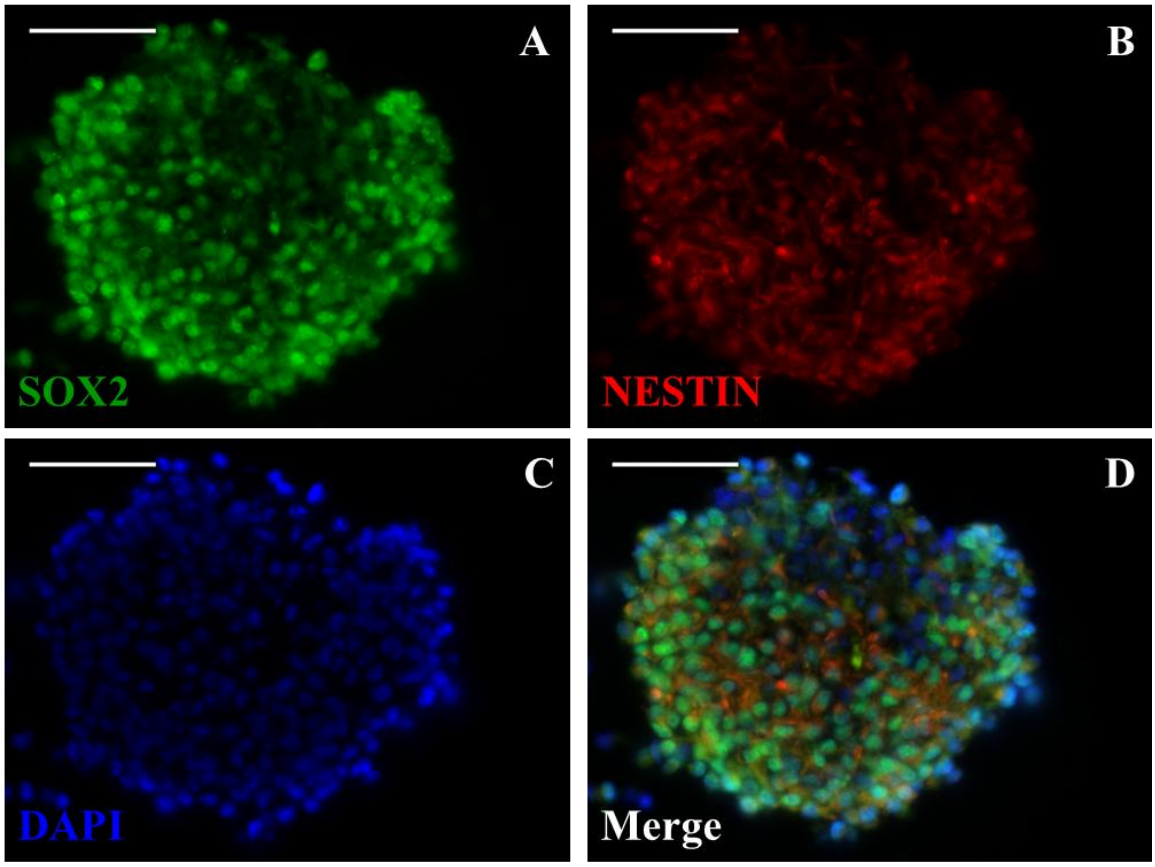

Figure 4. (A) SOX2 and (B) NESTIN expression in embryonic primary neurospheres. The neural stem cell marker SOX2 is expressed in the nuclei of approximately 82% of neurosphere cells (A). The signal for the neural stem cell marker NESTIN overlays with SOX2 positive regions (B). DAPI counterstain labels nuclei (C) and the merged image reveals the overlapping expression of SOX2 and NESTIN (D). Scale bar = 50 μm.

respectively, to label mature cells of these lineages. We found 5% of cells in our neurosphere assay were positive for NEUN (Fig. 5) and 4% were positive for GFAP expression (Fig. 6). Mature oligodendrocyte markers CNPase and O4 were not detected in the neurospheres. As was reported by Hack *et al*. (2003), our embryonic forebrain-derived neurospheres also expressed high levels of OLIG2 (60% of cells), which has an unknown role in neurospheres (Fig. 7) [128]. Because of its association with neuronal and oligodendrocyte differentiation from neurospheres, we traced OLIG2 expression through differentiation to provide evidence as to the number of oligodendrocytes being generated and maintained in culture. To control for non-specific signal in our immunofluorescent labelling experiments, we labeled the sectioned neurospheres with the immunoglobulin whole molecules that are isotype specific for the primary antibodies used (Fig. 8), and we labeled sectioned neurospheres with the secondary antibodies alone (primary omission control Fig. 9).

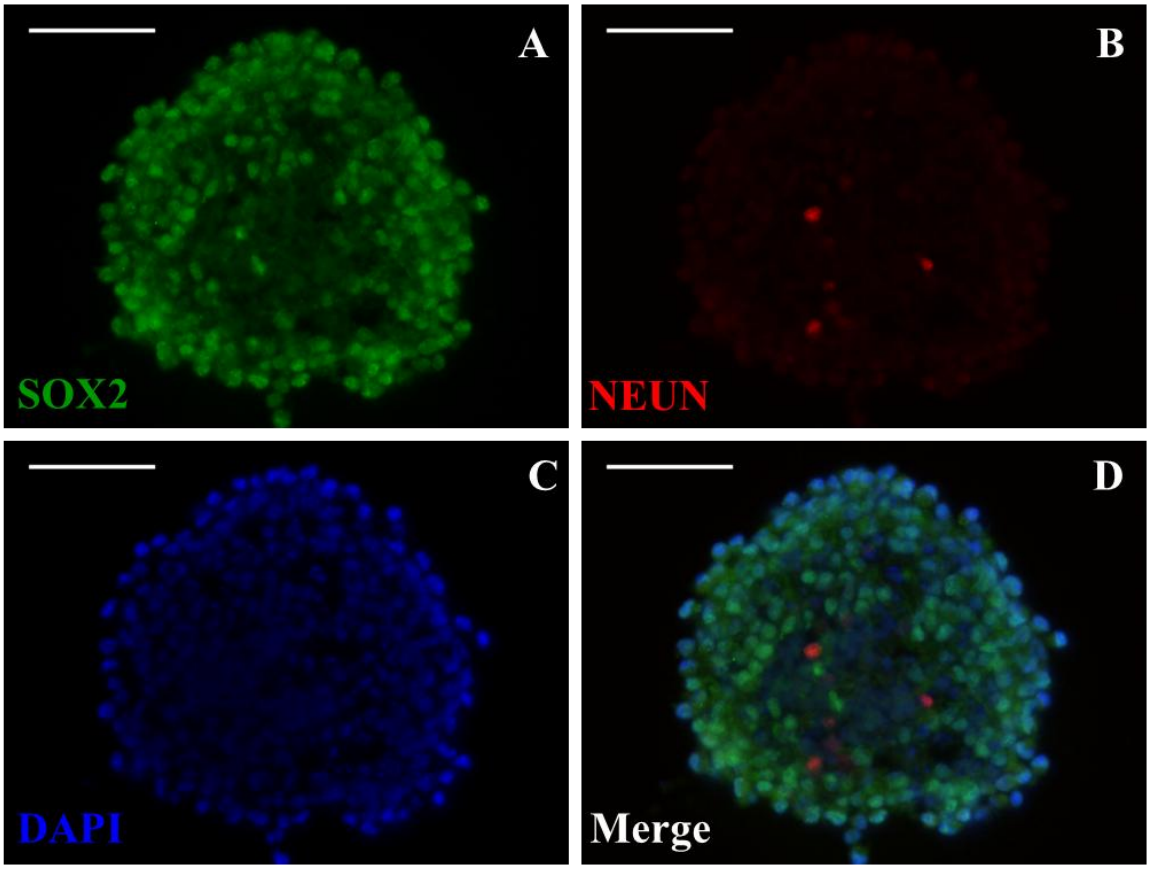

Figure 5. (A) SOX2 and (B) NEUN expression in embryonic primary neurospheres. SOX2 expression appears to be predominantly in the periphery of the neurospheres (A), while the mature neuron marker NEUN is detected in the core region (B). Appoximately 5% of cells are positive for NEUN. DAPI counterstain labels nuclei (C) and the merged image reveals the nonoverlapping expression of SOX2 and NEUN (D). Scale bar = 50 μm.

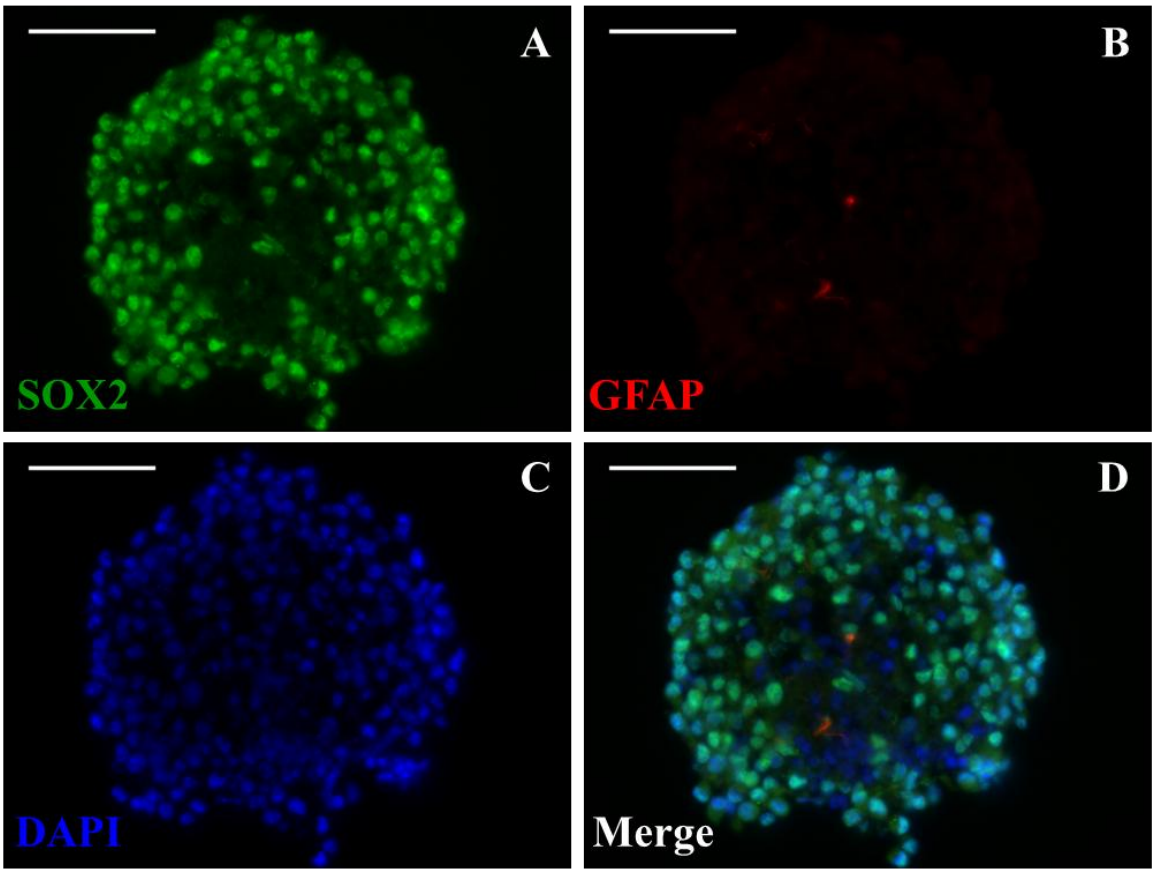

Figure 6. (A) SOX2 and (B) GFAP expression in embryonic primary neurospheres. SOX2 expression occurs more frequently in the periphery of the neurospheres (A), while the mature astrocyte marker GFAP is detected in the core region (B). Appoximately 4% of cells are positive for GFAP. DAPI counterstain labels nuclei (C) and the merged image reveals the nonoverlapping expression of SOX2 and GFAP (D). Scale bar = 50 μm.

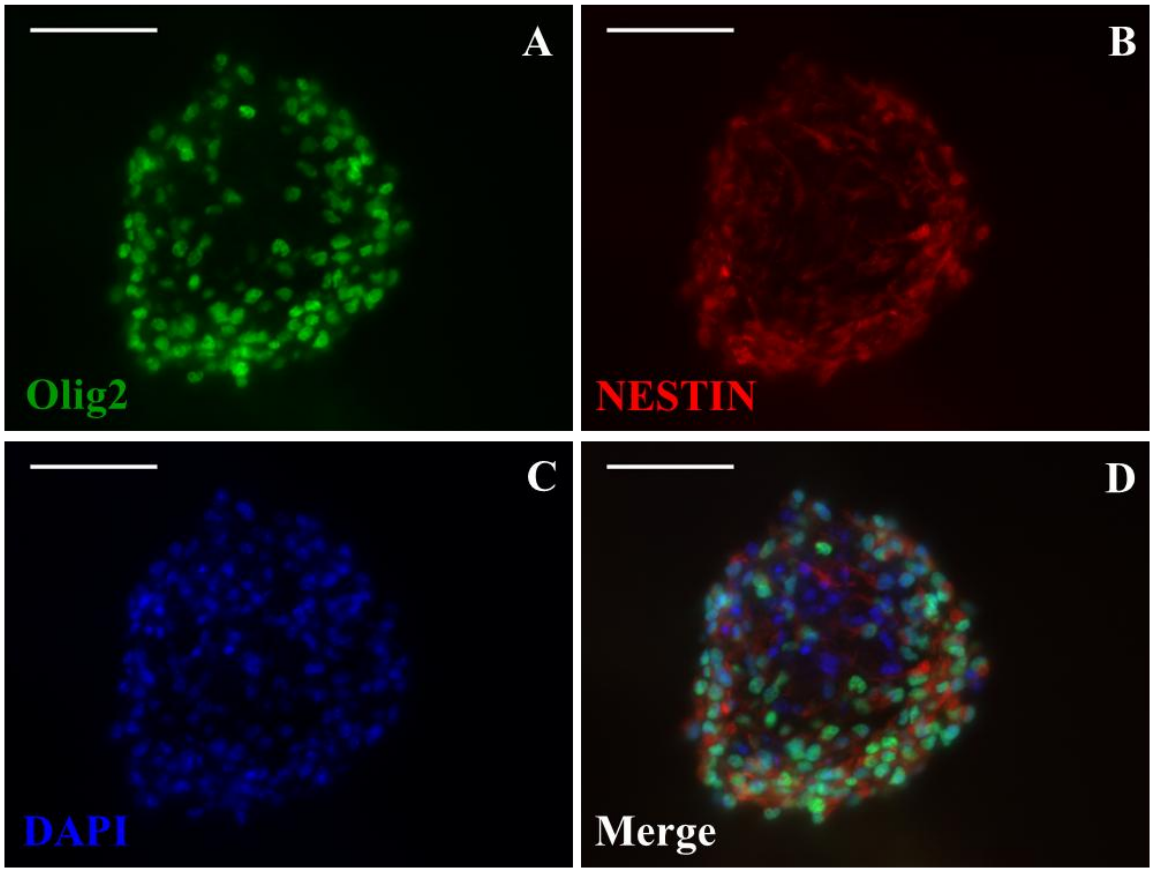

Figure 7. (A) OLIG2 and (B) NESTIN expression in embryonic primary neurospheres. Approximately 60% of nuclei label positively for OLIG2 in the neurosphere cells (A). The expression of NESTIN overlays with $OLIG2^{+}$ regions (B). DAPI counterstain labels nuclei (C) and the merged image reveals the overlapping expression of OLIG2 and NESTIN (D). Scale bar = 50 μm.

Marker	Cell type	Positive cells (%)
SOX2	Neural stem and progenitor	82
NEUN	Neuron	5
GFAP	Astrocyte	4
OLIG2	Unspecified neural precursor	60

Table 4. Expression of cell-type markers in primary neurospheres. The neurospheres are comprised of mainly stem cells and progenitors as indicated by the number of cells expressing SOX2. Differentiated neurons and astrocytes are also detected at much lower numbers. The majority of cells also express OLIG2, which frequently labels precursors in neuropheres, but has no established role in neurosphere cells.

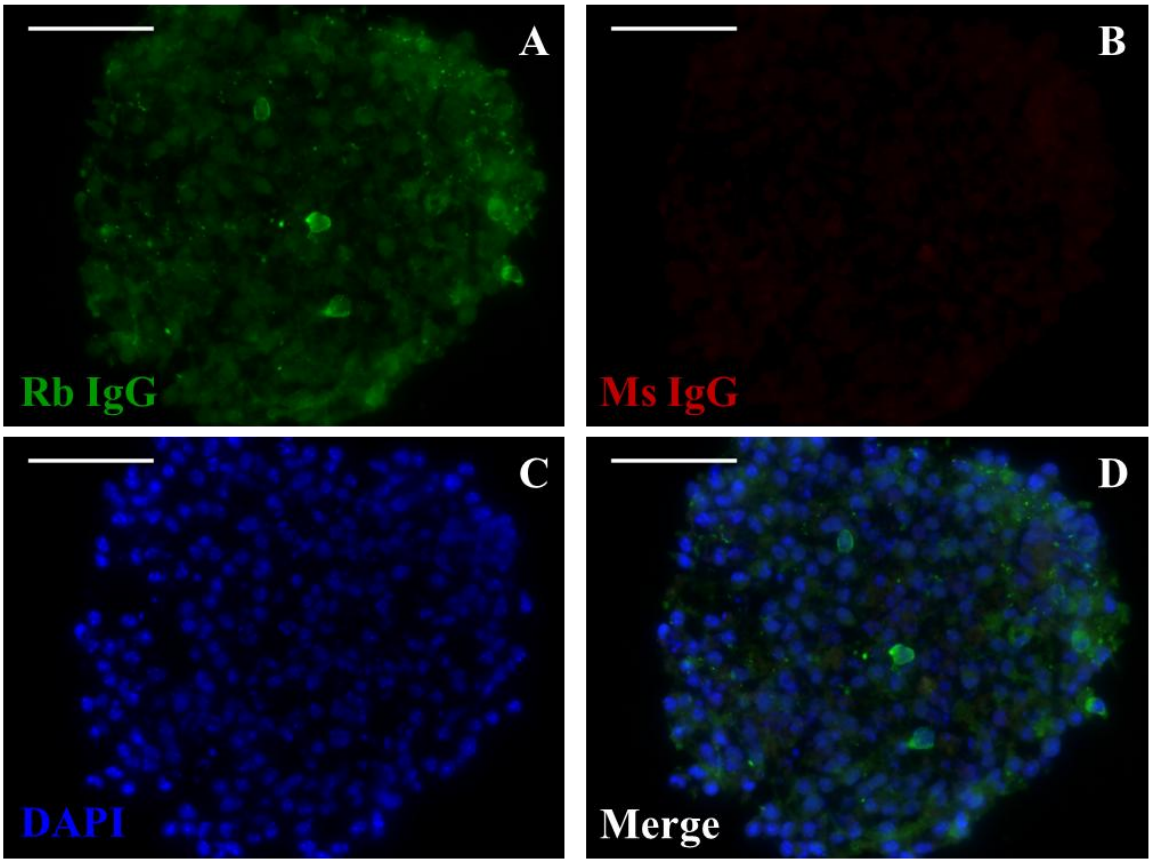

Figure 8. Immunoglobulin (Ig)G isotype control for antibodies used in immunofluorescent labeling of neurospheres. Rabbit (Rb) IgG (A) and mouse (Ms) IgG (B) adhere to the sectioned neurospheres very rarely and in a pattern that does not resemble that of the primary antibodies derived from these species (rabbit anti-SOX2 and anti-OLIG2, mouse anti-NESTIN, anti-NEUN and anti-GFAP). DAPI counterstains the nuclei (C) and the merged image shows the pattern of nonspecific immunolabeling (D). Scale bar = 50 μm.

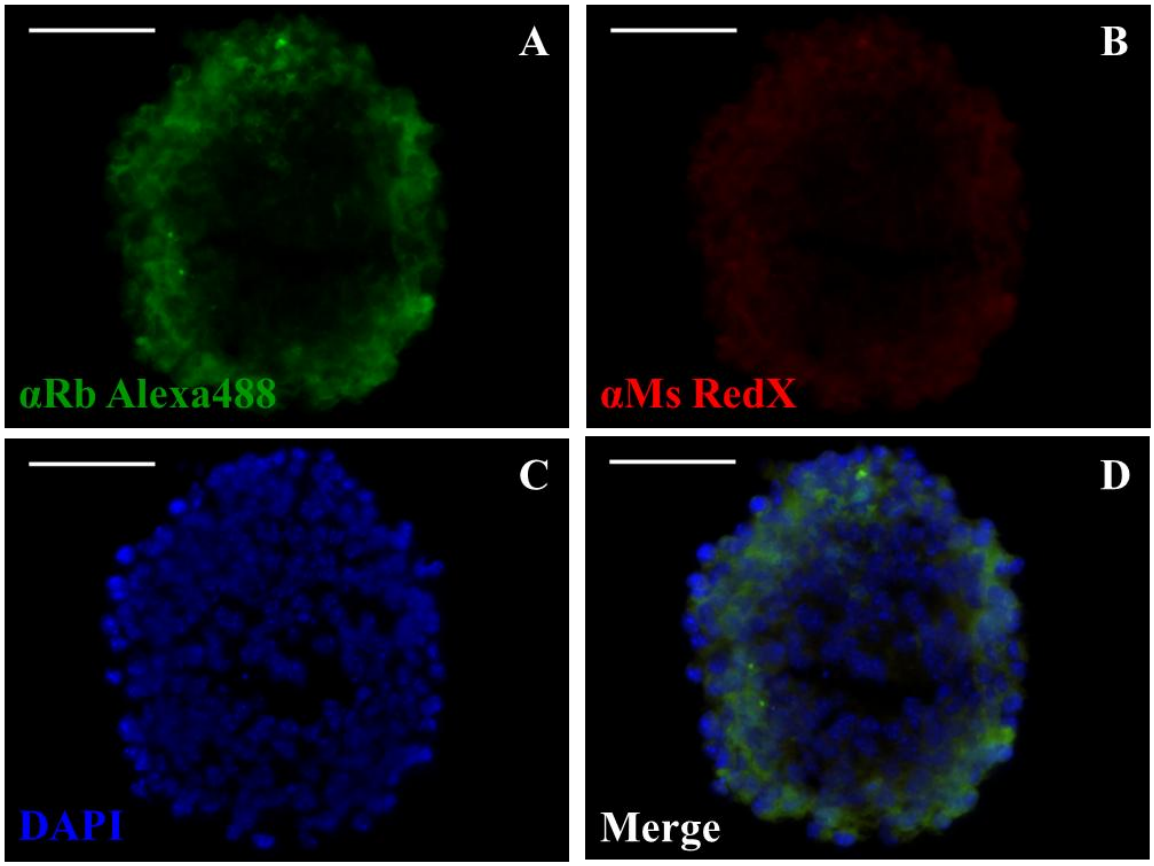

Figure 9. Primary antibody ommission control for immunofluorescent labeling of neurospheres. Without primary antibody there is labeling of the neurosphere cells by neither αRb Alexa488 (conjugated secondary antibody used for SOX2 and OLIG2 detection) (A) nor αMs RedX (conjugated secondary antibody used for NESTIN, NEUN and GFAP detection) (B) conjugated secondary antibodies. In both channels autofluorescence is visible mainly in the tissue periphery. DAPI counterstain labels nuclei (C) and the merged image shows overlapping regions of autofluorescence (D). Scale bar = 50 μm.

After one week in culture, the neurospheres were dissociated and the cells were plated in differentiation conditions for a period of 8 days. Protein and mRNA expression studies were carried out on neurospheres (D0) and cells that were differentiating for 1 day (D1) and 8 days (D8). At D8, 3% of the the differentiated cells derived from the dissociated neurospheres stained positive for the neuronal marker βTUBIII. Labelling with the astrocyte marker GFAP showed that approximately 80% of cells were positive for this marker. OLIG2 stained approximately 10% of cells including a portion of the $GFAP^+$ cells (Fig. 10), indicating that these were mature astrocytes. Astrocytes that express GFAP have previously been shown to express OLIG2 at decreasing levels while maturation occurs, while oligodendrocytes have been shown to maintain their level of OLIG2 expression [258]. Differentiated cells that were positive for OLIG2 at D8, and expressed neither βtubIII nor GFAP, were designated as oligodendrocytes. Appoximately 2% of cells were OLIG2+/GFAP- indicating that an estimated 2% of differentiated cells were of oligodendrocyte lineage. Previous reports on neurosphere differentiation indicate that this is an expected percentage for oligodendrocytes in the differentiated population of cells [126]. The isotype control was performed using immunoglobulin whole molecules mouse IgG, rabbit IgG and chicken IgY for the anti-GFAP, anti-OLIG2 and anti-βtubIII antibodies, respectively (Fig. 11).

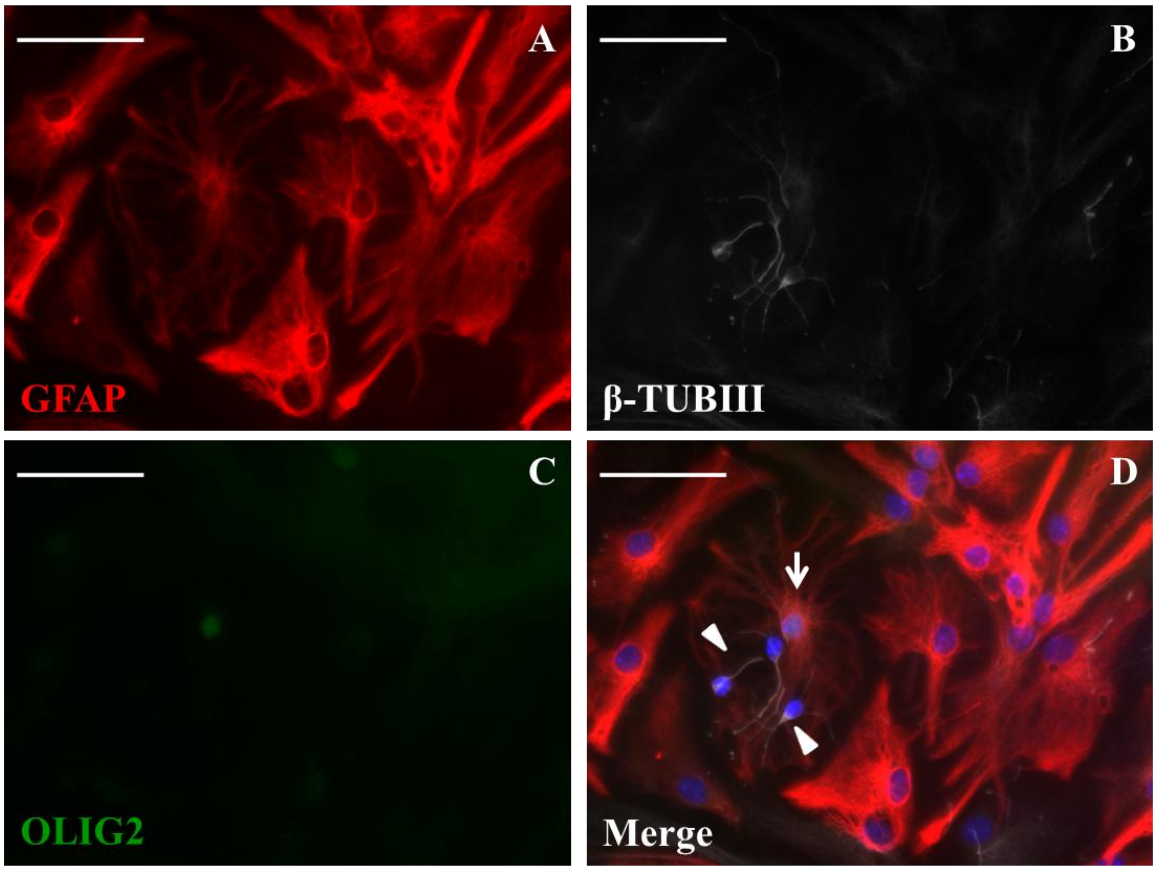

Figure 10. Immunofluorescent detection of cell type markers in differentiated neural stem cells. The astrocyte marker GFAP labelled approximately 80% of cells at D8 (A) and the neuron marker βtubIII labelled 3% of the D8 cells (B). OLIG2 was used to label and estimate the proportion of D8 cells that are oligodendrocytes; however, it was commonly co-expressed in $GFAP^+$ astrocytes (C). DAPI counterstain labels the nuclei and the merged image shows the heterogeneous differentiated cell population at D8. White arrow heads point to the $\beta tubIII^+$ neurons and the white arrow points to an $OLIG2^+$ astrocyte colabelled with GFAP (D). Scale bar = 50 μm.

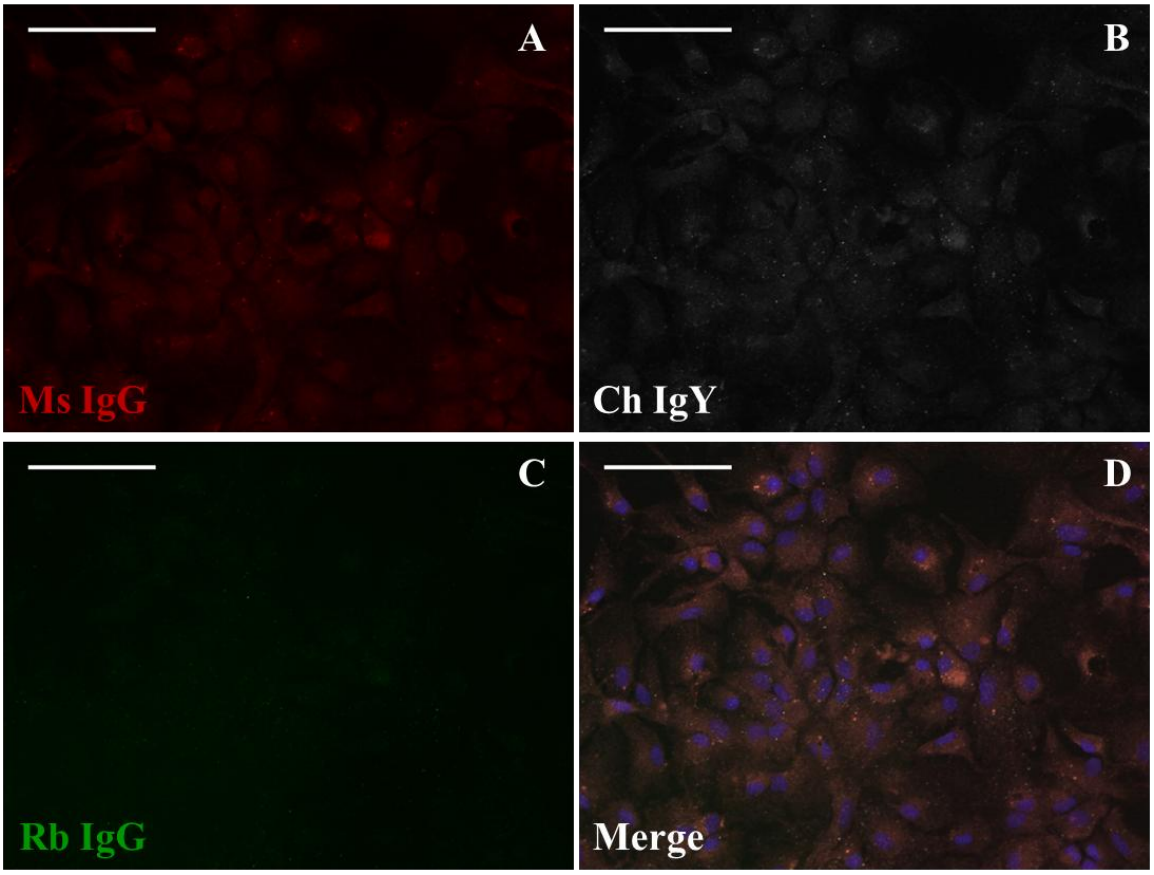

Figure 11. Immunoglobulin isotype control for antibodies used in immunofluorescent labelling of D8 differentiated cells. Mouse (Ms) IgG (A), Chicken (Ch) IgY (B) and Rabbit (Rb) IgG (C) adhere to differentiating cells very rarely and in a pattern that does not resemble that of the specific primary antibodies derived from these species (mouse anti-GFAP, chicken anti-βtubIII, rabbit anti-OLIG2). DAPI counterstains the nuclei and the merged image shows the pattern of nonspecific immunolabeling (D). Scale bar = 50 μm.

We next assayed the mRNA expression profile of the neurospheres, as well as the forebrains from which they are derived, and their differentiating progeny (Fig. 12). The purpose of this was to determine when lineage specific gene expression profiles were induced, indicating that the fate of the cells had likely been restricted. Given the presence of differentiated cells in the neurospheres and the sensitivity of the neurospheres to culture conditions, we did not restrict our analysis to cells in differentiation conditions and chose to include neurospheres. We found that *Gfap* was expressed at significantly higher levels in the neurospheres relative to the whole forebrain. In contrast, *βtubIII* and the oligodendrocyte lineage marker *Mbp* were expressed at significantly lower levels in the neurospheres relative to the whole forebrain. During the differentiation process between D1 and D8, *Gfap* detection continuously increased, which we attribute to differentiation of primitive cells along the astrocyte lineage as well as dividing astrocytes within the D1 and D8 populations. At D8, levels of *βtubIII* and *Mbp* were unchanged relative to the neurospheres, indicating there was no further differentiation of cells along these lineages from the neurospheres. The fold change results of the real-time PCR experiments are based on the averages of n=3 trials for E14.5 forebrain, E14.5 forebrain-derived neurospheres, D1 differentiating cells and D8 differentiating cells. Interestingly, *Sox2* expression at D8 showed a two fold increase over neurosphere levels. Given these findings, it appears that neurospheres cultured from the E14 forebrain, in the presence of EGF and FGF2, have an innate gene expression program that suggests their commitment to the astrocyte lineage. Furthermore, permitting the differentiation of these cells in minimal serum-containing conditions leads to increasing levels of *Gfap* transcript and protein, while leaving neuronal and oligodendrocyte marker transcripts unchanged.

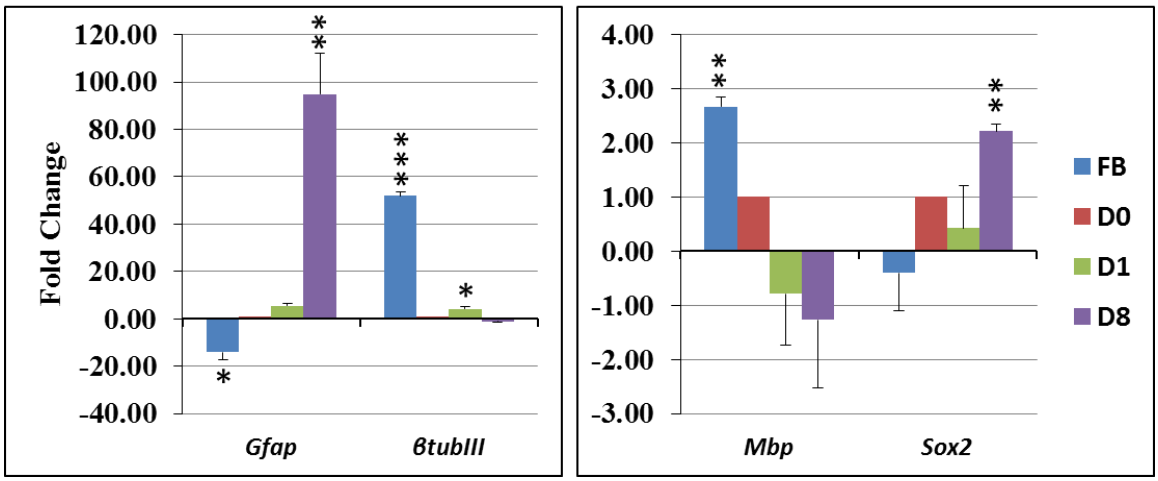

Figure 12. Fold change detection of specific cell type marker transcripts by real-time PCR. The mRNA transcript levels of *Gfap*, *βtubIII* and *Mbp* were detected as indicators of gene expression profiles of astrocytes, neurons and oligodendrocytes respectively. *Sox2* was assayed as an indicator of the neural stem cell gene expression profile. All transcripts were detected by real-time PCR in forebrain (FB), neurospheres (D0) and differentiating cells at day1 (D1) and day8 (D8) of differentiation. Threshold cycle (Ct) values were normalized to *gapdh* and the students t-test was used to detect significant differences between the normalized Ct values (ΔCt) at D0 versus FB, D1 and D8 based on a sample size of n = 3. (*) $P \leq 0.05$, (**) $P \leq 0.01$, (***) $P \leq 0.001$. Fold change in transcript levels is reported with standard error bars.

3.2 Differentiation of primary neural stem cells was accompanied by changes in the mRNA transcript levels of NOTCH and BMP signalling pathways.

In order to determine the activity of important NSC signalling pathways in our system, we performed real-time PCR to detect transcript levels of NOTCH receptors, ligands and downstream effectors, as well as BMP signalling molecules (*Bmp2*, *Bmp4* and *Bmp7*). These two pathways are particularly important to NSC self-renewal, differentiation specifically in our system, and neurogenesis *in vivo* and *in vitro* [95,259]. The specific roles of individual ligands and receptors, however, have yet to be determined. We observed minor changes in the mRNA expression of NOTCH receptors *Notch1* and *Notch3,* while much larger changes were observed in the expression of *Notch2* and *Notch4* (Fig. 13). There was a very small decrease in *Notch3* levels in neurospheres relative to the forebrain, and at D8 neither *Notch1* nor *Notch3* levels were significantly different from those detected in the neurospheres. *Notch4* was significantly decreased in neurospheres 12-fold relative to the whole forebrain while *Notch2* levels were relatively stable. The level of both transcripts significantly increased during differentiation and by D8 *Notch2* levels had increased 16-fold while *Notch4* levels increased but did not reach the levels that we detected in the forebrain. The diverse expression profile of the receptors in our system suggests that there are specific roles for the different receptor variants in the context of NOTCH signalling in neural stem cells.

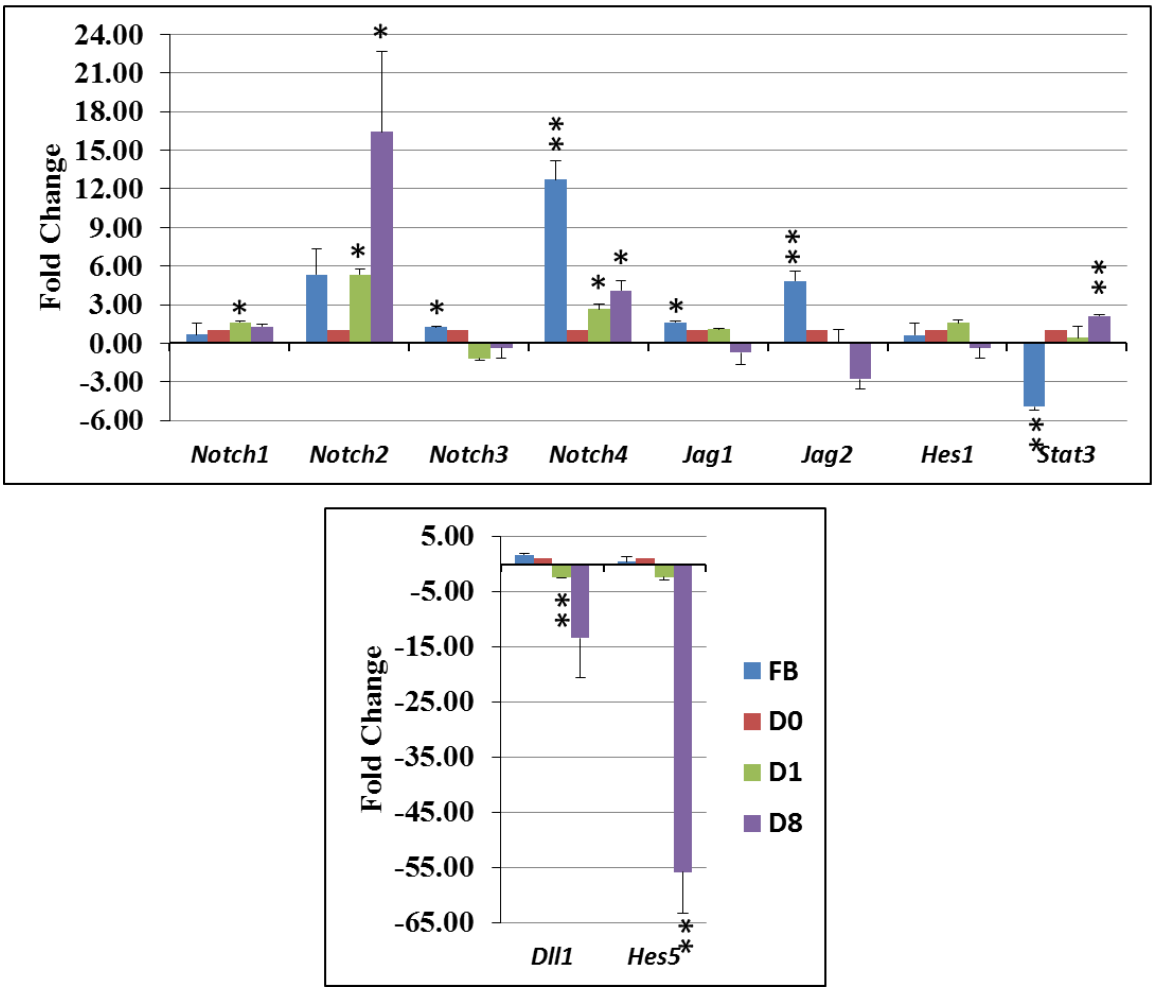

Figure 13. Fold change detection of NOTCH signalling pathway transcripts by real-time PCR. The mRNA transcript levels of *Notch* receptors (*Notch1-4*) , *Notch* ligands (*Jag1*, *Jag2* and *Dll1*) and downstream effectors (*Hes1*, *Hes5 and Stat3*) were detected as indicators of relative NOTCH pathway activity levels in neurospheres versus forebrain and differentiating cells. Threshold cycle values were normalized to *Gapdh* and the students t-test was used to detect significant differences between the ΔCt values at D0 versus FB, D1 and D8 based on a sample size of n = 3. (*) $P \leq 0.05$, (**) $P \leq 0.01$, (***) $P \leq 0.001$. Fold change in transcript levels is reported with standard error bars.

The transcript levels of NOTCH pathway ligands *Jagged1* (*Jag1*) and *Jagged2* (*Jag2*) were significantly decreased in neurospheres relative to forebrain, and these levels remained relatively unchanged throughout differentiation from neurospheres to D8 cells. The delta-like ligand *Dll1* was unchanged in neurospheres relative to forebrain but showed decreased levels in differentiated cells compared to neurospheres, and this was significant at D1 but not D8. The downstream effecter *Hes1* was relatively unchanged throughout the analysis but *Hes5* was largely and significantly reduced in the D8 samples compared to the neurospheres. Further to this, no change in expression levels was detected by D1 of differentiation, indicating that the effect on the *Hes5* transcript was delayed in comparison to the effects seen in the receptors and ligands. *Stat3* is known to interact with the NOTCH pathway and the expression of this gene is significantly higher in the neurospheres relative to the whole forebrain and significantly higher yet in D8 cells relative to the neurospheres. Again, the change in the transcript level during differentiation goes undetected until D8 as D1 levels are unchanged relative to neurospheres.

The expression profiles of *Bmp* transcripts also suggest non-redundant roles in the propagation and differentiation of neural stem cells. We detected increased levels of *Bmp2* in the forebrain and differentiating cells relative to neurospheres (Fig. 14). The differences were not significant with the exception of the very modest increase in expression levels detected in D1 cells. We detected significantly lower levels of *Bmp7* transcripts in the forebrain and differentiating cells relative to neurospheres and the fold decrease were very similar for forebrain and differentiating cells. *Bmp4* was significantly higher in the forebrain relative to neurospheres, and the transcripts greatly and

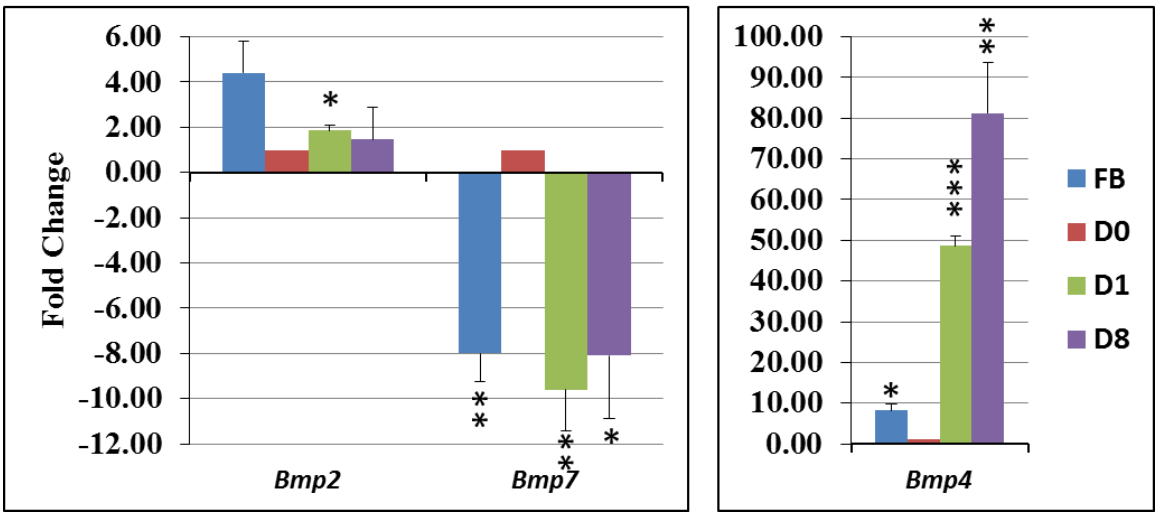

Figure 14. Fold change detection of BMP signalling molecule transcripts by real-time PCR. The mRNA transcript levels of *Bmp* signalling molecules were detected as indicators of relative *Bmp* signalling activity levels in neurospheres versus forebrain and differentiating cells. Threshold cycle (Ct) values were normalized to *gapdh* and the students t-test was used to detect significant differences between the ΔCt values at D0 versus FB, D1 and D8 based on a sample size of n = 3 . (*) $P \leq 0.05$, (**) $P \leq 0.01$, (***) $P \leq 0.001$. Fold change in transcript levels is reported with standard error bars.

significantly increased during differentiation relative to neurospheres.

In summary, differentiation of E14 forebrain-derived primary NSC was accompanied by specific changes in the mRNA expression of the NOTCH and BMP pathways, suggesting non-redundant roles amongst the receptors, ligands, downstream effectors and signalling molecules within these distinct pathways. While the canonical pathways are well understood, we have added to the evidence indicating that there are specific roles for the different variants of NOTCH receptors and the variants of BMP signalling molecules.

3.3 Mouse embryonic day E14.5 forebrain derived neural stem cells expressed lower mRNA transcript levels of genes important for forebrain neuronal development.

Based on the astrocyte gene expression profile we detected in the neurospheres, we were interested in detecting the relative expression levels of genes important to forebrain neuronal development in the E14.5 forebrain, neurospheres and differentiating cells (Fig. 15). These data would indicate the extent to which forebrain derived NSC in our system repress neuronal genes in neurospheres and during differentiation. These factors are important in deriving neurons from the progenitors in the ventral forebrain, and have important roles in neuronal maturation. Active repression of these genes, therefore, prevents neuronal differentiation. For instance, active NOTCH signalling has been shown to prevent the expression of the pro-neuronal gene *Mash1*. When NOTCH signalling is inhibited, *Mash1* expression is permitted, which leads to neuronal differentiation [260]. We found that the *Mash1* transcript levels did not change significantly between the different samples assayed. *Pax6, Dlx2* and *Dlx5* were detected at

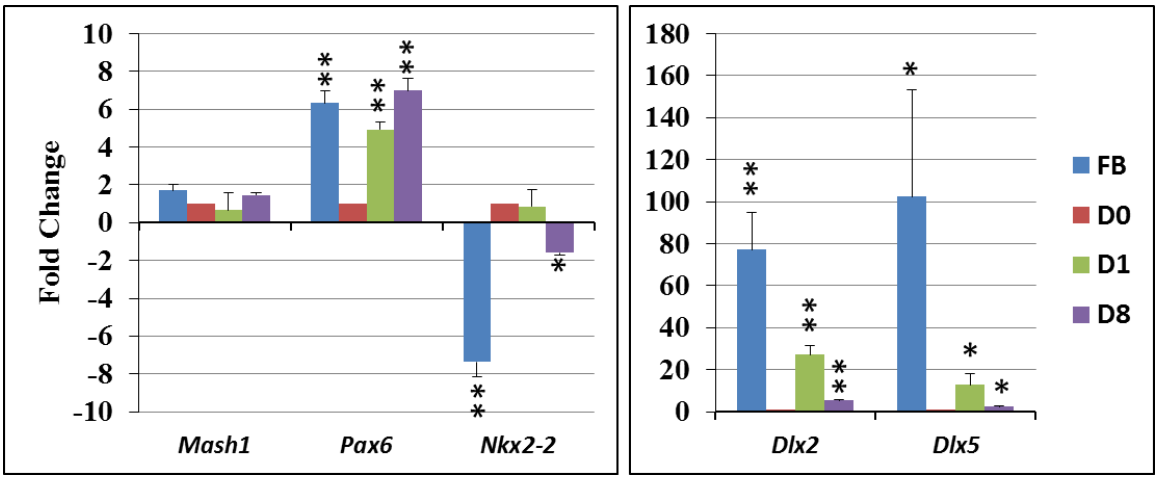

Figure 15. Fold change detection of developmentally important neuronal forebrain transcripts by real-time PCR. The mRNA transcript levels of several transcription factors involved in neuronal development in the embryonic forebrain were detected in neurospheres versus forebrain and differentiating cells. Threshold cycle (Ct) values were normalized to *gapdh* and the students t-test was used to detect significant differences between the ΔCt values at D0 versus FB, D1 and D8 based on a sample size of n=3. (*) $P \leq 0.05$, (**) $P \leq 0.01$, (***) $P \leq 0.001$. Fold change in transcript levels is reported with standard error bars.

significantly lower levels in neurospheres relative to forebrain and then at higher levels in the differentiating cells relative to neurospheres. The *Dlx* genes showed very large and significant fold decreases in transcript levels when compared to *Pax6*. When *Pax6* transcript levels increased again, they did so continuously through D1 and D8, while the *Dlx* transcripts increased at D1, to a fraction of what they were in the forebrain, and then decreased to levels that are just above the neurosphere levels. We also assayed for the expression of *Nkx2-2*, a gene associated with oligodendrocyte development [261]. The pattern of *Nkx2-2* was a sharp contrast to the neuronal genes, showing significantly lower levels in forebrain and D8 differentiated cells relative to neurospheres, although D8 levels were not much different from those in neurospheres. In summary, a group of transcription factors that have cooperative roles in ventral forebrain neurogenesis *in vivo* show temporally non-overlapping mRNA expression patterns in our NSC culture and differentiation system *in vitro*.

3.4 Three amino acid loop extension (TALE) gene mRNA transcripts and proteins were detected in the forebrain, neurospheres and differentiating cells.

It has been previously shown that TALE gene transcripts and proteins have been detected in the VZ and SVZ of the developing mouse forebrain [207]. In order to determine the expression level of the TALE transcription factors in our system, we performed real-time PCR for the PBX and MEINOX families in the whole forebrain, neurospheres and differentiating cells (Fig. 16). In all instances the expression of these transcripts was significantly lower in the neurospheres relative to the whole forebrain. At D8 of differentiation there was no significant difference in *Pbx1* and *Pbx2* levels relative to neurospheres, but *Pbx3* transcript levels approximately tripled. By D8 of differentiation

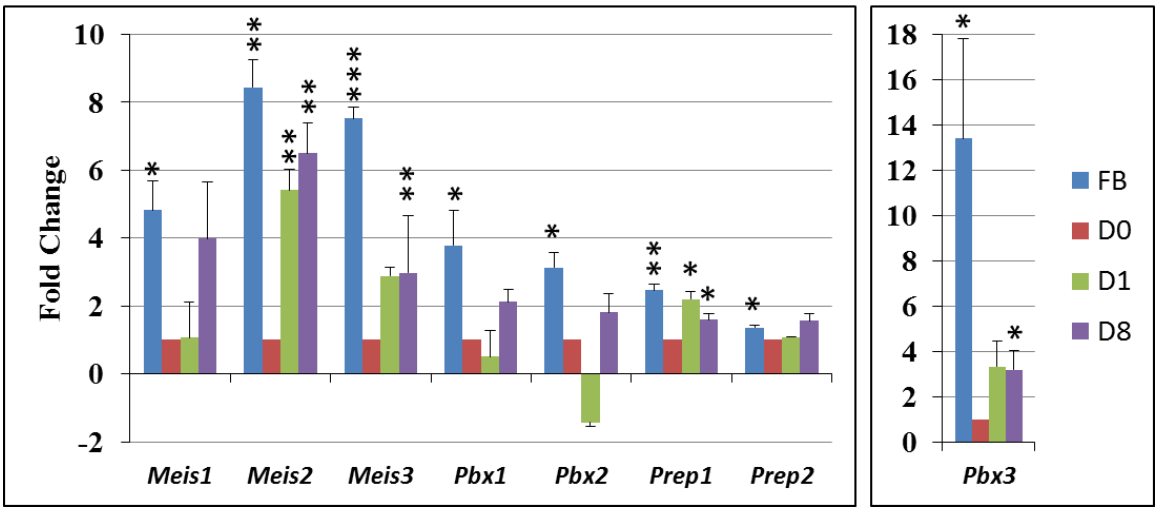

Figure 16. Fold change detection of TALE gene mRNA transcripts by real-time PCR. The mRNA transcript levels of the *Pbx*, *Meis* and *Prep* families of TALE genes were detected in neurospheres versus forebrain and differentiating cells as predictors for the relevance of these genes in forebrain development and NSC fate determination. Threshold cycle (Ct) values were normalized to *gapdh* and the students t-test was used to detect significant differences between ΔCt values at D0 versus FB, D1 and D8 based on a sample size of n=3. (*) $P \leq 0.05$, (**) $P \leq 0.01$, (***) $P \leq 0.001$. Fold change in transcript levels is reported with standard error bars.

Meis1, *Meis2* and *Meis3* levels were increased, however the change was not significant for *Meis1*. The levels of *Prep1* returned to forebrain levels during differentiation, increasing relative to neurospheres, but *Prep2* levels were unchanged during differentiation. In all samples, the TALE gene transcripts assayed were expressed at detectable levels, indicating that functional TALE proteins are potentially expressed in the forebrain as well as neurospheres and differentiating cells.

We chose to investigate the expression of PBX1 and MEIS1 proteins in our NSC culture system due to previously published data indicating that these proteins are present in the neurogenic regions surrounding the ventricles of the developing forebrain. Also, our transcript detection data indicates that these genes are actively expressed in the system we are studying. We further chose to investigate the expression of PREP1 and PREP2 based on the transcript detection data we generated, as well as the lack of data that exists regarding the expression patterns and functions of these TALE genes. We also proposed that if the TALE proteins are expressed in a system that does not express the *Hox* genes (results section 3.7), we may introduce a means to study the role of these genes in a *Hox*-independent context.

Each of the proteins was detected at high levels in the forebrain (Fig. 17). Western blot for PBX1 and PREP1 showed a sharp drop in the protein levels from forebrain to neurospheres and these levels remained very low. MEIS1 levels also dropped sharply from forebrain to neurospheres although not as drastically as PREP1 and PBX1. Unlike the formerly mentioned proteins, MEIS1 levels increased during differentiation and were detected at their highest levels in the D8 cells. The expression pattern of PREP2 was the

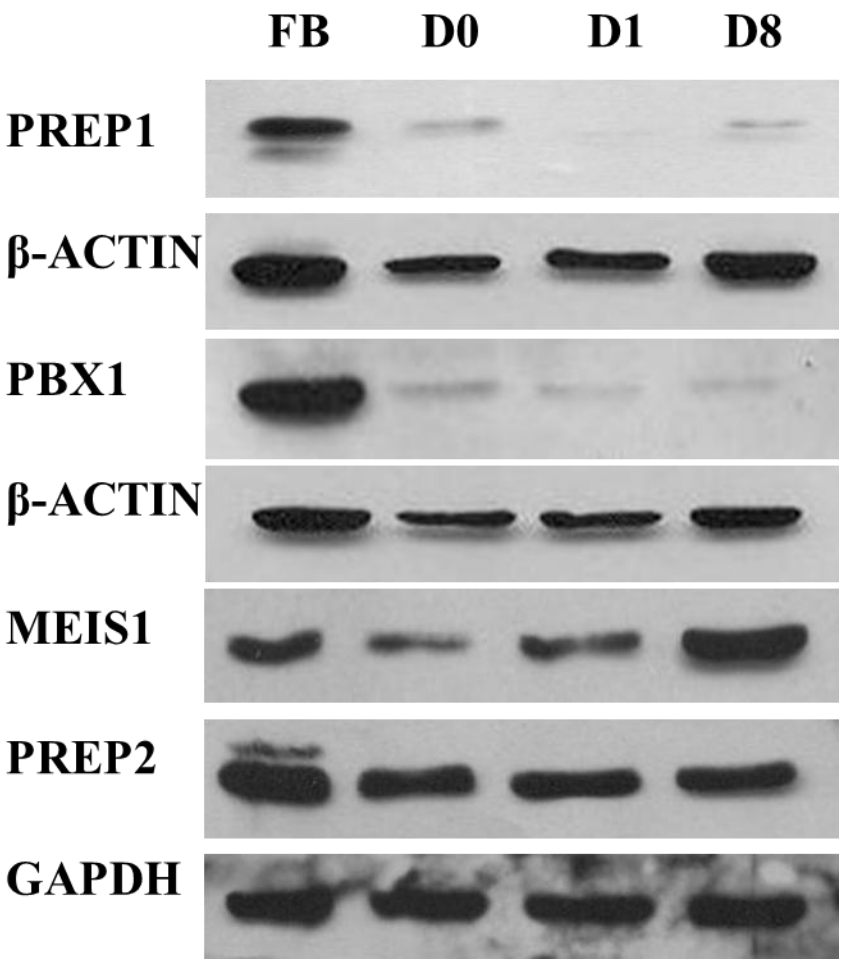

Figure 17. Protein level expression of TALE transcription factors detected by western blot. Immunoblotting for PREP1 and PBX1 protein revealed that these proteins are present in the E14.5 forebrain (FB) but are apparently expressed at very low levels in neurospheres (D0) and differentiating cells (D1 and D8). MEIS1 and PREP2 are also detected in the forebrain, as well as in the neurospheres and differentiating cells. The MEIS1 levels are reduced in neurospheres and significantly increased in differentiating cells while PREP2 levels are relatively unchanged. β-Actin and GAPDH act as the loading controls.

least variable, with strong levels detected in the forebrain, neurospheres and throughout differentiation. A higher molecular weight isoform of PREP2 also appears to be expressed in the forebrain at relatively lower levels, but this isoform is not detected in the other samples. The western blots were performed using a minimum of n=3 different sets of forebrains (FB), cultured neurospheres (D0) and differentiating cells (D1 and D8). The resulting expression patterns were consistent for each protein and the experiment was performed at least twice in each set of samples. When normalizing to GAPDH, there is a very small but statistically significant transient increase in PREP2 levels in the D1 cells versus D0 cells. MEIS1 levels are also significantly higher in D1 cells versus D0 and the level increases in D8 cells, however the difference is not statistically significant in D8 cells versus the neurospheres (Fig. 18).

To verify antibody specificities western blot was performed with each TALE antibody to detect protein levels in E14.5 forebrain, as well as verified positive and negative control samples. For the PREP antibodies, the positive control was the 293T cell line derived from human embryonic kidney (HEK) cells. The negative control used for PREP1 and PREP2 were adult heart and kidney respectively [220,222] (Fig 19 A). The MEIS1 and PBX1 antibodies were verified by western blot using an array of adult tissues harvested from C57 BL/6 mice [223,262] (Fig. 19 B).

To summarize, the mRNA transcripts of TALE genes are detectable in the forebrain, neurospheres and differentiating cells but show reduced levels in the neurospheres. The TALE proteins PBX1 and PREP1 are detected at very low levels in the neurospheres and differentiating cells while MEIS1 is detectable at high levels in D8 cells and PREP2 is detected at high levels in the neurospheres and differentiated cells.

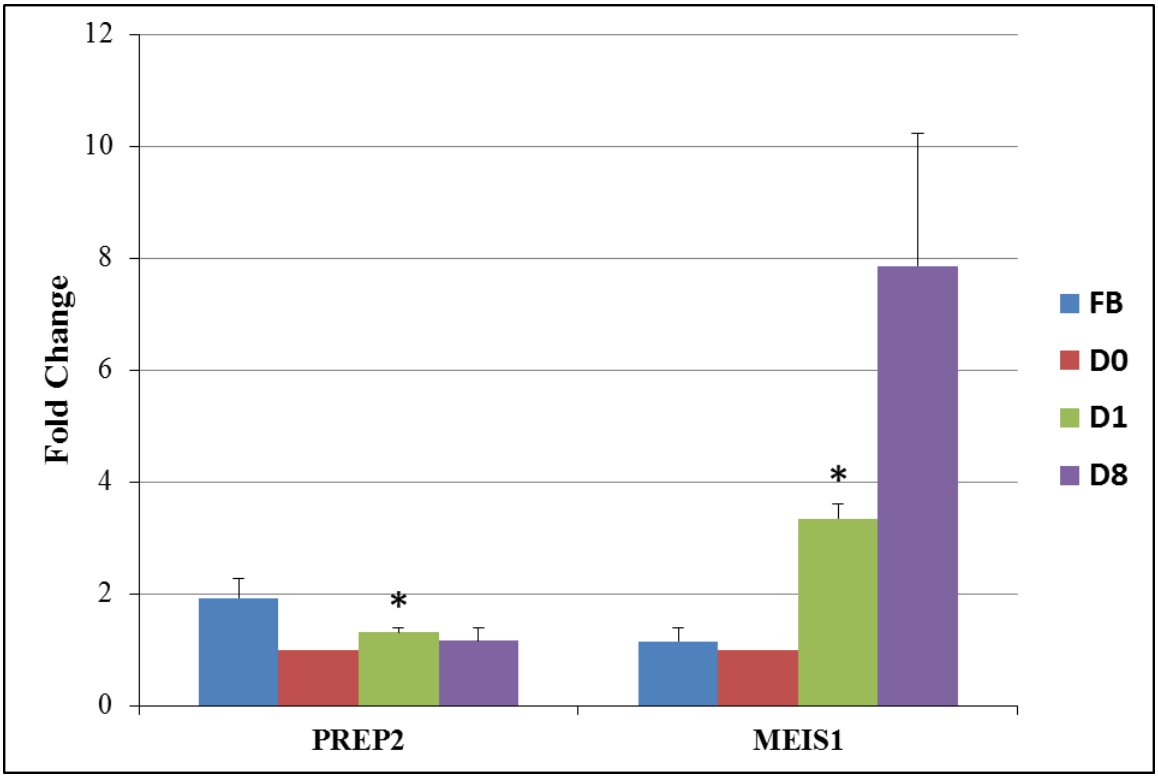

Figure 18. Fold change detection of PREP2 and MEIS1 protein by western blot. The expression levels of PREP2 and MEIS1 TALE proteins were detected in neurospheres versus forebrain and differentiating cells using western blot. Quantitative chemiluminescent values for the immunolabelled proteins were normalized to values of GAPDH. Fold change in the normalized values are reported with standard error bars. The students t-test was performed on the normalized values (n = 3, * indicates $P \leq 0.05$).

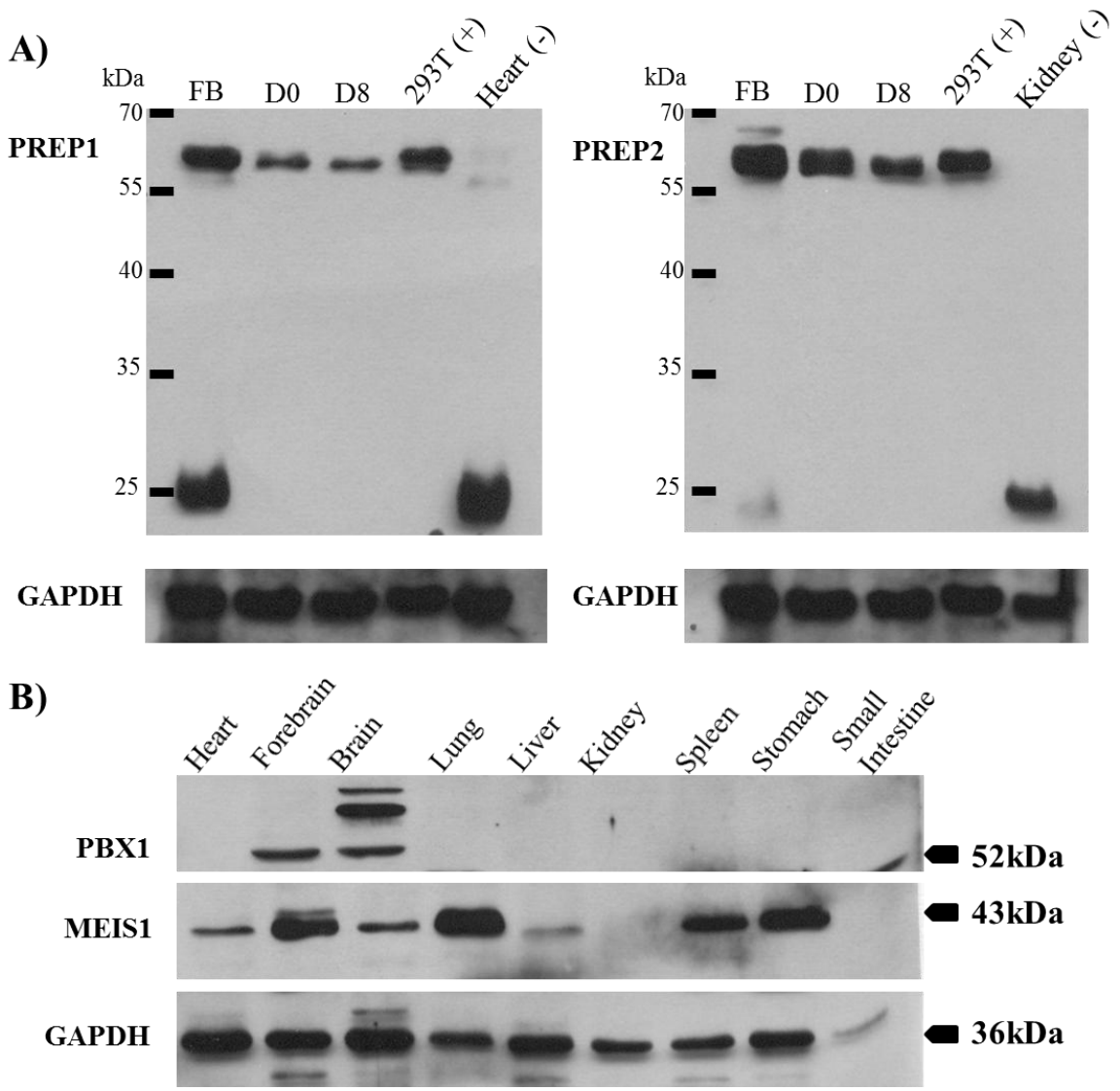

Figure 19. Western blot controls for anti-TALE antibodies. The PREP proteins are detectable at varying levels in the FB, D0 and D8 cells, and expressed in 293T cells that provide the positive control. Adult heart provides the negative control for PREP1 [222] and adult kidney provides the negative control for PREP2 [220] (A). We performed immunoblotting for PBX1 and MEIS1 in adult mouse tissues and E14 forebrain to verify the reliability of our antibodies. The MEIS1 antibody generated the pattern that we expected [262] and also detected an additional higher molecular weight band in the

embryonic forebrain (~45kDa). PBX1 was detected in adult and embryonic brain as expected (~53kDa) [223] (B). Previously unreported bands for PBX1 were detected in the adult brain at higher molecular weights (~60-65kDa). GAPDH provided the loading control.

3.5 The three amino acid loop extension (TALE) protein PREP2 was expressed at high levels in neural stem cells and neurons.

We were interested to find out which of the TALE proteins detected by western blot in neurospheres were being expressed in the neural stem cells. In order to address this, we used IF labelling on sectioned neurospheres to detect the expression of TALE proteins that coexpress with NSC markers SOX2 and NESTIN. As expected from the western blot data, PBX1 was not detected in the neurospheres (Fig. 20). The western blot data suggested that we should detect MEIS1 and PREP1 in either a small subpopulation of cells or faintly in a large population of the cells. PREP1 was not detected (preliminary data not shown), indicating that the protein levels may be too low or we must modify our immunolabeling approach. We detected only low levels of MEIS1 in the neurosphere cells above background levels making it difficult to determine the number of cells coexpressing NESTIN (Fig. 21). This was also hampered by the cytoplasmic staining pattern of NESTIN and the close proximity and overlapping nature of the cells in the neurosphere sections. PREP2 was detected in approximately 75% of cells in the neurospheres. Colabeling of SOX2 (Fig. 22) and Ki67 (Fig. 23) with PREP2 revealed that PREP2 was frequently coexpressed with these markers. Ki67 labelled approximately 75% of cells. The PREP2 signal was commonly localized to the periphery of the spheres which has previously been described as the region of more primitive cells as opposed to the core of the sphere where more differentiated cells are located [263].

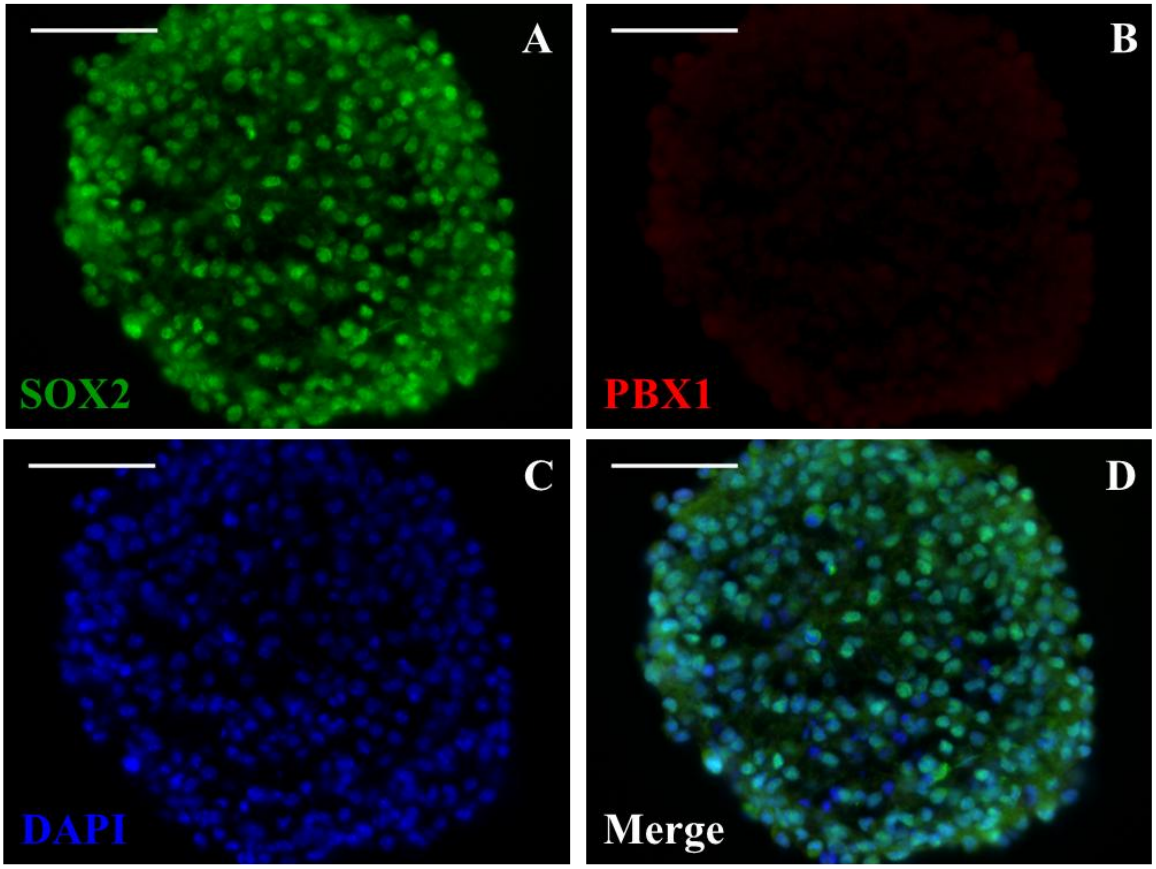

Figure 20. (A) SOX2 and (B) PBX1 expression in embryonic primary neurospheres. SOX2 labels the majority of cells in the spheres (A) while PBX1 is not detected (B). DAPI counterstain labels nuclei (C) and the merged image reveals the exclusive expression of SOX2 (D). Scale bar = 50 μm.

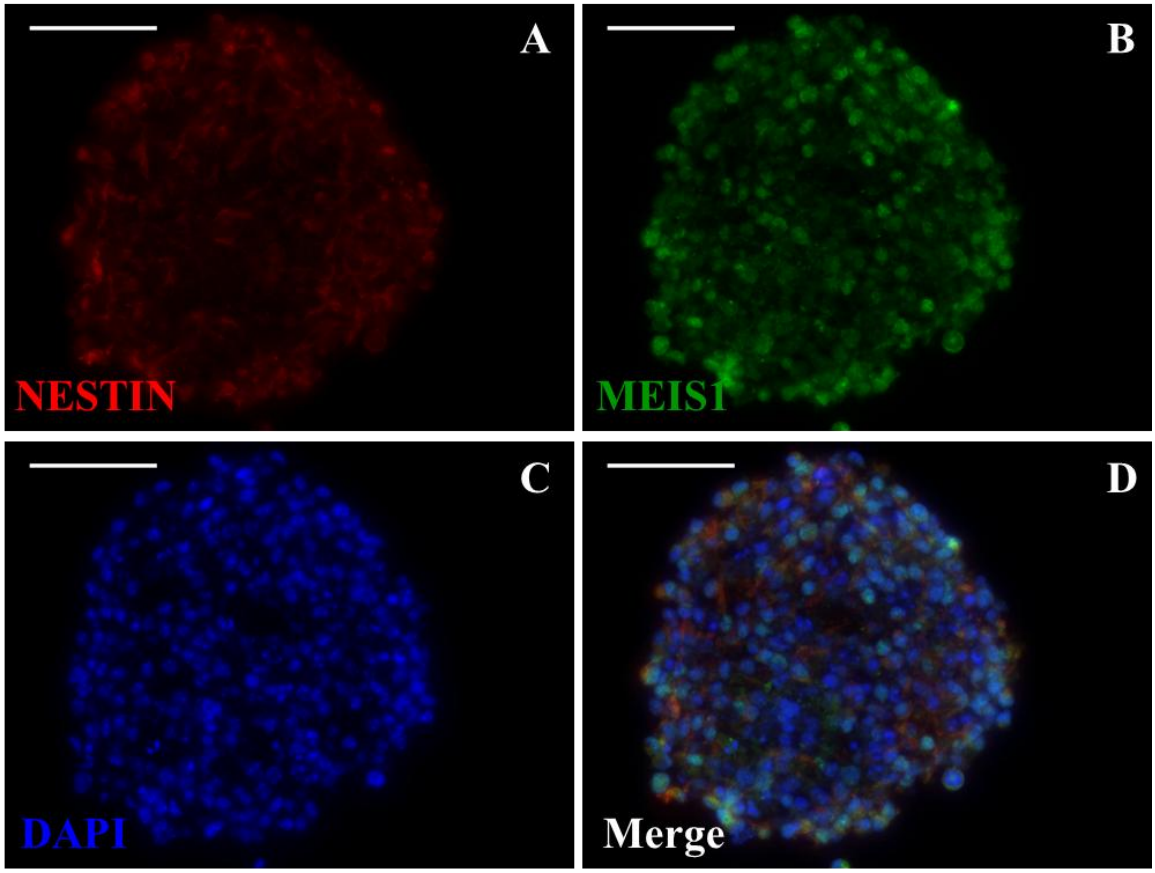

Figure 21. (A) NESTIN and (B) MEIS1 expression in embryonic primary neurospheres. NESTIN labels the majority of cells in the spheres (A) while MEIS1 appears to be expressed at low levels in some cells (B). DAPI counterstain labels nuclei (C) and the merged image reveals the overlapping expression of NESTIN and MEIS1 (D). Scale bar = 50 μm.

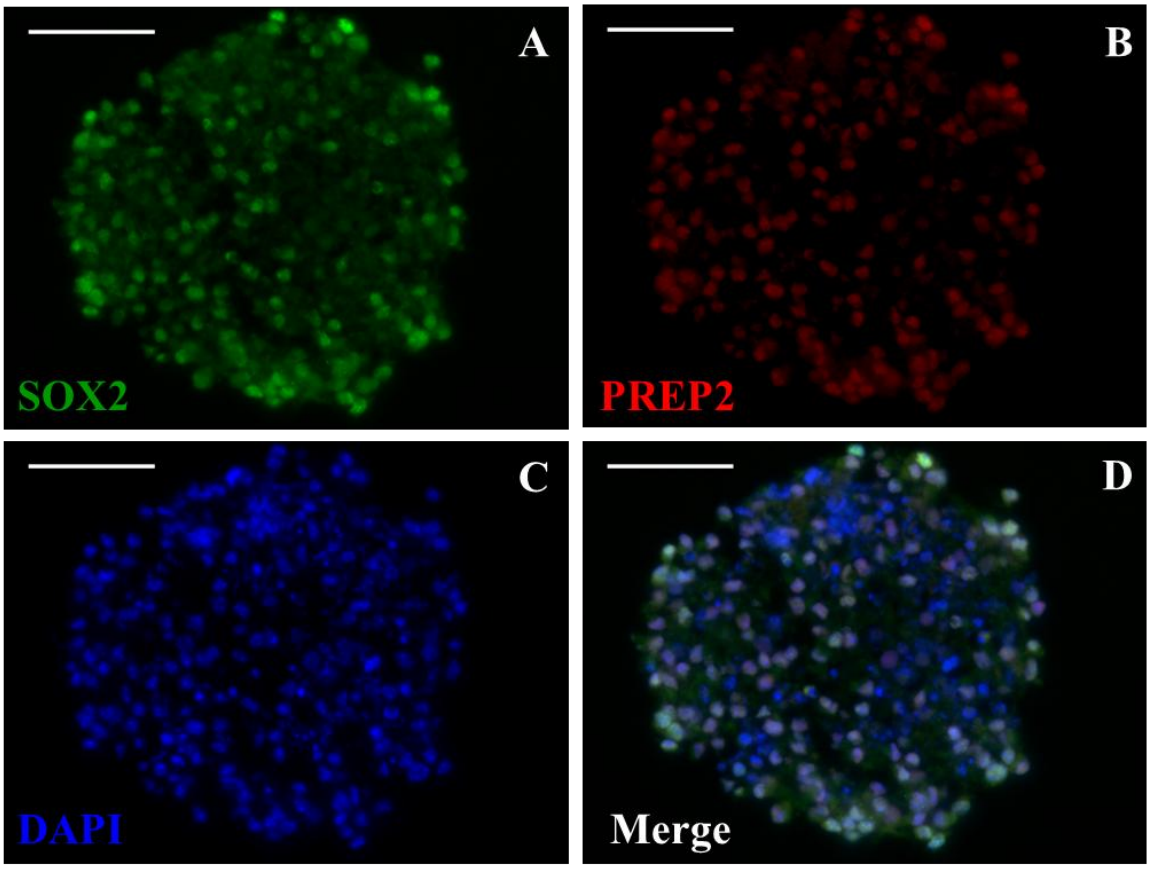

Figure 22. (A) SOX2 and (B) PREP2 expression in embryonic primary neurospheres. SOX2 labels the majority of cells (82%) in the spheres (A), as does PREP2 (75%), in overlapping regions (B). DAPI counterstain labels nuclei (C) and the merged image reveals the coexpression of SOX2 and PREP2 (D). Scale bar = 50 μm.

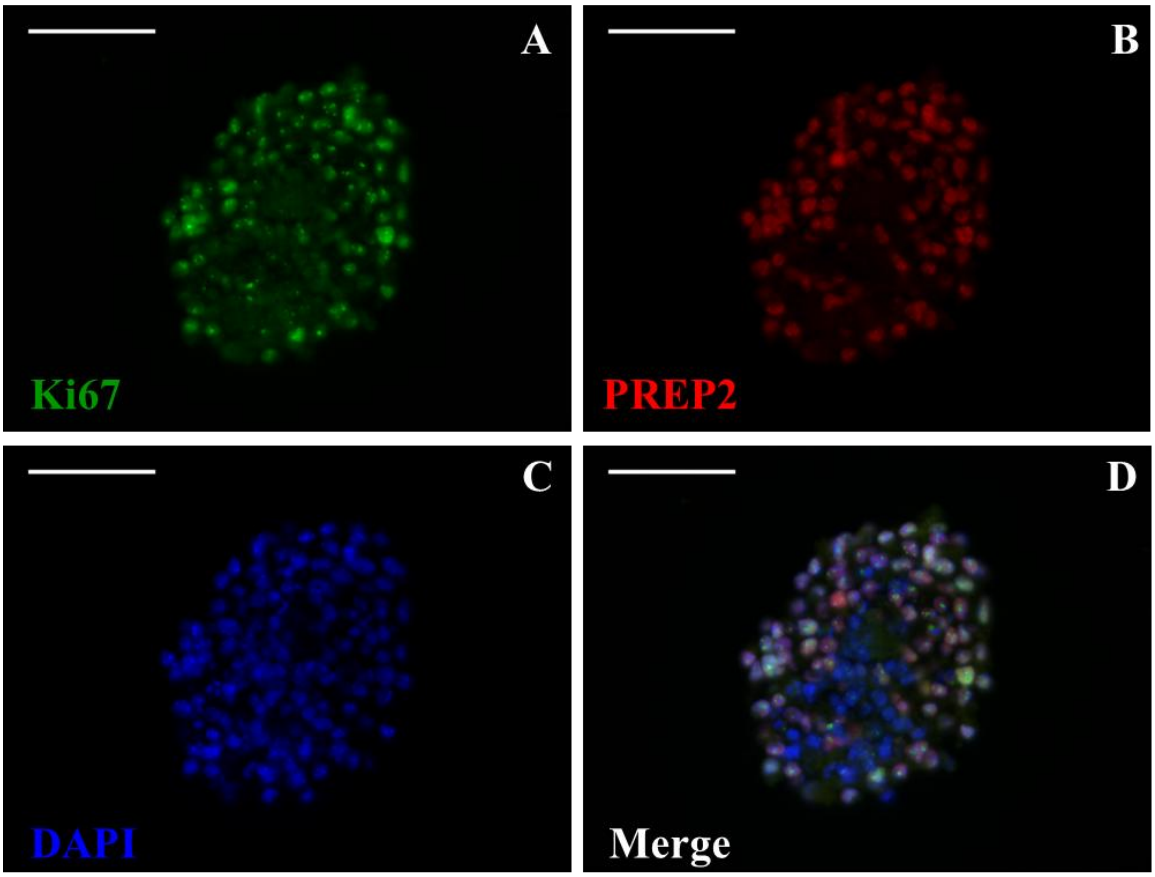

Figure 23. (A) Ki67 and (B) PREP2 expression in embryonic primary neurospheres. Ki67 labels the majority of cells (75%) in the spheres (A), as does PREP2 (75%) in overlapping regions (B). DAPI counterstain labels nuclei (C) and the merged image reveals the coexpression of Ki67 and PREP2 (D). Scale bar = 50 μm.

Western blot data revealed relatively stable levels of PREP2 protein from D0 to D8. Given the heterogeneity and dynamic nature of our culture system from D0 to D8, we were interested in investigating what cell types expressed PREP2. We found that cells expressing the neuronal marker βtubIII co-expressed PREP2, which was localized to the nucleus (Fig 24). We decided to validate our findings in primary neuron and astrocyte cultures that are differentiated *in vivo* (Fig. 25). Our data showed that PREP2 was expressed in primary cortical neurons, where its detection was localized to the nucleus, in euchromatic regions, and excluded from DAPI-rich heterochromatic regions. PREP2 was not detected in the primary cortical astrocyte cultures (preliminary data not shown). Primary antibody omission was performed to control for non-specific interactions involving the secondary antibodies. (Fig. 26). In summary, the TALE protein PREP2 is expressed in neural stem cells, and neurons that are differentiated *in vivo* or *in vitro*.

3.6 *Hox* mRNA transcript expression was tightly restricted in the developing forebrain, neurospheres, and differentiating cells.

In order to verify the expression levels of *Hox* homeobox genes in the forebrain and the forebrain derived NSC system, we performed real-time PCR analysis of 38 mammalian *Hox* genes. Reporter gene and biochemical assays have not previously detected expression of *Hox* genes in the forebrain. Reports of *Hox* detection in ESC-derived neural stem cells raised our interest in the potential of *Hox* genes being expressed in the NSC derived from forebrain and cultured *in vitro* [264]. The use of FGF2 in the culture media also raised the potential that we may see active *Hox* gene expression in the primary neurospheres. In addition to this, the mRNA transcript levels of HOX cofactors (TALE genes) were detected at moderate levels within our system, even in instances that

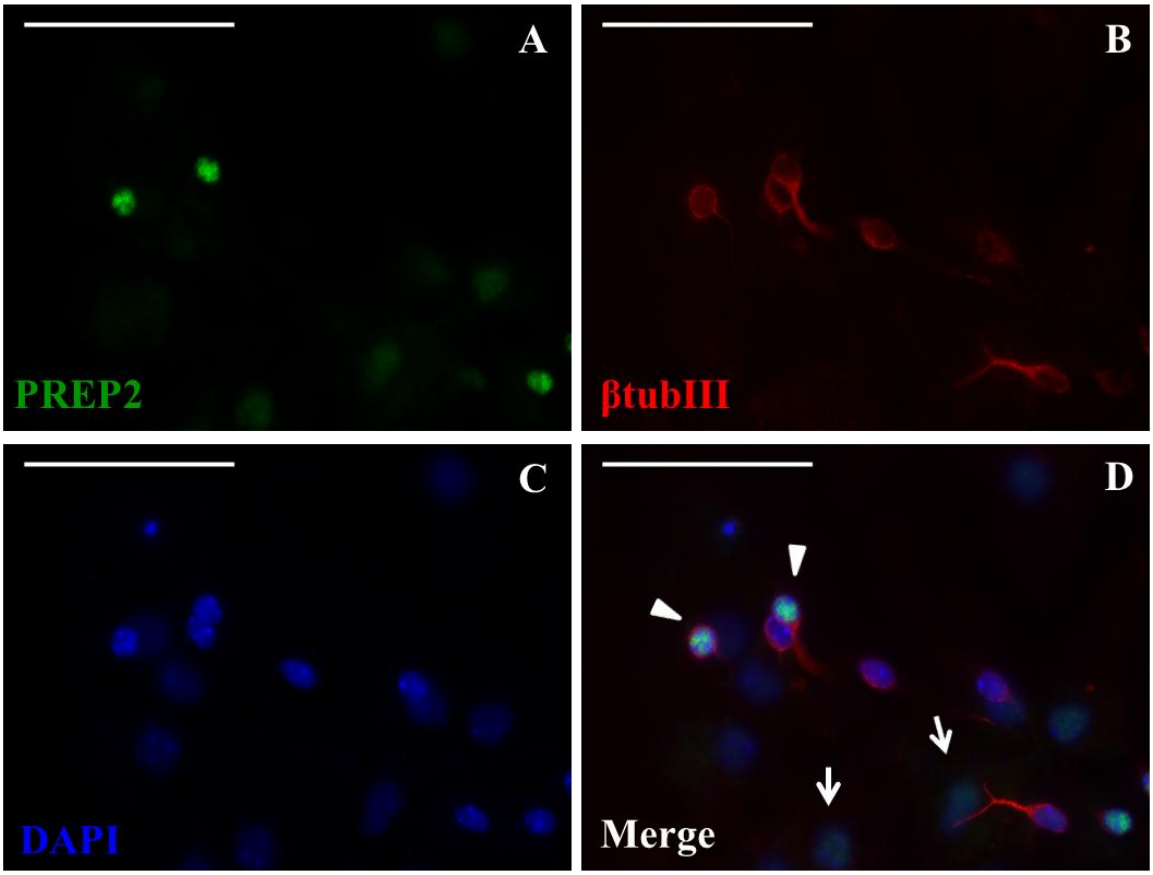

Figure 24. (A) PREP2 and (B) βtubIII expression in D8 differentiated cells. PREP2 (A) positively labels cells most strongly in the regions of βtubIII (B) detection. Much weaker signals are detected in nuclei of cells not expressing βtubIII, indicating PREP2 is expressed at its strongest levels in neurons. DAPI counterstain labels nuclei (C) and the merged image reveals the coexpression of PREP2 and βtubIII (D). The white arrow heads point to $\beta tubIII^{+}$ neurons strongly expressing PREP2, and the white arrows point to $\beta tubIII^{-}$ cells weakly expressing PREP2. Scale bar = 100 μm.

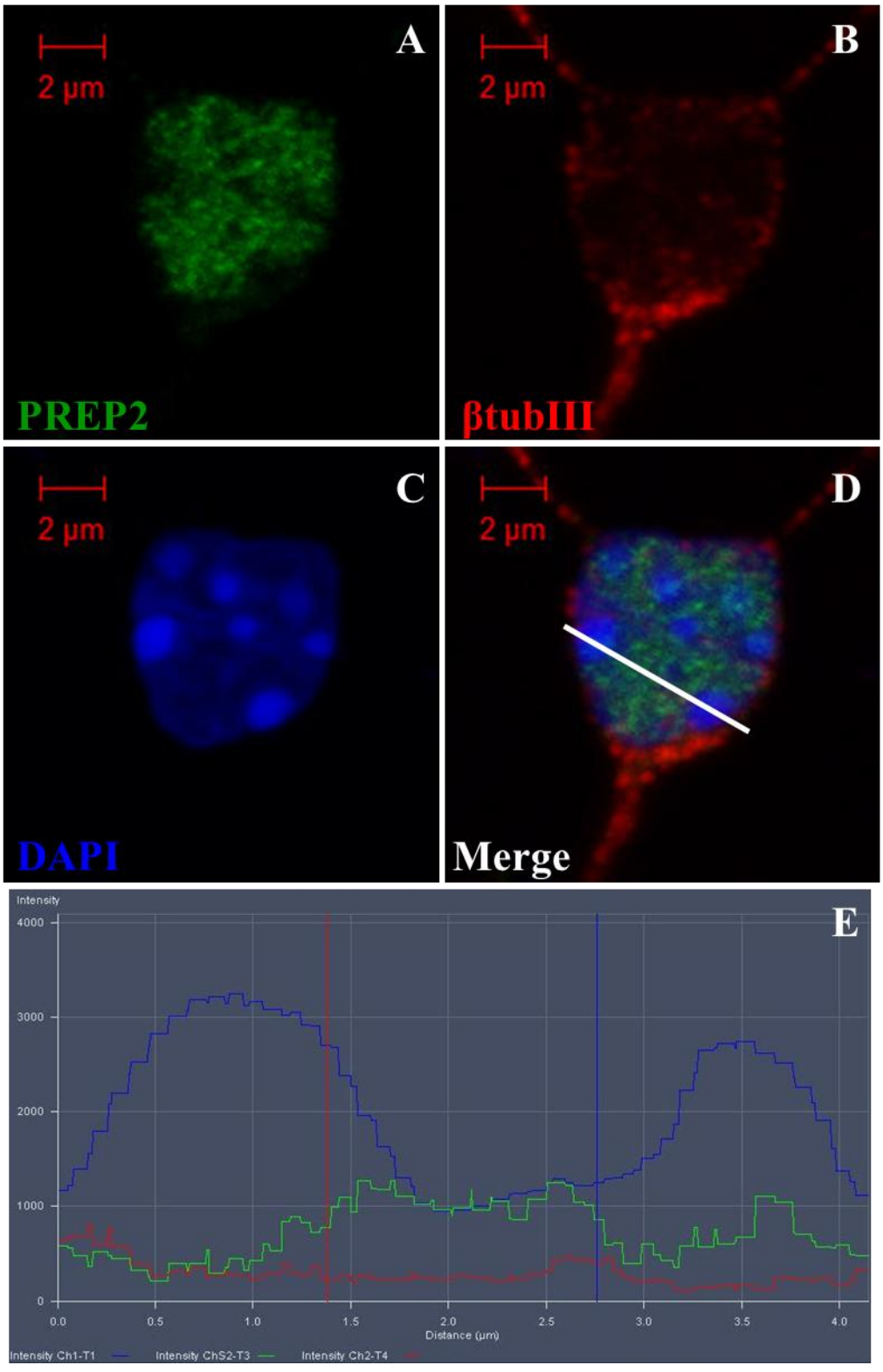
A
2 µm
PREP2
B
2 µm
βtubIII
C
2 µm
DAPI
D
2 µm
Merge
E
Intensity
4000
3000
2000
1000
0
0.0
0.5
1.0
1.5
2.0
2.5
3.0
3.5
4.0
Distance (µm)
Intensity Ch1-T1
Intensity ChS2-T3
Intensity Ch2-T4

Figure 25. PREP2 expression in primary cortical neurons. Embryonic day E18 primary cortical neurons were immunolabelled for PREP2 (A) and βtubIII (B). The nucleus, indicated by DAPI counterstain (C) is positive for PREP2 expression. The merged image (D) reveals that the PREP2 signal is situated throughout the nucleus but excluded from the DAPI-rich regions. Graphing the pixel intensity for each channel, situated along a single line drawn through the nucleus reveals that the signal for PREP2 has a profile that is opposite to that of DAPI (E). (*Robby Zachariah*).

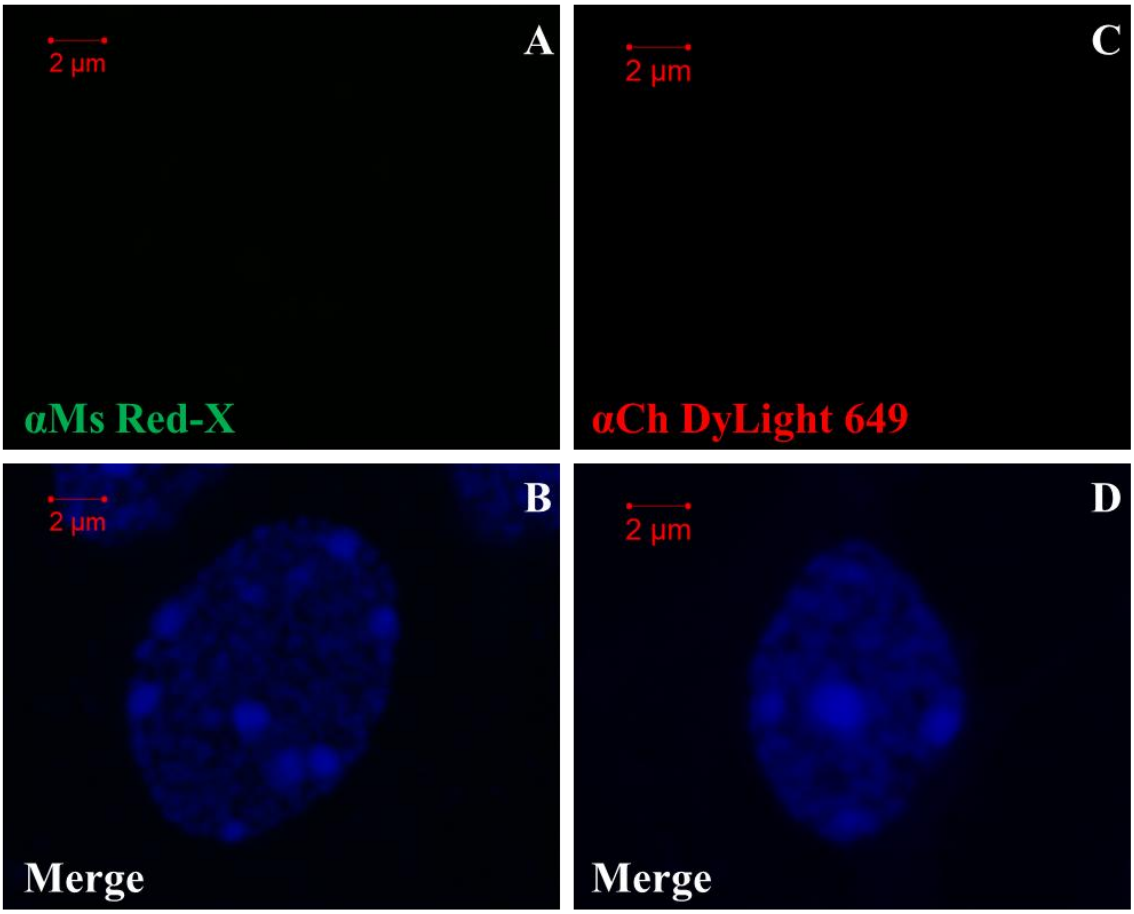

Figure 26. Primary antibody omission control for immunofluorescent labeling of primary cortical neurons. Omission of the mouse monoclonal anti-PREP2 antibody leads to no detectable signal from the anti-mouse IgG Red-X secondary antibody (A). Merged image of anti-PREP2 primary omission with DAPI counterstain (B). Omission of the chicken polyclonal anti-βtubIII antibody leads to no detectable signal from the anti-chicken IgY Dylight 649 secondary antibody (C). Merged image of anti-βtubIII primary omission with DAPI counterstain (D). (*Robby Zachariah*).

these were barely detectable at the protein level. The *Hox* transcripts were detected at extremely low levels relative to the housekeeping genes and other genes of interest. The Ct values for the majority of *Hox* genes were above 35, our threshold for considering transcripts to be expressed (Table 3). A proportion of *Hox* transcripts were observed to have Ct values of between 30-35 and none had Ct values below 30, indicating that they were not being actively expressed and suggesting these genes are not involved in the forebrain, neural stem cells, nor differentiation programs. More transcripts had Ct values below 35 in the whole forebrain than any of the other samples, indicating that expression from the *Hox* loci were even more tightly regulated in the neurospheres and differentiating cells.

Regulators of the *Hox* genes include the polycomb-group proteins, which are involved in chromatin remodelling and were originally identified in the fruit fly as *Hox* gene repressors. Trithorax-group proteins also regulate *Hox* gene expression, but antagonize polycomb-group repression; both protein groups are involved in the formation of complexes that modify histone methylation [265]. In order to investigate the potential role of such regulators in our NSC system, we used real-time PCR to analyze the mRNA expression levels of a group of epigenetic modifiers including histone methyl transferases (*Ezh2* and *Mll1*), histone demethylases (*Jmjd3* and *Utx*) and a mediator of histone ubiquitination (*Bmi1*) (Fig. 27). We did this to see whether the expression pattern of these genes could be associated with the changing levels of TALE transcription factors in forebrain, neurospheres and differentiating cell samples. There was a significant decrease in the transcripts of all epigenetic modifiers in the neurospheres relative to the whole forebrain with the exception of the histone demethylase *Jmjd3*. During differentiation, the

transcripts were significantly increased in D1 and D8 cells. *Jmjd3* showed approximately the same fold change pattern as the other histone modifier genes, but the results were not statistically significant. In summary, the *Hox* genes were found to be active in neither forebrain-derived NSC nor their differentiating progeny. We also found that cultured primary neurospheres, in general, showed decreasing expression of TALE homeobox genes and epigenetic modifiers, when compared to the whole forebrain and differentiating cells.

Hox mRNA	FB	D0	D1	D8
Hoxa1	34	37	33	35
Hoxa2	33	36	32	32
Hoxa3	36	40	39	40
Hoxa4	32	35	40	40
Hoxa5	35	39	37	38
Hoxa6	34	38	37	38
Hoxa7	37	38	37	39
Hoxa9	40	40	40	40
Hoxa10	40	40	38	35
Hoxa11	35	40	40	40
Hoxa13	36	40	33	40
Hoxb1	33	33	35	32
Hoxb2	31	40	37	36
Hoxb3	34	40	39	37
Hoxb4	34	40	38	40
Hoxb5	35	40	37	38
Hoxb6	34	35	35	35
Hoxb7	35	35	35	33
Hoxb8	37	39	39	40
Hoxb9	32	36	36	33
Hoxb13	38	33	39	40
Hoxc4	35	40	38	40
Hoxc5	34	36	37	36
Hoxc6	32	40	36	38
Hoxc8	39	40	40	40
Hoxc9	34	35	37	39
Hoxc10	35	37	39	37
Hoxc11	37	40	38	39
Hoxc12	30	30	31	30
Hoxc13	36	40	32	40
Hoxd1	33	40	35	40
Hoxd3	35	40	40	40
Hoxd4	34	40	40	39
Hoxd9	36	40	40	40
Hoxd10	38	39	35	38
Hoxd11	35	35	34	35
Hoxd12	35	38	38	40
Hoxd13	36	38	33	40

Table 5. *Hox* mRNA transcript threshold cycle (Ct) values from real-time PCR analysis. Real-time PCR analysis revealed that no *Hox* gene transcript had a Ct value below 30 in the E14 forebrain (FB), neurospheres (D0) or in differentiating cells (D1 and D8). Each Ct value presented is the average of three Ct values derived from three separate experiments.

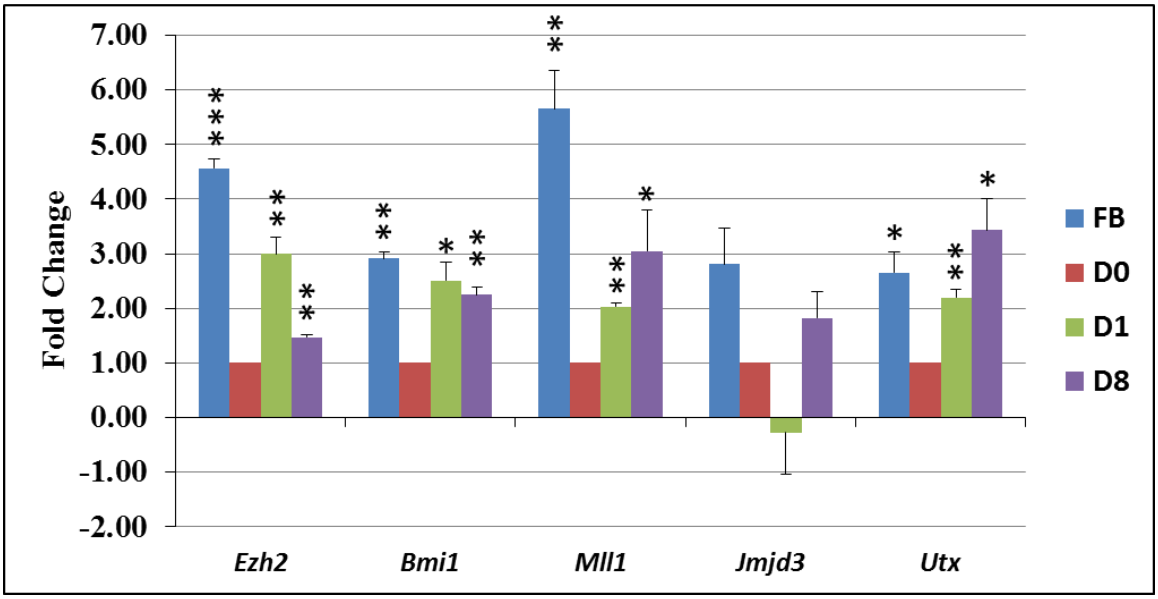

Figure 27. Fold change detection of epigenetic modifier mRNA transcripts by real-time PCR. The mRNA transcript levels of several histone modifiers were detected in neurospheres versus forebrain and differentiating cells. Threshold cycle (Ct) values were normalized to *gapdh* and the students t-test was used to detect significant differences between the normalized Ct values (ΔCt) at D0 versus FB, D1 and D8 based on a sample size of n=3. (*) $P \leq 0.05$, (**) $P \leq 0.01$, (***) $P \leq 0.001$. Fold change in transcript levels is reported with standard error bars.

4 Discussion

4.1 Character of E14 forebrain-derived primary neurospheres.

Embryonic day E14.5 forebrain-derived primary neural stem cells are isolated from the developing forebrain at a time when the NSC component is transitioning from a state of neurogenesis to gliogenesis [119]. The neurospheres generated by proliferating NSC *in vitro* have a gene expression profile that appears to be more astrocytic in nature, when compared with the whole forebrain. This is not supported by the protein expression levels, however, as the percentages of $GFAP^+$ and $NEUN^+$ cells are very low in these neurospheres. The advantage of labelling sectioned spheres versus whole spheres is that we can distinguish individual cell nuclei based on the detection of DAPI, for the purpose of quantifying the proportion of cells expressing a specific protein. The improved resolution when labelling sections versus whole spheres also makes it possible to describe the 3-dimensional position of the specific cell type markers. As previously described, the differentiated cells were localized to the core region of the neurospheres and the signals for neural stem cells were mainly found in the periphery [263]. In contrast, we observed that the OLIG2 signal is localized to the peripheral region where we detected SOX2 and NESTIN. This localization indicates that OLIG2 expression is mainly in the undifferentiated cells and may have a role in neural stem cell properties *in vitro*. A drawback of sectioning is that detecting cytoplasmic or fibrillary protein for the purpose of quantification is difficult due to overlapping cytoplasmic regions and mechanical damage from sectioning. This can be seen in the quality of GFAP labelling in the sectioned neurospheres when compared with the D8 astrocytes. However, because of the

dispersed nature of the $GFAP^+$ cells in the neurospheres it is still possible to quantify them without the concern of under counting $GFAP^+$ cells due to overlapping cytoplasms.

The embryonic forebrain as a whole, is a heterogeneous environment composed of neurons, glia and committed progenitors of different CNS cell type lineages as well as neural stem cells. The neurospheres are not pure clonal bodies and may be the product of aggregates conjoining in culture. However, they mainly consist of undifferentiated cells with the potential to give rise to enriched populations of neurons, astrocytes or oligodendrocytes depending on the specific culture conditions [129,266]. Assessing the transcript expression profile of our neurospheres (D0) takes place after one week in NSC culture conditions. At this point *Gfap* expression is significantly increased relative to forebrain while expression of the neuronal and oligodendrocyte lineage markers are significantly decreased. It would appear that these spheres are programmed to preferentially give rise to astrocytes, but they are not fully restricted to the astrocyte lineage as others have shown [267-268]. We suggest that this is attributable to a fate program associated with the developmental period from which they are isolated, which is maintained during expansion *in vitro*. The minimalist conditions used for differentiation then enables the cells to acquire the differentiated astrocyte fate, as is evident by the large majority of differentiated D8 cells positively labelled for GFAP. For consistency of the results, we only used primary brain-derived NSC neurospheres and have analyzed neither secondary nor tertiary spheres for GFAP protein expression. However, based on other reports it appears that translation of the accumulating *Gfap* transcripts is not permitted or is very inefficient, as the number of $GFAP^+$ cells detected in the spheres does not increase over time with increased passage number [269]. The fact that these cells maintain the fate

acquisition that is observed *in vivo* during NSC development suggests that our NSC culture system is a reliable model for detecting genes that are involved in the propagation and differentiation of neural stem cells. We suggest that the increase in *Sox2* expression observed in differentiating cells over neurospheres is due to the expanding population of astrocytes. It has been shown that non-quiescent astrocytes cultured directly form E13.5 VZ, or differentiated from E13.5 forebrain-derived NSC express SOX2 [109]. In our system we observe an increase in the confluency of astrocytes from day 1 through day 8. Therefore, although SOX2 is used as an NSC marker, it is actively expressed in the differentiating cells, and these cells are comprised mainly of expanding astrocytes. While this should be a caveat to using SOX2 as an NSC marker, it does support the inference that the *Gfap* signal detected by real-time RT-PCR in the neurospheres is largely coming from $SOX2^{+}$ precursor cells.

4.2 Neural stem cell signalling pathways and cell-type lineage associations.

Our analysis of *Notch1-4* transcripts supports the idea that these receptors have non-redundant and non-compensatory roles in NSC neurogenesis. A limitation in our approach was that the data directly address neither receptor-ligand interactions, nor activation of the signalling cascades. We were limited to making associations between the changing transcript expression levels of different genes and the different cell sources from which the RNA was derived. We would have expected compensation between NOTCH receptors if we had detected a decrease in one receptor's transcripts accompanied by the increase of another; however, this was not determined to be the case. The largest change seen in receptor expression is the increase in *Notch2* during differentiation of the cells, which are strongly enriched for astrocytes. The *Notch2*-

astrocyte fate association seems to be in agreement with recent findings that *Notch2* expression is reduced in differentiating E14.5-derived NSC that become neurogenic at the cost of gliogenesis, when *Stat3* is conditionally deleted [270]. Previous research studies show that NOTCH signalling is involved in NSC self-renewal, glial differentiation and repression of neuronal commitment [271-276]. Our results indicate that receptors *Notch2* and *Notch4* may have a larger role to play in glial differentiation versus *Notch1* and *Notch3,* based on their expression patterns. Decreased levels of *Hes5* are an indicator of differentiation in general, but also that this decrease is more pronounced in the context of glial differentiation versus neuronal. *Hes5* was also decreased in the differentiating NSC with the *Stat3* conditional deletion, which allows for increased expression of some neuronal genes but not *Mash1*. We also see no increase in *Mash1* despite the down-regulation of *Hes5*. Astrocyte differentiation is known to be induced by *Stat3* in E14.5 neural precursor cells [277] and our results show that *Stat3* induction is apparent in the neurospheres derived from E14 embryos, once again suggesting that the gliogenic nature of the neural stem cells in culture has already been established before isolation. Using NSC derived from the adult hippocampus, Tanigaki *et al*. (2001) demonstrated that *Notch1* and *Notch3* activation promotes astrogliogenesis in a *Stat3* independent manner, and this is accompanied by activation of *Hes1* [274]. In our system, we find that *Notch1*, *Notch3* and *Hes1* expression are relatively static indicating that these genes may compose a NOTCH signalling mechanism that is specific to adult hippocampal derived NSC fate as described by Tanigaki *et al*., while *Notch2* and *Notch4* might be the receptors involved in E14.5 forebrain-derived neural stem cell differentiation. While STAT3 potentiates expansion of E12.5-derived NPC *via* activation of *Dll1* [278], we observed no increase in

Dll1 in neurospheres relative to forebrain despite the selection for self-renewing NSC and the significant increase in *Stat3* transcript expression. *Dll1* is activated by pro-neuronal genes like *Mash1* so that differentiating neurons induce NOTCH signalling in adjacent NSC and prevent their neuronal differentiation (lateral inhibition) [279]. This could be one reason why in our system where neuronal differentiation is nearly absent, we see decreasing *Dll1* expression during differentiation. A similar argument is made for the decline in *Jagged* ligands, as it was recently shown that in the developing E14 brain *Jag1* is co-expressed with proneuronal genes [280]. We show NOTCH receptors either maintain or increase their mRNA expression levels during astrocyte differentiation, which corroborates previous evidence implicating NOTCH signalling in astrocyte fate commitment as well as astrocyte differentiation [281-282]. It is possible that the receptors that increase during differentiation are more involved in the later task of promoting astrocyte differentiation, whereas *Notch1* and *Notch3* are more involved in repressing neuronal differentiation. Each of the ligands show decreasing levels, which does not suggest that the variety of receptors and ligands implement specific receptor-ligand interactions with exclusive roles in the context of E14.5 forebrain-derived NSC self-renewal and differentiation. The declining levels of ligand transcripts do suggest that the ligands are not maintaining NSC populations *via* activation of NOTCH receptors when the cells are placed in differentiation conditions.

While BMP2 is involved in promoting astrocyte differentiation [283-284], we detect only a very minor increase in the expression of *Bmp2* in our system. This suggests that in our system BMP4 might be a much more relevant factor for differentiation as there is a drastic increase in its transcripts. BMP4 is known to be involved in generating astrocytes

from neural stem cells, and promoting the survival of astrocyte precursor cells [161,285-286]. The increase in *Bmp7* in neurospheres raises interest in whether BMP7 may be involved in the astrocyte commitment of neural stem cells versus the astrocyte differentiation process, in our system. It was recently shown that BMP7 activation was capable of inducing astrocyte differentiation from radial glia and this involved an increase in transition of radial glia (RG) to committed glial precursor cells [160]. In the study, the activation of BMP7 was the result of BDNF treatment and the induction was observed in neurons, possibly explaining why we see a decrease in *Bmp7* expression upon differentiation. In the context of primary NSC derived from the E14 forebrain, *Bmp4* may have a prevailing role in astrocyte differentiation with respect to BMP-induced astrocyte differentiation, and the role of *Bmp7* may be specific to early commitment of the neural stem cells.

Changing transcript levels can be used to draw associations with cell processes occurring simultaneously in culture. To go beyond this analysis, and draw conclusions regarding the impact of these gene expression changes requires further descriptive and functional assays. Detection of the signalling pathway protein levels as well as expression of target genes would be a starting point to reveal the activity level of these pathways at different stages. It is cautioned that, as discussed above, the role of these pathways is context dependent and our results are specific to the E14 primary forebrain-derived NSC differentiated *in vitro*, under fixed conditions.

4.3 *In vitro* expression of forebrain transcription factors in forebrain-derived neurospheres and their differentiating progeny.

The genes that we investigated due to their important roles in forebrain neuronal development were actively transcribed in our system. *Dlx2* is involved in later stages of striatal neuronal development. It has been shown that *Dlx2* expression is induced through repression of NOTCH signalling in the lateral ganglionic eminence and potentially repression of the early neuronal commitment gene *Mash1* [287]. *Dlx5* is essential for development of the olfactory bulb and postnatal neuronogenesis [288-289]. Like the neuronal marker *βtubIII*, there is a transient increase in the expression levels of these neuronal transcripts. This may have to do with the differentiation of the few neurons that arise in our system. While the levels of these transcripts are significantly reduced in the apparently astrocyte-committed neurospheres, a small percentage of cells likely still mature as neurons under our differentiation conditions. *Pax6* has long been studied for its role in neural stem cells and neuronogenesis in the forebrain; therefore, the decrease in *Pax6* in neurospheres relative to whole forebrain is understandable due to the contrast between the astrocyte committed neurospheres and neuron-rich forebrain samples. The rise in *Pax6* levels during astrocyte differentiation is in agreement with a recent discovery that *Pax6* expression is critical for forebrain NSC astrocyte differentiation [290]. *Nkx2-2* is important for the establishment of oligodendrocytes; however, a role for its expression specifically in the forebrain has not been deciphered. Despite the rare occurence of oligodendrocytes in differentiating cells, *Nkx2-2* showed increased expression levels in neurospheres over forebrain. The rise in *Nkx2-2* levels in neurospheres over forebrain may be due to the glial versus neuronal commitment of the cell populations being

assayed. This may be part of a transcription program that includes the expression of *Olig2*. Upon differentiation towards astrocytes, we therefore see an overall decrease in *Nkx2-2* levels relative to the neurospheres, when the glial precursors become astrocytes and not oligodendrocytes. Alternatively, Nkx2-2 may have a specific role in early commitment of astroglia, but not in the process of astrocyte differentiation.

4.4 Forebrain-derived NSC provide a convenient model system to study the role of TALE genes in neural development.

Previous reports indicate that human and mouse ESC-derived neural stem cells and their differentiating progeny express *Hox* genes [264,291]. *In vivo*, there is no evidence to suggest that *Hox* genes are expressed in the forebrain or involved in its development. Because of the detection of *Hox* in ESC-derived neural stem cells and the fact that their DNA binding cofactors, the TALE proteins are expressed in neurogenic regions of the developing forebrain, we decided to investigate the expression levels of *Hox* transcripts in forebrain derived primary NSC and their differentiating progeny. Detection of *Hox* transcripts was negative, indicating that *Hox* gene expression in ESC-derived neural stem cells is in contrast to primary NSC derived from the developing forebrain. The findings suggest that ESC may harbour intrinsic vulnerabilities to gene expression programming, making them a poor consideration as a cell source for regenerative therapies, particularly for forebrain insults. Retinoic acid, which is used to induce neuronal differentiation from ESC is a known inducer of *Hox* gene expression and it may be that the differentiating ESC, are suited for repair of other CNS regions [253,292-293], which involve regulated expression of *Hox* genes. The findings also indicate that a developmental role for TALE genes in the forebrain would be independent of interactions with HOX proteins.

Therefore, primary forebrain-derived neural stem cells may provide a convenient system to study the HOX-independent role of TALE genes.

To begin studying *Hox*-independent roles for TALE genes, it is first necessary to identify the TALE factors which are expressed in this system. MEIS1 and PBX1 have been described as being associated with the neuronal lineage. In the rat, PBX1 has been detected in proliferating cells of the post-natal SVZ and their neuronal progeny in the caudal-rostral migratory stream that is exploited by neurons replenishing the olfactory bulb [223]. MEIS1 is activated upon neuronal differentiation in P19 cells and has been detected in neuroblastoma [294-296]. MEIS1 and PBX1 proteins were detected at low levels by western blot and IF in the neurospheres, which we have described as astrocyte-commited. Therefore, based on this evidence it would appear that these TALE proteins are involved in the regulation of cells that are already commited to a neuronal fate. However, this does not address the role of MEIS1 detected in D8 cells. Previous data on the *Prep* genes make it difficult to speculate on what role they may play in NSC characteristics such as self-renewal and differentiation. PREP1 was not detected in the neurospheres, but the cells expressing PREP2 in neurospheres coexpressed the NSC marker SOX2 and the proliferating cell marker Ki67. We conclude that PREP2 is expressed in actively dividing cells of the neurospheres including neural stem cells, potentially implicating PREP2 as a regulator of these undifferentiated cells.

All of the TALE genes were expressed at significantly higher levels in the whole forebrain relative to the neurospheres and detection by real-time PCR showed specific expression patterns for the TALE transcripts in neurospheres and differentiating cells. However, many of the changes observed were not statistically significant. Increasing the

sample size would be one way to see whether the observed changes are significant. Recognizing that the transcripts were still detectable despite being down-regulated in neurospheres relative to the whole forebrain, we assayed the protein expression of these genes using western blot. PBX1 and PREP1 were barely detectable from D0 to D8, while MEIS1 showed an increase by D8. Based on their transcript levels we expected to detect PBX1 and PREP1 protein, but the lack of detection by western blot and IF labelling could be due to post transcriptional regulation whereby translation of the transcript is prevented, or active degradation of the protein as it is translated. The high levels of MEIS1 detected in the D8 differentiated cells indicate that MEIS1 may have a role in the late stages of astrocyte differentiation. We have attempted IF labelling experiments in D8 cells using anti-MEIS1 antibody; however, no MEIS1 signal was detected. The detection in neurospheres and sectioned E14.5 forebrains (data not shown) but not in D8 differentiated cells may be the result of the epitope being masked in differentiated cells. Protein modification in the context of D8 cells could be a reason for this, as could protein-protein interactions. The next step for investigating MEIS1 function in astrocyte differentiation is to verify the cell-type expression of MEIS1 in the D8 cells. Alternative approaches to do this include attempting antigen retrieval or using an antibody targeting a different epitope within the protein.

PREP2 was detected at much higher levels than the other TALE genes and this expression was relatively unchanged from D0 to D8. From our IF experiments the cell population that remains unchanged from D0 to D8 are neurons detected by NEUN and βtubIII staining. The neuronal lineage represents a small proportion of cells and can not explain the percentage of NSC and progenitors labelled positively by IF, for PREP2 in

the neurospheres. Mature astrocytes are ruled out as the source of PREP2 in the blots, since mature astrocytes overtake the cell population from D0 to D8 indicating that PREP2 detection would increase drastically. It is also apparent that PREP2 does not function eclusively as a self-renewal gene in NSC since there is an increase in PREP2 levels relative to GAPDH, upon differentiation. The PREP2 protein may have more than one role in the context of NSC development. In the neural stem and progenitor cells, PREP2 may be involved in maintenance or proliferation, and during differentiation it may have a role in lineage restriction. In initial experiements, western blots were performed for each TALE factor and normalized to β-Actin; however, we found that the levels of this housekeeping gene were variable making for a poor loading control. We found that GAPDH levels were less variable and chose to use this as our loading control for normalization and quantitative analysis. The GAPDH loading control data for PBX1 and PREP1 was not performed, a decrease in the levels of both of these proteins in the neurospheres and differentiating cells relative to the whole forebrain is evident.

Immunofluorescent labeling of PREP2 in D8 cells indicate that it is strongly detected in nuclei of neurons labelled with βtubIII^{+}. Co-labelling experiments in E18-derived primary cortical neurons showed that the PREP2 signal was co-localized with DAPI-poor regions and excluded from DAPI-rich regions in both the *in vitro* and *in vivo* differentiated neurons. This indicates that PREP2 protein in the nucleus is likely localized to euchromatic versus heterochromatic regions, which is characteristic of transcription factors actively involved in transcriptional regulation. We detected very faint PREP2 expression in non-neuronal cells, but have yet to perform successful colabelling experiments to determine in which cell types PREP2 is expressed. Given the proportion

of $GFAP^+$ cells in the population, it is reasonable to predict these are astrocytes. The subnuclear expression pattern was the same as neurons but the signal was very faint in comparison. These findings support the notion that PREP2 is involved in transcriptional regulation in neurons, and that *in vitro* neuronal differentiation of forebrain NSC is a reliable system to study the role of PREP2 in cortical neurogenesis. The absence of *Hox* and expression levels of PREP2 detected by our experiments suggest that there is an effective reconstruction of the *in vivo* expression programs of these genes, within our *in vitro* system.

Our results also indicate that the primary forebrain-derived NSC system would allow for experiments regarding the effect of aberrant *Hox* gene expression in the forebrain-derived neural stem cells. Studies have revealed that forebrain-derived tumours aberrantly express *Hox* genes [297-298]. In the context of ESC-derived neural stem cells, HOXB1 expression increases self-renewal capacity and resists differentiation [253]. Inducing *Hox* genes in forebrain-derived NSC *in vitro* would allow for investigating the effect of aberrant *Hox* expression on NSC proliferation rate and their inclination to differentiate. Deregulated *Hox* and TALE gene expression has been associated with leukemia and other cancers, and the interplay between these families of genes was shown to be important [246-248]. Introducing the potential for these proteins to interact and influence gene expression where they do not normally interact, for example HOX and PREP2 in the forebrain, could have a drastic effect on cell phenotype. One hypothesis is that this would lead to increased proliferation of stem cells and progenitors, reminiscent of cancer phenotypes. This would provide an *in vitro* system to study tumourogenesis in the context of NSC transformed by aberrant *Hox* gene expression.

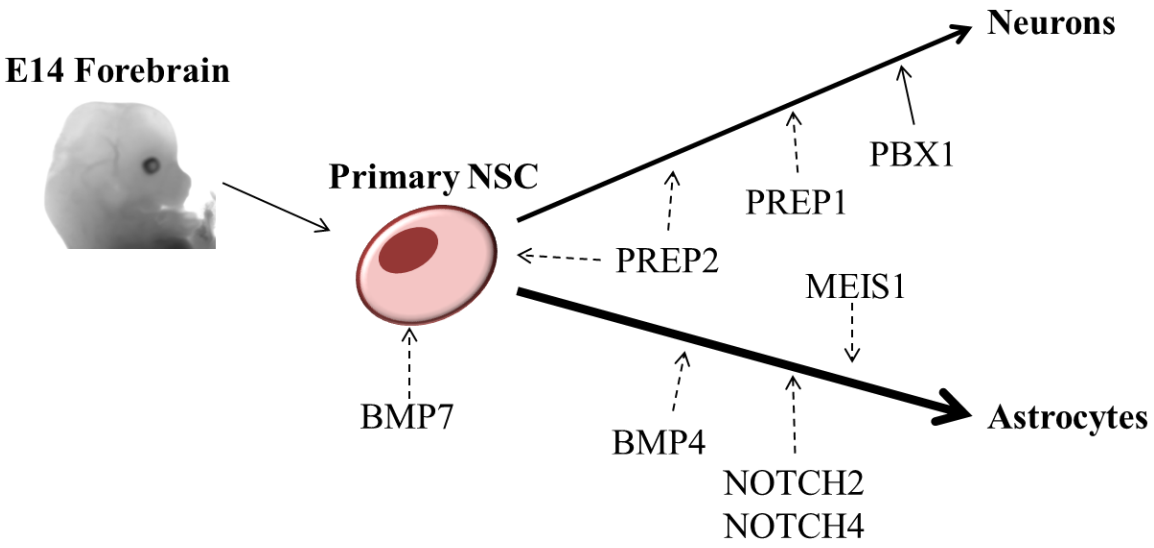

Figure 28. Proposed model of TALE protein influence on cell-type lineages. E14 forebrain-derived NSC differentiate into mainly astrocytes as depicted by the thicker arrow, and to a lesser extent neurons as indicated by the thinner arrow. Proposed roles for TALE proteins, as well as NOTCH and BMP proteins are indicated by the broken arrows. The solid arrow indicates the established role of PBX1 in neuron development.

5.1 Conclusion

We have shown that E14.5 forebrain-derived primary NSC cultured *in vitro* have an intrinsic astrocytic gene expression profile. These cells preferentially give rise to astrocytes. The TALE homeobox genes are actively transcribed in E14.5 forebrain-derived primary neural stem cells; however, expression at the protein level is tightly regulated. The expression profile of PREP2 suggests that this protein may have a role in NSC proliferation and neurogenesis, while the expression pattern of MEIS1 is suggestive of a role in astrocyte differentiation.

5.2 Future Directions

To more fully describe the association between the TALE genes and neural lineages acquired *in vitro,* we will perform triple immunofluorescent labelling for each of the TALE proteins with GFAP and βtubIII in the D8 differentiated cells. We will also perform co-labelling experiments, for each TALE protein and the neural stem cell markers in E14.5 forbrain sections, to verify *in vivo* whether the TALE proteins are expressed in neural stem cells. Similarly, the TALE proteins will be co-labelled with the astrocyte, neuron and oligodendrocyte markers in forebrain sections to compare their *in vitro* and *in vivo* expression patterns.

To investigate the role of PREP2 in neuronal differentiation we will begin by detecting the expression of PREP2 in P19 cells that have been treated with all trans-retinoic acid for neuronal differentiation. This system provides a convenient system to knock-down *Prep2* expression by means of siRNA plasmid transfection, if PREP2 is found to be expressed during or after neuronal differentiation. A role for PREP2 in P19

neuronal differentiation will further rationalize investigating the effects of lentivirus-mediated knock-down of PREP2 in primary neural stem cell. Similarly, lentiviral knock-down targeting MEIS1 in differentiating neural stem cells will reveal the role of MEIS1 in astrocyte maturation.

The results of these studies would describe the involvement of TALE genes in NSC fate decisions and increase our knowledge of how transcription factors can regulate the acquisition of specific cell types *in vitro*. This knowledge is important for regenerative therapies based on cell transplantation, as well as understanding the genetic programs involved in CNS development. The information acquired from these *in vitro* studies and mouse modelling can be used in conjunction with what is known about human disease and development to better predict not only the safety and efficacy of cell transplant therapies, but also the etiology of human disease.

5.3 References

1. Evans, M.J. & Kaufman, M.H. Establishment in culture of pluripotential cells from mouse embryos. *Nature* **292**, 154-156 (1981).

2. Reynolds, B.A. & Weiss, S. Generation of neurons and astrocytes from isolated cells of the adult mammalian central nervous system. *Science* **255**, 1707-1710 (1992).

3. Takahashi, K. & Yamanaka, S. Induction of pluripotent stem cells from mouse embryonic and adult fibroblast cultures by defined factors. *Cell* **126**, 663-676 (2006).

4. Williams, A.R. & Hare, J.M. Mesenchymal stem cells: biology, pathophysiology, translational findings, and therapeutic implications for cardiac disease. *Circ Res* **109**, 923-940 (2011).

5. Kriks, S., *et al.* Dopamine neurons derived from human ES cells efficiently engraft in animal models of Parkinson's disease. *Nature* **480**, 547-551 (2011).

6. Bhatia, S. Long-term health impacts of hematopoietic stem cell transplantation inform recommendations for follow-up. *Expert Rev Hematol* **4**, 437-452; quiz 453-434 (2011).

7. Weiss, S., *et al.* Multipotent CNS stem cells are present in the adult mammalian spinal cord and ventricular neuroaxis. *J Neurosci* **16**, 7599-7609 (1996).

8. Kukekov, V.G., *et al.* Multipotent stem/progenitor cells with similar properties arise from two neurogenic regions of adult human brain. *Exp Neurol* **156**, 333-344 (1999).

9. Albert, M. & Peters, A.H. Genetic and epigenetic control of early mouse development. *Curr Opin Genet Dev* **19**, 113-121 (2009).

10. Gage, F.H., Ray, J. & Fisher, L.J. Isolation, characterization, and use of stem cells from the CNS. *Annu Rev Neurosci* **18**, 159-192 (1995).

11. Beyer Nardi, N. & da Silva Meirelles, L. Mesenchymal stem cells: isolation, in vitro expansion and characterization. *Handb Exp Pharmacol*, 249-282 (2006).

12. Bhatia, M., Bonnet, D., Murdoch, B., Gan, O.I. & Dick, J.E. A newly discovered class of human hematopoietic cells with SCID-repopulating activity. *Nat Med* **4**, 1038-1045 (1998).

13. Wolpert, L. *Principles of development*, (Oxford University Press, Oxford ; New York, 2007).

14. Stevens, L.C. The development of transplantable teratocarcinomas from intratesticular grafts of pre- and postimplantation mouse embryos. *Dev Biol* **21**, 364-382 (1970).

15. Thomson, J.A., *et al.* Embryonic stem cell lines derived from human blastocysts. *Science* **282**, 1145-1147 (1998).

16. Niwa, H., Miyazaki, J. & Smith, A.G. Quantitative expression of Oct-3/4 defines differentiation, dedifferentiation or self-renewal of ES cells. *Nat Genet* **24**, 372-376 (2000).

17. Chambers, I., *et al.* Functional expression cloning of Nanog, a pluripotency sustaining factor in embryonic stem cells. *Cell* **113**, 643-655 (2003).

18. Berstine, E.G., Hooper, M.L., Grandchamp, S. & Ephrussi, B. Alkaline phosphatase activity in mouse teratoma. *Proc Natl Acad Sci U S A* **70**, 3899-3903 (1973).

19. O'Connor, M.D., Kardel, M.D. & Eaves, C.J. Functional assays for human embryonic stem cell pluripotency. *Methods Mol Biol* **690**, 67-80 (2011).

20. Martin, G.R. Teratocarcinomas and mammalian embryogenesis. *Science* **209**, 768-776 (1980).

21. Bradley, A., Evans, M., Kaufman, M.H. & Robertson, E. Formation of germ-line chimaeras from embryo-derived teratocarcinoma cell lines. *Nature* **309**, 255-256 (1984).

22. Rowland, J.W., *et al.* Generation of neural stem cells from embryonic stem cells using the default mechanism: in vitro and in vivo characterization. *Stem Cells Dev* **20**, 1829-1845 (2011).

23. Tropepe, V., *et al.* Direct neural fate specification from embryonic stem cells: a primitive mammalian neural stem cell stage acquired through a default mechanism. *Neuron* **30**, 65-78 (2001).

24. Gaspard, N., *et al.* An intrinsic mechanism of corticogenesis from embryonic stem cells. *Nature* **455**, 351-357 (2008).

25. Bouhon, I.A., Joannides, A., Kato, H., Chandran, S. & Allen, N.D. Embryonic stem cell-derived neural progenitors display temporal restriction to neural patterning. *Stem Cells* **24**, 1908-1913 (2006).

26. Smukler, S.R., Runciman, S.B., Xu, S. & van der Kooy, D. Embryonic stem cells assume a primitive neural stem cell fate in the absence of extrinsic influences. *J Cell Biol* **172**, 79-90 (2006).

27. Bain, G., Kitchens, D., Yao, M., Huettner, J.E. & Gottlieb, D.I. Embryonic stem cells express neuronal properties in vitro. *Dev Biol* **168**, 342-357 (1995).

28. Kim, M., *et al.* Regulation of mouse embryonic stem cell neural differentiation by retinoic acid. *Dev Biol* **328**, 456-471 (2009).

29. Fraichard, A., *et al.* In vitro differentiation of embryonic stem cells into glial cells and functional neurons. *J Cell Sci* **108 (Pt 10)**, 3181-3188 (1995).

30. Strubing, C., *et al.* Differentiation of pluripotent embryonic stem cells into the neuronal lineage in vitro gives rise to mature inhibitory and excitatory neurons. *Mech Dev* **53**, 275-287 (1995).

31. Kawasaki, H., *et al.* Induction of midbrain dopaminergic neurons from ES cells by stromal cell-derived inducing activity. *Neuron* **28**, 31-40 (2000).

32. Wichterle, H., Lieberam, I., Porter, J.A. & Jessell, T.M. Directed differentiation of embryonic stem cells into motor neurons. *Cell* **110**, 385-397 (2002).

33. Salero, E. & Hatten, M.E. Differentiation of ES cells into cerebellar neurons. *Proc Natl Acad Sci U S A* **104**, 2997-3002 (2007).

34. Papalopulu, N. & Kintner, C. A posteriorising factor, retinoic acid, reveals that anteroposterior patterning controls the timing of neuronal differentiation in Xenopus neuroectoderm. *Development* **122**, 3409-3418 (1996).

35. Avantaggiato, V., Acampora, D., Tuorto, F. & Simeone, A. Retinoic acid induces stage-specific repatterning of the rostral central nervous system. *Dev Biol* **175**, 347-357 (1996).

36. Cunningham, M.L., Mac Auley, A. & Mirkes, P.E. From gastrulation to neurulation: transition in retinoic acid sensitivity identifies distinct stages of neural patterning in the rat. *Dev Dyn* **200**, 227-241 (1994).

37. Dresser, R. Stem cell research as innovation: expanding the ethical and policy conversation. *J Law Med Ethics* **38**, 332-341 (2010).

38. Blendon, R.J., Kim, M.K. & Benson, J.M. The public, political parties, and stem-cell research. *N Engl J Med* **365**, 1853-1856 (2011).

39. Robinton, D.A. & Daley, G.Q. The promise of induced pluripotent stem cells in research and therapy. *Nature* **481**, 295-305 (2012).

40. Wilmut, I., Schnieke, A.E., McWhir, J., Kind, A.J. & Campbell, K.H. Viable offspring derived from fetal and adult mammalian cells. *Nature* **385**, 810-813 (1997).

41. Takahashi, K., *et al.* Induction of pluripotent stem cells from adult human fibroblasts by defined factors. *Cell* **131**, 861-872 (2007).

42. Okita, K., Hong, H., Takahashi, K. & Yamanaka, S. Generation of mouse-induced pluripotent stem cells with plasmid vectors. *Nat Protoc* **5**, 418-428 (2010).

43. Mack, A.A., Kroboth, S., Rajesh, D. & Wang, W.B. Generation of induced pluripotent stem cells from CD34+ cells across blood drawn from multiple donors with non-integrating episomal vectors. *PLoS One* **6**, e27956 (2011).

44. Kim, D., *et al.* Generation of human induced pluripotent stem cells by direct delivery of reprogramming proteins. *Cell Stem Cell* **4**, 472-476 (2009).

45. Eminli, S., *et al.* Differentiation stage determines potential of hematopoietic cells for reprogramming into induced pluripotent stem cells. *Nat Genet* **41**, 968-976 (2009).

46. Tat, P.A., Sumer, H., Jones, K.L., Upton, K. & Verma, P.J. The efficient generation of induced pluripotent stem (iPS) cells from adult mouse adipose tissue-derived and neural stem cells. *Cell Transplant* **19**, 525-536 (2010).

47. Kim, J.B., *et al.* Pluripotent stem cells induced from adult neural stem cells by reprogramming with two factors. *Nature* **454**, 646-650 (2008).

48. Fusaki, N., Ban, H., Nishiyama, A., Saeki, K. & Hasegawa, M. Efficient induction of transgene-free human pluripotent stem cells using a vector based on

Sendai virus, an RNA virus that does not integrate into the host genome. *Proc Jpn Acad Ser B Phys Biol Sci* **85**, 348-362 (2009).

49. Okita, K. & Yamanaka, S. Induced pluripotent stem cells: opportunities and challenges. *Philos Trans R Soc Lond B Biol Sci* **366**, 2198-2207 (2011).

50. Amabile, G. & Meissner, A. Induced pluripotent stem cells: current progress and potential for regenerative medicine. *Trends Mol Med* **15**, 59-68 (2009).

51. Lowry, W.E., *et al.* Generation of human induced pluripotent stem cells from dermal fibroblasts. *Proc Natl Acad Sci U S A* **105**, 2883-2888 (2008).

52. Chin, M.H., *et al.* Induced pluripotent stem cells and embryonic stem cells are distinguished by gene expression signatures. *Cell Stem Cell* **5**, 111-123 (2009).

53. Vierbuchen, T., *et al.* Direct conversion of fibroblasts to functional neurons by defined factors. *Nature* **463**, 1035-1041 (2010).

54. Marro, S., *et al.* Direct lineage conversion of terminally differentiated hepatocytes to functional neurons. *Cell Stem Cell* **9**, 374-382 (2011).

55. Kajimura, S., *et al.* Initiation of myoblast to brown fat switch by a PRDM16-C/EBP-beta transcriptional complex. *Nature* **460**, 1154-1158 (2009).

56. Ieda, M., *et al.* Direct reprogramming of fibroblasts into functional cardiomyocytes by defined factors. *Cell* **142**, 375-386 (2010).

57. Graf, T. Historical origins of transdifferentiation and reprogramming. *Cell Stem Cell* **9**, 504-516 (2011).

58. Barber, B.A. & Rastegar, M. Epigenetic control of Hox genes during neurogenesis, development, and disease. *Ann Anat* **192**, 261-274 (2010).

59. Streit, A., Berliner, A.J., Papanayotou, C., Sirulnik, A. & Stern, C.D. Initiation of neural induction by FGF signalling before gastrulation. *Nature* **406**, 74-78 (2000).

60. Wilson, P.A. & Hemmati-Brivanlou, A. Induction of epidermis and inhibition of neural fate by Bmp-4. *Nature* **376**, 331-333 (1995).

61. Pera, E.M., Ikeda, A., Eivers, E. & De Robertis, E.M. Integration of IGF, FGF, and anti-BMP signals via Smad1 phosphorylation in neural induction. *Genes Dev* **17**, 3023-3028 (2003).

62. Keynes, R. & Lumsden, A. Segmentation and the origin of regional diversity in the vertebrate central nervous system. *Neuron* **4**, 1-9 (1990).

63. Wilson, L. & Maden, M. The mechanisms of dorsoventral patterning in the vertebrate neural tube. *Dev Biol* **282**, 1-13 (2005).

64. Stamataki, D., Ulloa, F., Tsoni, S.V., Mynett, A. & Briscoe, J. A gradient of Gli activity mediates graded Sonic Hedgehog signaling in the neural tube. *Genes Dev* **19**, 626-641 (2005).

65. Lumsden, A. & Krumlauf, R. Patterning the vertebrate neuraxis. *Science* **274**, 1109-1115 (1996).

66. Megason, S.G. & McMahon, A.P. A mitogen gradient of dorsal midline Wnts organizes growth in the CNS. *Development* **129**, 2087-2098 (2002).

67. Tanabe, Y. & Jessell, T.M. Diversity and pattern in the developing spinal cord. *Science* **274**, 1115-1123 (1996).

68. Doniach, T. Basic FGF as an inducer of anteroposterior neural pattern. *Cell* **83**, 1067-1070 (1995).

69. Bel-Vialar, S., Itasaki, N. & Krumlauf, R. Initiating Hox gene expression: in the early chick neural tube differential sensitivity to FGF and RA signaling subdivides the HoxB genes in two distinct groups. *Development* **129**, 5103-5115 (2002).

70. Liu, J.P., Laufer, E. & Jessell, T.M. Assigning the positional identity of spinal motor neurons: rostrocaudal patterning of Hox-c expression by FGFs, Gdf11, and retinoids. *Neuron* **32**, 997-1012 (2001).

71. Jung, H., *et al.* Global control of motor neuron topography mediated by the repressive actions of a single hox gene. *Neuron* **67**, 781-796 (2010).

72. Tsuchida, T., *et al.* Topographic organization of embryonic motor neurons defined by expression of LIM homeobox genes. *Cell* **79**, 957-970 (1994).

73. Hentges, K., Thompson, K. & Peterson, A. The flat-top gene is required for the expansion and regionalization of the telencephalic primordium. *Development* **126**, 1601-1609 (1999).

74. Caviness, V.S., Jr., Nowakowski, R.S. & Bhide, P.G. Neocortical neurogenesis: morphogenetic gradients and beyond. *Trends Neurosci* **32**, 443-450 (2009).

75. Gotz, M. & Huttner, W.B. The cell biology of neurogenesis. *Nat Rev Mol Cell Biol* **6**, 777-788 (2005).

76. Georgala, P.A., Carr, C.B. & Price, D.J. The role of Pax6 in forebrain development. *Dev Neurobiol* **71**, 690-709 (2011).

77. Stoykova, A., Fritsch, R., Walther, C. & Gruss, P. Forebrain patterning defects in Small eye mutant mice. *Development* **122**, 3453-3465 (1996).

78. Toresson, H., Potter, S.S. & Campbell, K. Genetic control of dorsal-ventral identity in the telencephalon: opposing roles for Pax6 and Gsh2. *Development* **127**, 4361-4371 (2000).

79. Stoykova, A., Treichel, D., Hallonet, M. & Gruss, P. Pax6 modulates the dorsoventral patterning of the mammalian telencephalon. *J Neurosci* **20**, 8042-8050 (2000).

80. Englund, C., *et al.* Pax6, Tbr2, and Tbr1 are expressed sequentially by radial glia, intermediate progenitor cells, and postmitotic neurons in developing neocortex. *J Neurosci* **25**, 247-251 (2005).

81. Yun, K., Potter, S. & Rubenstein, J.L. Gsh2 and Pax6 play complementary roles in dorsoventral patterning of the mammalian telencephalon. *Development* **128**, 193-205 (2001).

82. Hallonet, M., *et al.* Vax1 is a novel homeobox-containing gene expressed in the developing anterior ventral forebrain. *Development* **125**, 2599-2610 (1998).

83. Oliver, G., *et al.* Six3, a murine homologue of the sine oculis gene, demarcates the most anterior border of the developing neural plate and is expressed during eye development. *Development* **121**, 4045-4055 (1995).

84. Stoykova, A., Gotz, M., Gruss, P. & Price, J. Pax6-dependent regulation of adhesive patterning, R-cadherin expression and boundary formation in developing forebrain. *Development* **124**, 3765-3777 (1997).

85. Holmberg, J. & Frisen, J. Ephrins are not only unattractive. *Trends Neurosci* **25**, 239-243 (2002).

86. Kriegstein, A. & Alvarez-Buylla, A. The glial nature of embryonic and adult neural stem cells. *Annu Rev Neurosci* **32**, 149-184 (2009).

87. Schmechel, D.E. & Rakic, P. Arrested proliferation of radial glial cells during midgestation in rhesus monkey. *Nature* **277**, 303-305 (1979).

88. Feng, L., Hatten, M.E. & Heintz, N. Brain lipid-binding protein (BLBP): a novel signaling system in the developing mammalian CNS. *Neuron* **12**, 895-908 (1994).

89. Shibata, T., *et al.* Glutamate transporter GLAST is expressed in the radial glia-astrocyte lineage of developing mouse spinal cord. *J Neurosci* **17**, 9212-9219 (1997).

90. Aaku-Saraste, E., Hellwig, A. & Huttner, W.B. Loss of occludin and functional tight junctions, but not ZO-1, during neural tube closure--remodeling of the neuroepithelium prior to neurogenesis. *Dev Biol* **180**, 664-679 (1996).

91. Molnar, Z. & Clowry, G. Cerebral cortical development in rodents and primates. *Prog Brain Res* **195**, 45-70 (2012).

92. Basak, O. & Taylor, V. Identification of self-replicating multipotent progenitors in the embryonic nervous system by high Notch activity and Hes5 expression. *Eur J Neurosci* **25**, 1006-1022 (2007).

93. Yoon, K.J., *et al.* Mind bomb 1-expressing intermediate progenitors generate notch signaling to maintain radial glial cells. *Neuron* **58**, 519-531 (2008).

94. Brand, A.H. & Livesey, F.J. Neural stem cell biology in vertebrates and invertebrates: more alike than different? *Neuron* **70**, 719-729 (2011).

95. Lui, J.H., Hansen, D.V. & Kriegstein, A.R. Development and evolution of the human neocortex. *Cell* **146**, 18-36 (2011).

96. Bjornson, C.R., Rietze, R.L., Reynolds, B.A., Magli, M.C. & Vescovi, A.L. Turning brain into blood: a hematopoietic fate adopted by adult neural stem cells in vivo. *Science* **283**, 534-537 (1999).

97. Clarke, D.L., *et al.* Generalized potential of adult neural stem cells. *Science* **288**, 1660-1663 (2000).

98. Galli, R., *et al.* Skeletal myogenic potential of human and mouse neural stem cells. *Nat Neurosci* **3**, 986-991 (2000).

99. Wang, Y.Z., Plane, J.M., Jiang, P., Zhou, C.J. & Deng, W. Concise review: Quiescent and active states of endogenous adult neural stem cells: identification and characterization. *Stem Cells* **29**, 907-912 (2011).

100. Morshead, C.M., *et al.* Neural stem cells in the adult mammalian forebrain: a relatively quiescent subpopulation of subependymal cells. *Neuron* **13**, 1071-1082 (1994).

101. Seri, B., Garcia-Verdugo, J.M., McEwen, B.S. & Alvarez-Buylla, A. Astrocytes give rise to new neurons in the adult mammalian hippocampus. *J Neurosci* **21**, 7153-7160 (2001).

102. Battaglia, F.P., Benchenane, K., Sirota, A., Pennartz, C.M. & Wiener, S.I. The hippocampus: hub of brain network communication for memory. *Trends Cogn Sci* **15**, 310-318 (2011).

103. Gould, E., Beylin, A., Tanapat, P., Reeves, A. & Shors, T.J. Learning enhances adult neurogenesis in the hippocampal formation. *Nat Neurosci* **2**, 260-265 (1999).

104. Tamai, S., Sanada, K. & Fukada, Y. Time-of-day-dependent enhancement of adult neurogenesis in the hippocampus. *PLoS One* **3**, e3835 (2008).

105. Matsumoto, Y., *et al.* Differential proliferation rhythm of neural progenitor and oligodendrocyte precursor cells in the young adult hippocampus. *PLoS One* **6**, e27628 (2011).

106. Conover, J.C. & Shook, B.A. Aging of the Subventricular Zone Neural Stem Cell Niche. *Aging Dis* **2**, 149-163 (2011).

107. Li, W., Cogswell, C.A. & LoTurco, J.J. Neuronal differentiation of precursors in the neocortical ventricular zone is triggered by BMP. *J Neurosci* **18**, 8853-8862 (1998).

108. Gross, R.E., *et al.* Bone morphogenetic proteins promote astroglial lineage commitment by mammalian subventricular zone progenitor cells. *Neuron* **17**, 595-606 (1996).

109. Bani-Yaghoub, M., *et al.* Role of Sox2 in the development of the mouse neocortex. *Dev Biol* **295**, 52-66 (2006).

110. Chojnacki, A. & Weiss, S. Isolation of a novel platelet-derived growth factor-responsive precursor from the embryonic ventral forebrain. *J Neurosci* **24**, 10888-10899 (2004).

111. Andreu-Agullo, C., Maurin, T., Thompson, C.B. & Lai, E.C. Ars2 maintains neural stem-cell identity through direct transcriptional activation of Sox2. *Nature* **481**, 195-198 (2012).

112. Conti, L. & Cattaneo, E. Neural stem cell systems: physiological players or in vitro entities? *Nat Rev Neurosci* **11**, 176-187 (2010).

113. Suslov, O.N., Kukekov, V.G., Ignatova, T.N. & Steindler, D.A. Neural stem cell heterogeneity demonstrated by molecular phenotyping of clonal neurospheres. *Proc Natl Acad Sci U S A* **99**, 14506-14511 (2002).

114. Keyoung, H.M., *et al.* High-yield selection and extraction of two promoter-defined phenotypes of neural stem cells from the fetal human brain. *Nat Biotechnol* **19**, 843-850 (2001).

115. Singh, S.K., *et al.* Identification of a cancer stem cell in human brain tumors. *Cancer Res* **63**, 5821-5828 (2003).

116. Doering, L.C. *Protocols for neural cell culture*, (Humana, New York, 2010).

117. Johe, K.K., Hazel, T.G., Muller, T., Dugich-Djordjevic, M.M. & McKay, R.D. Single factors direct the differentiation of stem cells from the fetal and adult central nervous system. *Genes Dev* **10**, 3129-3140 (1996).

118. Hermanson, O., Jepsen, K. & Rosenfeld, M.G. N-CoR controls differentiation of neural stem cells into astrocytes. *Nature* **419**, 934-939 (2002).

119. Qian, X., *et al.* Timing of CNS cell generation: a programmed sequence of neuron and glial cell production from isolated murine cortical stem cells. *Neuron* **28**, 69-80 (2000).

120. Kouroupi, G., *et al.* Lentivirus-mediated expression of insulin-like growth factor-I promotes neural stem/precursor cell proliferation and enhances their potential to generate neurons. *J Neurochem* **115**, 460-474 (2010).

121. Katsimpardi, L., *et al.* BM88/Cend1 expression levels are critical for proliferation and differentiation of subventricular zone-derived neural precursor cells. *Stem Cells* **26**, 1796-1807 (2008).

122. Lagace, D.C., *et al.* Dynamic contribution of nestin-expressing stem cells to adult neurogenesis. *J Neurosci* **27**, 12623-12629 (2007).

123. Ninkovic, J., Mori, T. & Gotz, M. Distinct modes of neuron addition in adult mouse neurogenesis. *J Neurosci* **27**, 10906-10911 (2007).

124. Merkle, F.T., Mirzadeh, Z. & Alvarez-Buylla, A. Mosaic organization of neural stem cells in the adult brain. *Science* **317**, 381-384 (2007).

125. Suhonen, J.O., Peterson, D.A., Ray, J. & Gage, F.H. Differentiation of adult hippocampus-derived progenitors into olfactory neurons in vivo. *Nature* **383**, 624-627 (1996).

126. Hitoshi, S., Tropepe, V., Ekker, M. & van der Kooy, D. Neural stem cell lineages are regionally specified, but not committed, within distinct compartments of the developing brain. *Development* **129**, 233-244 (2002).

127. Gabay, L., Lowell, S., Rubin, L.L. & Anderson, D.J. Deregulation of dorsoventral patterning by FGF confers trilineage differentiation capacity on CNS stem cells in vitro. *Neuron* **40**, 485-499 (2003).

128. Hack, M.A., Sugimori, M., Lundberg, C., Nakafuku, M. & Gotz, M. Regionalization and fate specification in neurospheres: the role of Olig2 and Pax6. *Mol Cell Neurosci* **25**, 664-678 (2004).

129. Coles-Takabe, B.L., *et al.* Don't look: growing clonal versus nonclonal neural stem cell colonies. *Stem Cells* **26**, 2938-2944 (2008).

130. Kim, H.Y., *et al.* Effects of intermittent media replacement on the gene expression of differentiating neural progenitor cells. *Mol Biosyst* **8**, 602-608 (2012).

131. Seaberg, R.M., Smukler, S.R. & van der Kooy, D. Intrinsic differences distinguish transiently neurogenic progenitors from neural stem cells in the early postnatal brain. *Dev Biol* **278**, 71-85 (2005).

132. Martens, D.J., Tropepe, V. & van Der Kooy, D. Separate proliferation kinetics of fibroblast growth factor-responsive and epidermal growth factor-responsive neural stem cells within the embryonic forebrain germinal zone. *J Neurosci* **20**, 1085-1095 (2000).

133. Sun, T., *et al.* A comparison of proliferative capacity and passaging potential between neural stem and progenitor cells in adherent and neurosphere cultures. *Int J Dev Neurosci* **29**, 723-731 (2011).

134. Nakatomi, H., *et al.* Regeneration of hippocampal pyramidal neurons after ischemic brain injury by recruitment of endogenous neural progenitors. *Cell* **110**, 429-441 (2002).

135. Kang, S.H., Fukaya, M., Yang, J.K., Rothstein, J.D. & Bergles, D.E. NG2+ CNS glial progenitors remain committed to the oligodendrocyte lineage in postnatal life and following neurodegeneration. *Neuron* **68**, 668-681 (2010).

136. Buffo, A., *et al.* Origin and progeny of reactive gliosis: A source of multipotent cells in the injured brain. *Proc Natl Acad Sci U S A* **105**, 3581-3586 (2008).

137. Park, K.I., Teng, Y.D. & Snyder, E.Y. The injured brain interacts reciprocally with neural stem cells supported by scaffolds to reconstitute lost tissue. *Nat Biotechnol* **20**, 1111-1117 (2002).

138. Teng, Y.D., *et al.* Functional recovery following traumatic spinal cord injury mediated by a unique polymer scaffold seeded with neural stem cells. *Proc Natl Acad Sci U S A* **99**, 3024-3029 (2002).

139. Yandava, B.D., Billinghurst, L.L. & Snyder, E.Y. "Global" cell replacement is feasible via neural stem cell transplantation: evidence from the dysmyelinated shiverer mouse brain. *Proc Natl Acad Sci U S A* **96**, 7029-7034 (1999).

140. Jeong, S.W., *et al.* Human neural stem cell transplantation promotes functional recovery in rats with experimental intracerebral hemorrhage. *Stroke* **34**, 2258-2263 (2003).

141. Aschheim, K., Defrancesco, L., Hare, P. & Mak, C. Research highlights. *Nat Biotechnol* **27**, 1134 (2009).

142. Fujikawa, T., *et al.* Teratoma formation leads to failure of treatment for type I diabetes using embryonic stem cell-derived insulin-producing cells. *Am J Pathol* **166**, 1781-1791 (2005).

143. Knoepfler, P.S. Deconstructing stem cell tumorigenicity: a roadmap to safe regenerative medicine. *Stem Cells* **27**, 1050-1056 (2009).

144. Samson, D., Chanarin, I. & Reid, C.D. Recent advances in haematology. *Postgrad Med J* **57**, 139-149 (1981).

145. Reynolds, B.A., Tetzlaff, W. & Weiss, S. A multipotent EGF-responsive striatal embryonic progenitor cell produces neurons and astrocytes. *J Neurosci* **12**, 4565-4574 (1992).

146. Imayoshi, I., Sakamoto, M., Yamaguchi, M., Mori, K. & Kageyama, R. Essential roles of Notch signaling in maintenance of neural stem cells in developing and adult brains. *J Neurosci* **30**, 3489-3498 (2010).

147. Neri, M., *et al.* Robust generation of oligodendrocyte progenitors from human neural stem cells and engraftment in experimental demyelination models in mice. *PLoS One* **5**, e10145 (2010).

148. Liu, J., Wei, Y., Chen, Y., Xu, X. & Zhang, H. Differentiation of neural stem cells influences their chemotactic responses to vascular endothelial growth factor. *J Neurosci Res* **89**, 1173-1184 (2011).

149. Ables, J.L., Breunig, J.J., Eisch, A.J. & Rakic, P. Not(ch) just development: Notch signalling in the adult brain. *Nat Rev Neurosci* **12**, 269-283 (2011).

150. Simpson, P. Notch signalling in development: on equivalence groups and asymmetric developmental potential. *Curr Opin Genet Dev* **7**, 537-542 (1997).

151. Axelrod, J.D. Delivering the lateral inhibition punchline: it's all about the timing. *Sci Signal* **3**, pe38 (2010).

152. Henrique, D., *et al.* Expression of a Delta homologue in prospective neurons in the chick. *Nature* **375**, 787-790 (1995).

153. Hatakeyama, J. & Kageyama, R. Notch1 expression is spatiotemporally correlated with neurogenesis and negatively regulated by Notch1-independent Hes genes in the developing nervous system. *Cereb Cortex* **16 Suppl 1**, i132-137 (2006).

154. Hammerle, B. & Tejedor, F.J. A novel function of DELTA-NOTCH signalling mediates the transition from proliferation to neurogenesis in neural progenitor cells. *PLoS One* **2**, e1169 (2007).

155. Ross, S.E., Greenberg, M.E. & Stiles, C.D. Basic helix-loop-helix factors in cortical development. *Neuron* **39**, 13-25 (2003).

156. Ohtsuka, T., *et al.* Hes1 and Hes5 as notch effectors in mammalian neuronal differentiation. *EMBO J* **18**, 2196-2207 (1999).

157. Miyazono, K., Kamiya, Y. & Morikawa, M. Bone morphogenetic protein receptors and signal transduction. *J Biochem* **147**, 35-51 (2010).

158. Ying, Q.L., Nichols, J., Chambers, I. & Smith, A. BMP induction of Id proteins suppresses differentiation and sustains embryonic stem cell self-renewal in collaboration with STAT3. *Cell* **115**, 281-292 (2003).

159. See, J., *et al.* BMP signaling mutant mice exhibit glial cell maturation defects. *Mol Cell Neurosci* **35**, 171-182 (2007).

160. Ortega, J.A. & Alcantara, S. BDNF/MAPK/ERK-induced BMP7 expression in the developing cerebral cortex induces premature radial glia differentiation and impairs neuronal migration. *Cereb Cortex* **20**, 2132-2144 (2010).

161. Kim, M.Y., Kaduwal, S., Yang, D.H. & Choi, K.Y. Bone morphogenetic protein 4 stimulates attachment of neurospheres and astrogenesis of neural stem cells in neurospheres via phosphatidylinositol 3 kinase-mediated upregulation of N-cadherin. *Neuroscience* **170**, 8-15 (2010).

162. Piper, D.E., Batchelor, A.H., Chang, C.P., Cleary, M.L. & Wolberger, C. Structure of a HoxB1-Pbx1 heterodimer bound to DNA: role of the hexapeptide and a fourth homeodomain helix in complex formation. *Cell* **96**, 587-597 (1999).

163. Billeter, M., *et al.* Determination of the nuclear magnetic resonance solution structure of an Antennapedia homeodomain-DNA complex. *J Mol Biol* **234**, 1084-1093 (1993).

164. Mallo, M., Wellik, D.M. & Deschamps, J. Hox genes and regional patterning of the vertebrate body plan. *Dev Biol* **344**, 7-15 (2010).

165. Potts, M.B., Wang, D.P. & Cameron, S. Trithorax, Hox, and TALE-class homeodomain proteins ensure cell survival through repression of the BH3-only gene egl-1. *Dev Biol* **329**, 374-385 (2009).

166. Rogulja-Ortmann, A., Renner, S. & Technau, G.M. Antagonistic roles for Ultrabithorax and Antennapedia in regulating segment-specific apoptosis of differentiated motoneurons in the Drosophila embryonic central nervous system. *Development* **135**, 3435-3445 (2008).

167. Hombria, J.C. & Lovegrove, B. Beyond homeosis--HOX function in morphogenesis and organogenesis. *Differentiation* **71**, 461-476 (2003).

168. Lohmann, I., McGinnis, N., Bodmer, M. & McGinnis, W. The Drosophila Hox gene deformed sculpts head morphology via direct regulation of the apoptosis activator reaper. *Cell* **110**, 457-466 (2002).

169. Kanzler, B., *et al.* Differential expression of two different homeobox gene families during mouse tegument morphogenesis. *Int J Dev Biol* **38**, 633-640 (1994).

170. Lewis, E.B. A gene complex controlling segmentation in Drosophila. *Nature* **276**, 565-570 (1978).

171. Regulski, M., *et al.* Homeo box genes of the Antennapedia and bithorax complexes of Drosophila. *Cell* **43**, 71-80 (1985).

172. Boulet, A.M. & Capecchi, M.R. Multiple roles of Hoxa11 and Hoxd11 in the formation of the mammalian forelimb zeugopod. *Development* **131**, 299-309 (2004).

173. Brison, N., Tylzanowski, P. & Debeer, P. Limb skeletal malformations - What the HOX is going on? *Eur J Med Genet* (2011).

174. Davis, A.P., Witte, D.P., Hsieh-Li, H.M., Potter, S.S. & Capecchi, M.R. Absence of radius and ulna in mice lacking hoxa-11 and hoxd-11. *Nature* **375**, 791-795 (1995).

175. Lufkin, T., Dierich, A., LeMeur, M., Mark, M. & Chambon, P. Disruption of the Hox-1.6 homeobox gene results in defects in a region corresponding to its rostral domain of expression. *Cell* **66**, 1105-1119 (1991).

176. Ramirez-Solis, R., Zheng, H., Whiting, J., Krumlauf, R. & Bradley, A. Hoxb-4 (Hox-2.6) mutant mice show homeotic transformation of a cervical vertebra and defects in the closure of the sternal rudiments. *Cell* **73**, 279-294 (1993).

177. Noro, B., Lelli, K., Sun, L. & Mann, R.S. Competition for cofactor-dependent DNA binding underlies Hox phenotypic suppression. *Genes Dev* **25**, 2327-2332 (2011).

178. Wassef, M.A., *et al.* Rostral hindbrain patterning involves the direct activation of a Krox20 transcriptional enhancer by Hox/Pbx and Meis factors. *Development* **135**, 3369-3378 (2008).

179. Ferretti, E., *et al.* Hoxb1 enhancer and control of rhombomere 4 expression: complex interplay between PREP1-PBX1-HOXB1 binding sites. *Mol Cell Biol* **25**, 8541-8552 (2005).

180. Tumpel, S., *et al.* Expression of Hoxa2 in rhombomere 4 is regulated by a conserved cross-regulatory mechanism dependent upon Hoxb1. *Dev Biol* **302**, 646-660 (2007).

181. Huang, H., *et al.* MEIS C termini harbor transcriptional activation domains that respond to cell signaling. *J Biol Chem* **280**, 10119-10127 (2005).

182. Penkov, D., *et al.* Cooperative interactions between PBX, PREP, and HOX proteins modulate the activity of the alpha 2(V) collagen (COL5A2) promoter. *J Biol Chem* **275**, 16681-16689 (2000).

183. Chisaka, O. & Capecchi, M.R. Regionally restricted developmental defects resulting from targeted disruption of the mouse homeobox gene hox-1.5. *Nature* **350**, 473-479 (1991).

184. Studer, M., Lumsden, A., Ariza-McNaughton, L., Bradley, A. & Krumlauf, R. Altered segmental identity and abnormal migration of motor neurons in mice lacking Hoxb-1. *Nature* **384**, 630-634 (1996).

185. Wong, E.Y., *et al.* Hoxb3 negatively regulates Hoxb1 expression in mouse hindbrain patterning. *Dev Biol* **352**, 382-392 (2011).

186. Kobrossy, L., Rastegar, M. & Featherstone, M. Interplay between chromatin and trans-acting factors regulating the Hoxd4 promoter during neural differentiation. *J Biol Chem* **281**, 25926-25939 (2006).

187. Coy, S.E. & Borycki, A.G. Expression analysis of TALE family transcription factors during avian development. *Dev Dyn* **239**, 1234-1245 (2010).

188. Shen, W.F., *et al.* AbdB-like Hox proteins stabilize DNA binding by the Meis1 homeodomain proteins. *Mol Cell Biol* **17**, 6448-6458 (1997).

189. Chang, C.P., Brocchieri, L., Shen, W.F., Largman, C. & Cleary, M.L. Pbx modulation of Hox homeodomain amino-terminal arms establishes different DNA-binding specificities across the Hox locus. *Mol Cell Biol* **16**, 1734-1745 (1996).

190. Capellini, T.D., Zappavigna, V. & Selleri, L. Pbx homeodomain proteins: TALEnted regulators of limb patterning and outgrowth. *Dev Dyn* **240**, 1063-1086 (2011).

191. Vitobello, A., *et al.* Hox and Pbx factors control retinoic acid synthesis during hindbrain segmentation. *Dev Cell* **20**, 469-482 (2011).

192. Ferretti, E., *et al.* Hypomorphic mutation of the TALE gene Prep1 (pKnox1) causes a major reduction of Pbx and Meis proteins and a pleiotropic embryonic phenotype. *Mol Cell Biol* **26**, 5650-5662 (2006).

193. Pineault, N., Helgason, C.D., Lawrence, H.J. & Humphries, R.K. Differential expression of Hox, Meis1, and Pbx1 genes in primitive cells throughout murine hematopoietic ontogeny. *Exp Hematol* **30**, 49-57 (2002).

194. Rauskolb, C., Peifer, M. & Wieschaus, E. extradenticle, a regulator of homeotic gene activity, is a homolog of the homeobox-containing human proto-oncogene pbx1. *Cell* **74**, 1101-1112 (1993).

195. Kamps, M.P., Murre, C., Sun, X.H. & Baltimore, D. A new homeobox gene contributes the DNA binding domain of the t(1;19) translocation protein in pre-B ALL. *Cell* **60**, 547-555 (1990).

196. Nourse, J., *et al.* Chromosomal translocation t(1;19) results in synthesis of a homeobox fusion mRNA that codes for a potential chimeric transcription factor. *Cell* **60**, 535-545 (1990).

197. Monica, K., Galili, N., Nourse, J., Saltman, D. & Cleary, M.L. PBX2 and PBX3, new homeobox genes with extensive homology to the human proto-oncogene PBX1. *Mol Cell Biol* **11**, 6149-6157 (1991).

198. Wagner, K., Mincheva, A., Korn, B., Lichter, P. & Popperl, H. Pbx4, a new Pbx family member on mouse chromosome 8, is expressed during spermatogenesis. *Mech Dev* **103**, 127-131 (2001).

199. Selleri, L., *et al.* Requirement for Pbx1 in skeletal patterning and programming chondrocyte proliferation and differentiation. *Development* **128**, 3543-3557 (2001).

200. Di Giacomo, G., *et al.* Spatio-temporal expression of Pbx3 during mouse organogenesis. *Gene Expr Patterns* **6**, 747-757 (2006).

201. Selleri, L., *et al.* The TALE homeodomain protein Pbx2 is not essential for development and long-term survival. *Mol Cell Biol* **24**, 5324-5331 (2004).

202. Wong, P., Iwasaki, M., Somervaille, T.C., So, C.W. & Cleary, M.L. Meis1 is an essential and rate-limiting regulator of MLL leukemia stem cell potential. *Genes Dev* **21**, 2762-2774 (2007).

203. Burglin, T.R. The PBC domain contains a MEINOX domain: coevolution of Hox and TALE homeobox genes? *Dev Genes Evol* **208**, 113-116 (1998).

204. Moskow, J.J., Bullrich, F., Huebner, K., Daar, I.O. & Buchberg, A.M. Meis1, a PBX1-related homeobox gene involved in myeloid leukemia in BXH-2 mice. *Mol Cell Biol* **15**, 5434-5443 (1995).

205. Hisa, T., *et al.* Hematopoietic, angiogenic and eye defects in Meis1 mutant animals. *EMBO J* **23**, 450-459 (2004).

206. Azcoitia, V., Aracil, M., Martinez, A.C. & Torres, M. The homeodomain protein Meis1 is essential for definitive hematopoiesis and vascular patterning in the mouse embryo. *Dev Biol* **280**, 307-320 (2005).

207. Toresson, H., Parmar, M. & Campbell, K. Expression of Meis and Pbx genes and their protein products in the developing telencephalon: implications for regional differentiation. *Mech Dev* **94**, 183-187 (2000).

208. Molotkova, N., Molotkov, A. & Duester, G. Role of retinoic acid during forebrain development begins late when Raldh3 generates retinoic acid in the ventral subventricular zone. *Dev Biol* **303**, 601-610 (2007).

209. Bumsted-O'Brien, K.M., Hendrickson, A., Haverkamp, S., Ashery-Padan, R. & Schulte, D. Expression of the homeodomain transcription factor Meis2 in the embryonic and postnatal retina. *J Comp Neurol* **505**, 58-72 (2007).

210. Heine, P., Dohle, E., Bumsted-O'Brien, K., Engelkamp, D. & Schulte, D. Evidence for an evolutionary conserved role of homothorax/Meis1/2 during vertebrate retina development. *Development* **135**, 805-811 (2008).

211. Elkouby, Y.M., *et al.* Mesodermal Wnt signaling organizes the neural plate via Meis3. *Development* **137**, 1531-1541 (2010).

212. Vlachakis, N., Choe, S.K. & Sagerstrom, C.G. Meis3 synergizes with Pbx4 and Hoxb1b in promoting hindbrain fates in the zebrafish. *Development* **128**, 1299-1312 (2001).

213. Dibner, C., Elias, S. & Frank, D. XMeis3 protein activity is required for proper hindbrain patterning in Xenopus laevis embryos. *Development* **128**, 3415-3426 (2001).

214. Fernandez-Diaz, L.C., *et al.* The absence of Prep1 causes p53-dependent apoptosis of mouse pluripotent epiblast cells. *Development* **137**, 3393-3403 (2010).

215. Longobardi, E., *et al.* Prep1 (pKnox1)-deficiency leads to spontaneous tumor development in mice and accelerates EmuMyc lymphomagenesis: a tumor suppressor role for Prep1. *Mol Oncol* **4**, 126-134 (2010).

216. Iotti, G., *et al.* Homeodomain transcription factor and tumor suppressor Prep1 is required to maintain genomic stability. *Proc Natl Acad Sci U S A* **108**, E314-322 (2011).

217. Iotti, G., *et al.* Homeodomain transcription factor and tumor suppressor Prep1 is required to maintain genomic stability. *Proc Natl Acad Sci U S A* **108**, E314-322.

218. Longobardi, E., *et al.* Prep1 (pKnox1)-deficiency leads to spontaneous tumor development in mice and accelerates EmuMyc lymphomagenesis: a tumor suppressor role for Prep1. *Mol Oncol* **4**, 126-134.

219. Villaescusa, J.C., Verrotti, A.C., Ferretti, E., Farookhi, R. & Blasi, F. Expression of Hox cofactor genes during mouse ovarian follicular development and oocyte maturation. *Gene* **330**, 1-7 (2004).

220. Haller, K., Rambaldi, I., Kovacs, E.N., Daniels, E. & Featherstone, M. Prep2: cloning and expression of a new prep family member. *Dev Dyn* **225**, 358-364 (2002).

221. Haller, K., Rambaldi, I., Daniels, E. & Featherstone, M. Subcellular localization of multiple PREP2 isoforms is regulated by actin, tubulin, and nuclear export. *J Biol Chem* **279**, 49384-49394 (2004).

222. Ferretti, E., Schulz, H., Talarico, D., Blasi, F. & Berthelsen, J. The PBX-regulating protein PREP1 is present in different PBX-complexed forms in mouse. *Mech Dev* **83**, 53-64 (1999).

223. Redmond, L., Hockfield, S. & Morabito, M.A. The divergent homeobox gene PBX1 is expressed in the postnatal subventricular zone and interneurons of the olfactory bulb. *J Neurosci* **16**, 2972-2982 (1996).

224. Carroll, A.J., *et al.* Pre-B cell leukemia associated with chromosome translocation 1;19. *Blood* **63**, 721-724 (1984).

225. Sykes, D.B. & Kamps, M.P. E2a/Pbx1 induces the rapid proliferation of stem cell factor-dependent murine pro-T cells that cause acute T-lymphoid or myeloid leukemias in mice. *Mol Cell Biol* **24**, 1256-1269 (2004).

226. Kawagoe, H., Humphries, R.K., Blair, A., Sutherland, H.J. & Hogge, D.E. Expression of HOX genes, HOX cofactors, and MLL in phenotypically and functionally defined subpopulations of leukemic and normal human hematopoietic cells. *Leukemia* **13**, 687-698 (1999).

227. Rozovskaia, T., *et al.* Upregulation of Meis1 and HoxA9 in acute lymphocytic leukemias with the t(4 : 11) abnormality. *Oncogene* **20**, 874-878 (2001).

228. Imamura, T., *et al.* Frequent co-expression of HoxA9 and Meis1 genes in infant acute lymphoblastic leukaemia with MLL rearrangement. *Br J Haematol* **119**, 119-121 (2002).

229. Argiropoulos, B., Yung, E. & Humphries, R.K. Unraveling the crucial roles of Meis1 in leukemogenesis and normal hematopoiesis. *Genes Dev* **21**, 2845-2849 (2007).

230. Yang, J., *et al.* Enhanced self-renewal of hematopoietic stem/progenitor cells mediated by the stem cell gene Sall4. *J Hematol Oncol* **4**, 38 (2011).

231. Monteiro, M.C., *et al.* PBX1: a novel stage-specific regulator of adipocyte development. *Stem Cells* **29**, 1837-1848 (2011).

232. Peifer, M. & Wieschaus, E. Mutations in the Drosophila gene extradenticle affect the way specific homeo domain proteins regulate segmental identity. *Genes Dev* **4**, 1209-1223 (1990).

233. Rauskolb, C., Smith, K.M., Peifer, M. & Wieschaus, E. extradenticle determines segmental identities throughout Drosophila development. *Development* **121**, 3663-3673 (1995).

234. Berthelsen, J., Kilstrup-Nielsen, C., Blasi, F., Mavilio, F. & Zappavigna, V. The subcellular localization of PBX1 and EXD proteins depends on nuclear import and export signals and is modulated by association with PREP1 and HTH. *Genes Dev* **13**, 946-953 (1999).

235. Huang, H., Paliouras, M., Rambaldi, I., Lasko, P. & Featherstone, M. Nonmuscle myosin promotes cytoplasmic localization of PBX. *Mol Cell Biol* **23**, 3636-3645 (2003).

236. Abu-Shaar, M., Ryoo, H.D. & Mann, R.S. Control of the nuclear localization of Extradenticle by competing nuclear import and export signals. *Genes Dev* **13**, 935-945 (1999).

237. Saleh, M., Huang, H., Green, N.C. & Featherstone, M.S. A conformational change in PBX1A is necessary for its nuclear localization. *Exp Cell Res* **260**, 105-115 (2000).

238. Kilstrup-Nielsen, C., Alessio, M. & Zappavigna, V. PBX1 nuclear export is regulated independently of PBX-MEINOX interaction by PKA phosphorylation of the PBC-B domain. *EMBO J* **22**, 89-99 (2003).

239. Dintilhac, A., *et al.* PBX1 intracellular localization is independent of MEIS1 in epithelial cells of the developing female genital tract. *Int J Dev Biol* **49**, 851-858 (2005).

240. Longobardi, E. & Blasi, F. Overexpression of PREP-1 in F9 teratocarcinoma cells leads to a functionally relevant increase of PBX-2 by preventing its degradation. *J Biol Chem* **278**, 39235-39241 (2003).

241. Mojsin, M. & Stevanovic, M. PBX1 and MEIS1 up-regulate SOX3 gene expression by direct interaction with a consensus binding site within the basal promoter region. *Biochem J* **425**, 107-116 (2010).

242. Knoepfler, P.S., Calvo, K.R., Chen, H., Antonarakis, S.E. & Kamps, M.P. Meis1 and pKnox1 bind DNA cooperatively with Pbx1 utilizing an interaction surface disrupted in oncoprotein E2a-Pbx1. *Proc Natl Acad Sci U S A* **94**, 14553-14558 (1997).

243. Ferretti, E., *et al.* Segmental expression of Hoxb2 in r4 requires two separate sites that integrate cooperative interactions between Prep1, Pbx and Hox proteins. *Development* **127**, 155-166 (2000).

244. Jacobs, Y., Schnabel, C.A. & Cleary, M.L. Trimeric association of Hox and TALE homeodomain proteins mediates Hoxb2 hindbrain enhancer activity. *Mol Cell Biol* **19**, 5134-5142 (1999).

245. Chang, C.P., *et al.* Meis proteins are major in vivo DNA binding partners for wild-type but not chimeric Pbx proteins. *Mol Cell Biol* **17**, 5679-5687 (1997).

246. Schnabel, C.A., Jacobs, Y. & Cleary, M.L. HoxA9-mediated immortalization of myeloid progenitors requires functional interactions with TALE cofactors Pbx and Meis. *Oncogene* **19**, 608-616 (2000).

247. Fernandez, L.C., *et al.* Oncogenic HoxB7 requires TALE cofactors and is inactivated by a dominant-negative Pbx1 mutant in a cell-specific manner. *Cancer Lett* **266**, 144-155 (2008).

248. Delval, S., *et al.* The Pbx interaction motif of Hoxa1 is essential for its oncogenic activity. *PLoS One* **6**, e25247 (2011).

249. Bisaillon, R., Wilhelm, B.T., Krosl, J. & Sauvageau, G. C-terminal domain of MEIS1 converts PKNOX1 (PREP1) into a HOXA9-collaborating oncoprotein. *Blood* **118**, 4682-4689 (2011).

250. Niederreither, K., Subbarayan, V., Dolle, P. & Chambon, P. Embryonic retinoic acid synthesis is essential for early mouse post-implantation development. *Nat Genet* **21**, 444-448 (1999).

251. Zhao, D., *et al.* Molecular identification of a major retinoic-acid-synthesizing enzyme, a retinaldehyde-specific dehydrogenase. *Eur J Biochem* **240**, 15-22 (1996).

252. Jurgens, A.S., *et al.* PBX1 is dispensable for neural commitment of RA-treated murine ES cells. *In Vitro Cell Dev Biol Anim* **45**, 252-263 (2009).

253. Gouti, M. & Gavalas, A. Hoxb1 controls cell fate specification and proliferative capacity of neural stem and progenitor cells. *Stem Cells* **26**, 1985-1997 (2008).

254. Gaspar, N., *et al.* MGMT-independent temozolomide resistance in pediatric glioblastoma cells associated with a PI3-kinase-mediated HOX/stem cell gene signature. *Cancer Res* **70**, 9243-9252 (2010).

255. Rastegar, M., *et al.* MECP2 isoform-specific vectors with regulated expression for Rett syndrome gene therapy. *PLoS One* **4**, e6810 (2009).

256. Slack, R.S., El-Bizri, H., Wong, J., Belliveau, D.J. & Miller, F.D. A critical temporal requirement for the retinoblastoma protein family during neuronal determination. *J Cell Biol* **140**, 1497-1509 (1998).

257. Wegner, M. SOX after SOX: SOXession regulates neurogenesis. *Genes Dev* **25**, 2423-2428 (2011).

258. Marshall, C.A., Novitch, B.G. & Goldman, J.E. Olig2 directs astrocyte and oligodendrocyte formation in postnatal subventricular zone cells. *J Neurosci* **25**, 7289-7298 (2005).

259. Takahashi, H. & Liu, F.C. Genetic patterning of the mammalian telencephalon by morphogenetic molecules and transcription factors. *Birth Defects Res C Embryo Today* **78**, 256-266 (2006).

260. Kageyama, R., Ohtsuka, T., Hatakeyama, J. & Ohsawa, R. Roles of bHLH genes in neural stem cell differentiation. *Exp Cell Res* **306**, 343-348 (2005).

261. Rowitch, D.H. Glial specification in the vertebrate neural tube. *Nat Rev Neurosci* **5**, 409-419 (2004).

262. Nakamura, T., Jenkins, N.A. & Copeland, N.G. Identification of a new family of Pbx-related homeobox genes. *Oncogene* **13**, 2235-2242 (1996).

263. Campos, L.S., *et al.* Beta1 integrins activate a MAPK signalling pathway in neural stem cells that contributes to their maintenance. *Development* **131**, 3433-3444 (2004).

264. Fathi, A., *et al.* Comprehensive gene expression analysis of human embryonic stem cells during differentiation into neural cells. *PLoS One* **6**, e22856 (2011).

265. Schuettengruber, B., Martinez, A.M., Iovino, N. & Cavalli, G. Trithorax group proteins: switching genes on and keeping them active. *Nat Rev Mol Cell Biol* **12**, 799-814 (2011).

266. Mori, H., Fujitani, T., Kanemura, Y., Kino-Oka, M. & Taya, M. Observational examination of aggregation and migration during early phase of neurosphere culture of mouse neural stem cells. *J Biosci Bioeng* **104**, 231-234 (2007).

267. Copray, S., *et al.* Olig2 overexpression induces the in vitro differentiation of neural stem cells into mature oligodendrocytes. *Stem Cells* **24**, 1001-1010 (2006).

268. Aranha, M.M., Santos, D.M., Sola, S., Steer, C.J. & Rodrigues, C.M. miR-34a regulates mouse neural stem cell differentiation. *PLoS One* **6**, e21396 (2011).

269. Reynolds, B.A. & Weiss, S. Clonal and population analyses demonstrate that an EGF-responsive mammalian embryonic CNS precursor is a stem cell. *Dev Biol* **175**, 1-13 (1996).

270. Cao, F., Hata, R., Zhu, P., Nakashiro, K. & Sakanaka, M. Conditional deletion of Stat3 promotes neurogenesis and inhibits astrogliogenesis in neural stem cells. *Biochem Biophys Res Commun* **394**, 843-847 (2010).

271. Grandbarbe, L., *et al.* Delta-Notch signaling controls the generation of neurons/glia from neural stem cells in a stepwise process. *Development* **130**, 1391-1402 (2003).

272. Ohtsuka, T., Sakamoto, M., Guillemot, F. & Kageyama, R. Roles of the basic helix-loop-helix genes Hes1 and Hes5 in expansion of neural stem cells of the developing brain. *J Biol Chem* **276**, 30467-30474 (2001).

273. Ge, W., *et al.* Notch signaling promotes astrogliogenesis via direct CSL-mediated glial gene activation. *J Neurosci Res* **69**, 848-860 (2002).

274. Tanigaki, K., *et al.* Notch1 and Notch3 instructively restrict bFGF-responsive multipotent neural progenitor cells to an astroglial fate. *Neuron* **29**, 45-55 (2001).

275. Alexson, T.O., Hitoshi, S., Coles, B.L., Bernstein, A. & van der Kooy, D. Notch signaling is required to maintain all neural stem cell populations--irrespective of spatial or temporal niche. *Dev Neurosci* **28**, 34-48 (2006).

276. Hitoshi, S., *et al.* Notch pathway molecules are essential for the maintenance, but not the generation, of mammalian neural stem cells. *Genes Dev* **16**, 846-858 (2002).

277. Sanosaka, T., *et al.* Identification of genes that restrict astrocyte differentiation of midgestational neural precursor cells. *Neuroscience* **155**, 780-788 (2008).

278. Yoshimatsu, T., *et al.* Non-cell-autonomous action of STAT3 in maintenance of neural precursor cells in the mouse neocortex. *Development* **133**, 2553-2563 (2006).

279. Tokunaga, A., *et al.* Mapping spatio-temporal activation of Notch signaling during neurogenesis and gliogenesis in the developing mouse brain. *J Neurochem* **90**, 142-154 (2004).

280. Namihira, M., *et al.* Committed neuronal precursors confer astrocytic potential on residual neural precursor cells. *Dev Cell* **16**, 245-255 (2009).

281. Kamakura, S., *et al.* Hes binding to STAT3 mediates crosstalk between Notch and JAK-STAT signalling. *Nat Cell Biol* **6**, 547-554 (2004).

282. Gaiano, N., Nye, J.S. & Fishell, G. Radial glial identity is promoted by Notch1 signaling in the murine forebrain. *Neuron* **26**, 395-404 (2000).

283. Nakashima, K., Yanagisawa, M., Arakawa, H. & Taga, T. Astrocyte differentiation mediated by LIF in cooperation with BMP2. *FEBS Lett* **457**, 43-46 (1999).

284. Nakashima, K., *et al.* BMP2-mediated alteration in the developmental pathway of fetal mouse brain cells from neurogenesis to astrocytogenesis. *Proc Natl Acad Sci U S A* **98**, 5868-5873 (2001).

285. Andersson, T., *et al.* Noggin and Wnt3a enable BMP4-dependent differentiation of telencephalic stem cells into GluR-agonist responsive neurons. *Mol Cell Neurosci* **47**, 10-18 (2011).

286. Cai, N., Kurachi, M., Shibasaki, K., Okano-Uchida, T. & Ishizaki, Y. CD44-Positive Cells Are Candidates for Astrocyte Precursor Cells in Developing Mouse Cerebellum. *Cerebellum* (2011).

287. Yun, K., *et al.* Modulation of the notch signaling by Mash1 and Dlx1/2 regulates sequential specification and differentiation of progenitor cell types in the subcortical telencephalon. *Development* **129**, 5029-5040 (2002).

288. Levi, G., *et al.* The Dlx5 homeodomain gene is essential for olfactory development and connectivity in the mouse. *Mol Cell Neurosci* **22**, 530-543 (2003).

289. Perera, M., *et al.* Defective neuronogenesis in the absence of Dlx5. *Mol Cell Neurosci* **25**, 153-161 (2004).

290. Gomez-Lopez, S., *et al.* Sox2 and Pax6 maintain the proliferative and developmental potential of gliogenic neural stem cells In vitro. *Glia* **59**, 1588-1599 (2011).

291. Martinez-Ceballos, E. & Gudas, L.J. Hoxa1 is required for the retinoic acid-induced differentiation of embryonic stem cells into neurons. *J Neurosci Res* **86**, 2809-2819 (2008).

292. Murata, H., Yamaguchi, D., Nagai, A. & Shimada, N. Reduction of deoxynivalenol contaminating corn silage by short-term ultraviolet irradiation: a pilot study. *J Vet Med Sci* **73**, 1059-1060 (2011).

293. Kashyap, V., *et al.* Epigenomic reorganization of the clustered Hox genes in embryonic stem cells induced by retinoic acid. *J Biol Chem* **286**, 3250-3260 (2011).

294. Freemantle, S.J., Kerley, J.S., Olsen, S.L., Gross, R.H. & Spinella, M.J. Developmentally-related candidate retinoic acid target genes regulated early during neuronal differentiation of human embryonal carcinoma. *Oncogene* **21**, 2880-2889 (2002).

295. Spieker, N., *et al.* The MEIS1 oncogene is highly expressed in neuroblastoma and amplified in cell line IMR32. *Genomics* **71**, 214-221 (2001).

296. Geerts, D., Schilderink, N., Jorritsma, G. & Versteeg, R. The role of the MEIS homeobox genes in neuroblastoma. *Cancer Lett* **197**, 87-92 (2003).

297. Abdel-Fattah, R., *et al.* Differential expression of HOX genes in neoplastic and non-neoplastic human astrocytes. *J Pathol* **209**, 15-24 (2006).

298. Murat, A., *et al.* Stem cell-related "self-renewal" signature and high epidermal growth factor receptor expression associated with resistance to concomitant chemoradiotherapy in glioblastoma. *J Clin Oncol* **26**, 3015-3024 (2008).